

The self-resonance and self-capacitance of solenoid coils: applicable theory, models and calculation methods.

By David W Knight¹

Version² 1.00, 4th May 2016.

DOI: 10.13140/RG.2.1.1472.0887

Abstract

The data on which Medhurst's semi-empirical self-capacitance formula is based are re-analysed in a way that takes the permittivity of the coil-former into account. The updated formula is compared with theories attributing self-capacitance to the capacitance between adjacent turns, and also with transmission-line theories. The inter-turn capacitance approach is found to have no predictive power. Transmission-line behaviour is corroborated by measurements using an induction loop and a receiving antenna, and by visualising the electric field using a gas discharge tube. In-circuit solenoid self-capacitance determinations show long-coil asymptotic behaviour corresponding to a wave propagating along the helical conductor with a phase-velocity governed by the local refractive index (i.e., $v = c$ if the medium is air). This is consistent with measurements of transformer phase error vs. frequency, which indicate a constant time delay. These observations are at odds with the fact that a long solenoid in free space will exhibit helical propagation with a frequency-dependent phase velocity $> c$. The implication is that unmodified helical-waveguide theories are not appropriate for the prediction of self-capacitance, but they remain applicable in principle to open-circuit systems, such as Tesla coils, helical resonators and loaded vertical antennas, despite poor agreement with actual measurements. A semi-empirical method is given for predicting the first self-resonance frequencies of free coils by treating the coil as a helical transmission-line terminated by its own axial-field and fringe-field capacitances.

Keywords: circuit modelling, solenoid coil, self-capacitance, self-resonance, helical waveguide, sheet helix, sheath helix.

Acknowledgements

I would like to thank Prof. Tuck Choy (M0TCC) for detailed reading and discussion of this work, and for providing reference materials and corrections. I would also like to thank Bob Weaver for discussions, corrections, inductance calculation programs, and reference materials; Alex Pettit (KK4VB) for the long coil measurements discussed in the text; Dr Duncan Cadd (G0UTY) for the donation of a large PTFE-cored test coil; and Dr Richard Craven for discussions and for introducing me to the literature on folded helical resonators.

¹ Ottery St Mary, Devon, UK. website: <http://g3ynh.info/>
<http://orcid.org/0000-0003-0499-3938>

² Please check the author's website for updates and supplementary material.
<http://g3ynh.info/zdocs/magnetics/appendix/self-res.html>

© D. W. Knight, 2009 - 2016.

Contents

Abstract	1
Acknowledgements	1
1.0 The inductor modelling problem	3
1.1 Scattering experiment	8
1.2 Conductor length vs. SRF	12
1.3 Single-conductor transmission-line	14
1.4 Normal-mode antennas and Tesla coils	18
1.5 Helical resonators	20
1.6 Helical waveguide models overview	21
1.7 Velocity-factor for a finite free helix	23
Simple fringe-field correction	27
Decline of velocity factor with frequency	29
1.8 Velocity factor for an infinite free helix	30
Kandoian & Sichak	34
2.0 Self-capacitance	39
2.1 Propagation of uncertainty from SRF to self-capacitance	39
2.2 Self-capacitance derived from the conductor-length	41
3. Medhurst's formula	43
Repeat of Medhurst's data analysis	44
4. Coil-former dielectric	45
5. Empirically-corrected formula for self-capacitance	50
6. Inter-turn capacitance	53
7. Comparison of self-capacitance formulae	55
8. Tubular coil formers	60
9. Axial induced electric-field capacitance	62
Correction for internal dielectric	65
10. Velocity limiting	70
11. Free coil SRF calculation	77
Helical-line surge resistance	79
Uniform current surge resistance	80
Nominal VF - short coil limiting case	81
Nominal VF - Iterative solution	83
Pitch-angle correction	88
Long-coil correction	89
Coil former dielectric	91
Model properties, limitations and overall calculation procedure	95
12. Pseudo self-capacitance	98
13. Discussion and summary	101
Glossary	103
Revision history	105

1.0 The inductor modelling problem

Of the circuit theory elements: resistance, capacitance and inductance; the latter is the least amenable to realisation in practical devices. The reason is that the lumped-component theory depends on the assumption that every physical dimension is negligible in comparison to the operating wavelength. In a wound inductor, the difficulty lies with the length of the piece of wire inside it. Although that wire might be coiled-up in a small volume, its full length nevertheless dictates the inductor's high-frequency behaviour.

When a solenoid coil is operated in the regime in which wire length is negligible in comparison to wavelength, its partial inductance³ can be calculated with good accuracy from magnetic considerations alone. A straightforward basis for so doing is the hypothetical current-sheet inductor that, with corrections for realistic wire, allows the inductance of coils of small pitch-angle to be determined from physical parameters to an accuracy of around one part-per-thousand⁴. Magnetic theory must, of course, be respected in the asymptotic behaviour of any hypothesis that purports to describe inductors at high frequencies, and this has been a weakness in some of the more influential studies.

At audio and low-radio frequencies, the situation is complicated by the onset of the skin effect, and its companion, the proximity effect. The internal impedance of isolated wires is however fairly easy to calculate⁵; and the proximity effect, albeit more difficult to quantify, is nevertheless susceptible to attack^{6, 7}. We can also note that the redistribution of electric current that affects external inductance is physically constrained; i.e., the loop radius is always determined to a point that lies within the body of the conductor. Hence, with a little empiricism, we can push the inductor model into the radio-frequency range and still obtain respectable accuracy. More relevant to the present discussion however, we can envisage the existence of data corrected for minor non-idealities, which frees us from distractions when looking to higher frequencies still.

As the lumped element theory would have it: corrected for strays and losses (and better-still also corrected for the effects of non-uniform current distribution over the wire cross section); the reactance of a coil looks like the reactance of a pure inductance in parallel with a capacitance. This so-called self-capacitance is often attributed to capacitances presumed to exist between adjacent turns; and although that is partly true for multi-layer coils and flat spirals, the hypothesis turns out to be a hopeless predictor of the reactance of single-layer high-Q solenoids.

The lumped element approach also fails to give the correct impedance in the vicinity of the principal self-resonance frequency (the SRF⁸), a difficulty that gives rise to inaccuracies in circuit simulation. A possible solution lies in recognising that the coil is a transmission-line; although the line in question turns out to be a rather complicated one.

Even for resistors and capacitors, the lumped approximation is just a special limiting case of transmission-line theory. It is just that those components can generally be made small in comparison to wavelength; and when they do become large, the distributed parameter models remain fairly simple. Not so for the inductor; a device in which different regions of the line overlap, giving rise to hybridisation between what would otherwise be distinct propagation processes.

3 i.e., its theoretical inductance prior to adding connecting wires and closing the circuit.

4 See, for example: **Inductance Calculations: Working Formulas and Tables**, F. W. Grover, 1946, 1973. Dover Phoenix 2004, ISBN: 0-486-49577-9.

5 **Practical continuous functions for the internal impedance of solid cylindrical conductors**. D. W. Knight. DOI: 10.13140/RG.2.1.3865.1284 <https://www.researchgate.net/publication/301674351>

6 **Practical Model and Calculation of AC resistance of Long Solenoids**. E. Fraga, C Prados, and D.-X Chen. IEEE Transactions on Magnetics, Vol 34, No. 1. Jan 1998.

7 **Solid State Tesla Coil**. Gary L Johnson, 2001. Chapter 6. <http://ece.k-state.edu/people/faculty/gjohnson/> (accessed 18th March 2016)

8 There are actually numerous resonances. The SRF is usually taken to be the lowest parallel-resonance frequency of the disconnected coil.

If it were just a matter of replacing the expression for the reactance of a pure inductance in parallel with a pure capacitance with the expression for a short-circuited conventional line, then inductor modelling would present no serious challenge. Actual measurements remain anomalous when compared against either model however; an issue that came to this author's attention some years ago while investigating and attempting to predict the behaviour of broadband current transformers.

The lumped component and the simple transmission-line models agree over a fairly wide frequency range. Hence there is a correspondence between self-capacitance and time delay, which might be exploited in the modelling of phase-sensitive circuits. In the interests of predicting self-capacitance therefore (and in view of what appeared to be the consensus in this matter) attention was turned to the classic 1947 work of R G Medhurst⁹, which offers a widely used empirical formula for solenoids that can, in principle, be adapted to deal with toroids and other shapes.

It soon became apparent that Medhurst's formula was not good enough for the task in hand. It is clearly on the right track, because it gives results that are accurate within about $\pm 75\%$; but, for coil length-to-diameter ratios of >1 , a fair degree of accuracy can be obtained by accounting for static stray capacitance and otherwise assuming that waves propagate along the coil wire with a phase velocity equal to that of light in the surrounding medium ($v_p = c$ if the medium is air). The latter approach incidentally, does not agree with helical transmission-line models (for reasons that will be explained later); but it definitely works. Instead of abandoning Medhurst however; an attempt was made to find the cause of the errors. That investigation, reported in this article, results in a formula that brings the uncertainty in estimating the self-capacitance of typical RF inductors to a more respectable $\pm 2\%$.

It was actually the business of acquiring self-capacitance data, rather than that of predicting it, that produced the greatest difficulty. Measurements, for want of exotic test equipment at the time, were made using the ancient but venerable resonance method of G W O Howe¹⁰. This involves resonating the test coil against a series of known capacitances, then fitting the data to a regression line. If we take, for the purpose of illustration, the simple case where the Q is sufficiently high to permit the neglect of losses, the parallel resonance formula reduces to:

$$(2\pi f_0)^2 = \frac{1}{L(C_L + C_{\text{ref}})}$$

Where C_L is the self-capacitance, and C_{ref} is the added parallel capacitance including all strays. Rearranging gives:

$$C_{\text{ref}} = -C_L + \frac{1}{(2\pi f_0)^2 L} \quad (1.1)$$

which, insofar as the lumped component representation is valid, is a straight-line graph of the form $y = a + xb$. Hence, if $1/(2\pi f_0)^2$ is chosen as x , a linear regression procedure returns the slope $1/L$ and the y-axis intercept $-C_L$.

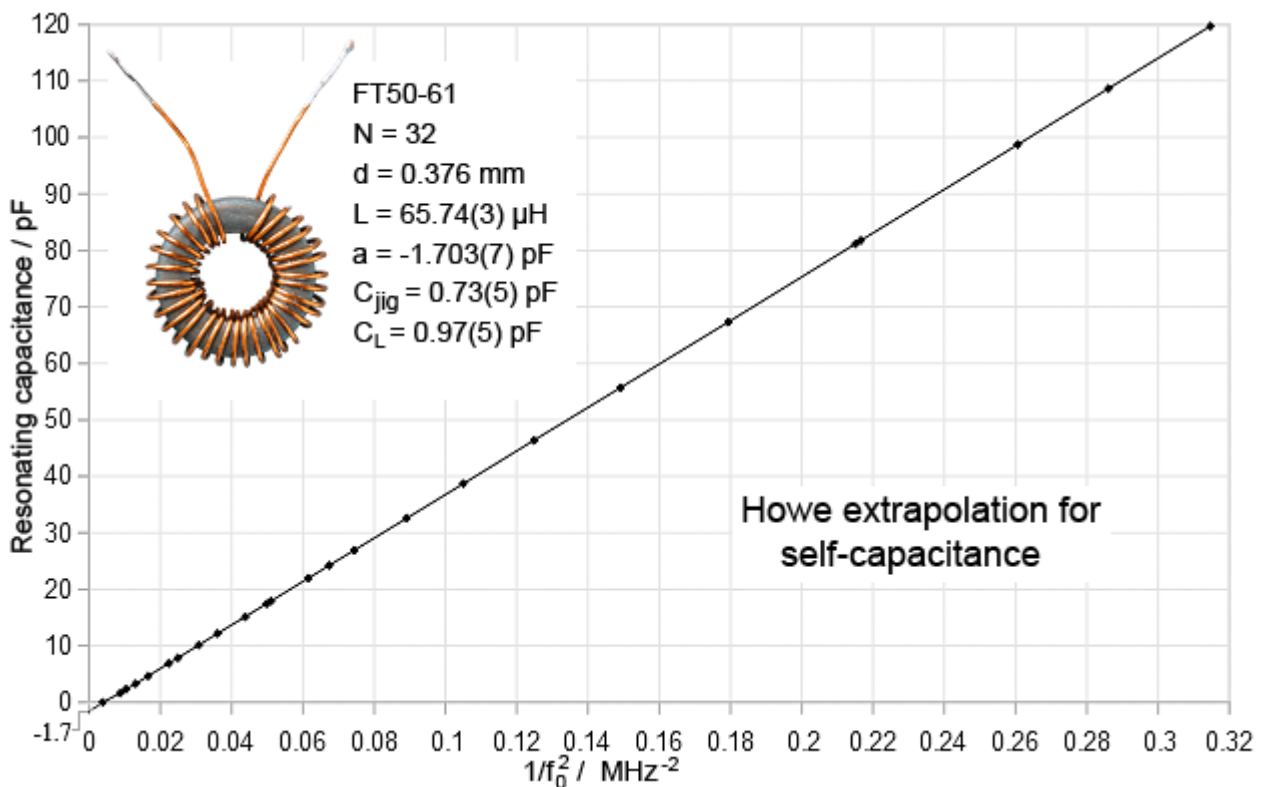
Medhurst's measurements were made using a variant of Howe's method, but there is no effective difference. For a given test coil, he acquired data using reference capacitances considerably greater than C_L . That amounts to shooting at the graph intercept from a distance; and although the measurements were performed with great care, the limited perspective precludes discovery of deviations from the model in the vicinity of the SRF.

For the measurements made by this author, data were taken over a wide frequency range:

9 **H. F. Resistance and Self-Capacitance of Single-Layer Solenoids.** R G Medhurst (GEC Research Labs.). *Wireless Engineer*, Feb. 1947 p35-43, Mar. 1947 p80-92. Corresp. June 1947 p185, Sept. 1947 p281. [Medhurst 1947]
10 **The calibration of wave meters for radio-telegraphy.** G W O Howe. *Proc. Phys. Soc.* 1911, Vol 24, p251-259.

generally at least three and sometimes as many as six octaves for each test coil. A method was developed using a set of pre-calibrated plug-in mica reference capacitors¹¹, and a simple jig with a stray capacitance of only 0.73 pF was constructed on the back of a BNC socket¹². The small jig capacitance meant that, for most of the coils, measurements at the high end of the frequency range involved external capacitances of less than C_L . The results turned out to have both explicable and, initially, inexplicable deviations from linearity.

One feature of the datasets covering sufficient range was the dispersion due to skin and proximity effects. This however, in cases where it caused statistically-significant deviations, could be corrected-for using well known methods. Hence, in the discussion to follow, we will concern ourselves only with what remains after that correction¹³, if it is actually needed.



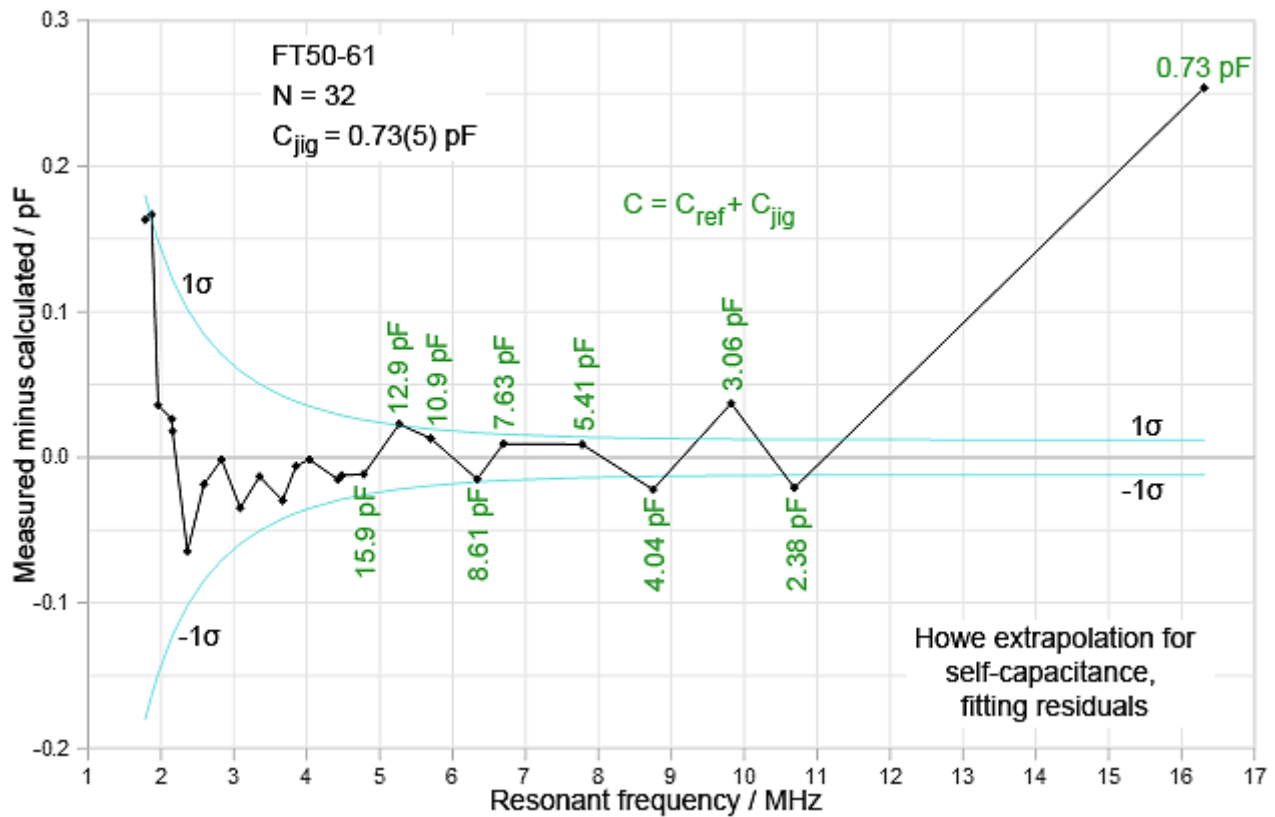
Self-capacitance determination using Howe's method: In this example¹⁴, the coil is a 32 turn toroid wound on a Fair-rite ½" type 61 ferrite bead. The graph of reference capacitance vs. $1/f_0^2$ is a convincing straight line, with a y-axis intercept, $a = -1.703 \pm 0.007$ pF. This value however, also contains the jig capacitance (0.73 ± 0.05 pF), and so the actual coil self-capacitance is 0.97 ± 0.05 pF. Note however, that a toroid has an additional static capacitance beyond the solenoid-like self-capacitance, because the ends are close together. This gap capacitance was estimated to be 0.5 ± 0.05 pF, and so the solenoid-like self-capacitance component for this coil is 0.47 ± 0.07 pF. There is more interesting information however in the statistical analysis (next graph).

11 **Capacitor standardisation using a reference inductor.** D W Knight. (Method description and data analysis). Available from <http://g3ynh.info/zdocs/magnetics/appendix/refcoil.html>

12 **Self-capacitance of toroidal inductors.** D W Knight. (Method description and data analysis). Available from www.g3ynh.info/zdocs/magnetics/

13 We can also usually neglect the internal inductance correction for thick-wire coils, because the dispersion occurs at low frequency; and we can approximate the proximity-effect correction on external inductance for thick-wire coils by calculating the inductance using the internal diameter of the coil.

14 See worksheet **F61-32T.ods**, downloadable from <http://g3ynh.info/zdocs/magnetics/appendix/self-res.html>



Fitting residuals for a 3-octave extrapolation: This graph shows the scatter of residuals (measured minus calculated capacitance) for the preceding self-capacitance determination. Also shown are the one-standard-deviation limits ($\pm 1\sigma$) for an observation. These are obtained by using a realistic error function for the reference-capacitor standardisation and adjusting it slightly to give a variance of fit (reduced χ^2) close to 1. If the model is realistic, the data should be normally distributed over the $\pm 1\sigma$ bound, with a 68% probability of being inside it. The capacitors were standardised to about $\pm 0.15\% \pm 0.012 \text{ pF}$, and so for the largest values, the absolute uncertainty is $>0.1 \text{ pF}$ and the scatter is large. In the 2½ to 10 MHz region however, the scatter has settled down, and we see a slight (but not statistically significant) upward curvature due to falling internal inductance (onset of the skin-effect). When no reference capacitor is connected however, all we have is the jig capacitance (here $0.73 \pm 0.5 \text{ pF}$). In that case the data point does not lie close to the regression line and has to be excluded from the fit. The 'self-capacitance' appears to have mysteriously diminished by 0.25 pF at that point. All solenoids and toroids measured by the author exhibited this type of deviation for shunt capacitances comparable to the extrapolated self-capacitance.

If a coil behaves as a conventional short-circuited transmission line, we should see a low frequency agreement between the data and the lumped component model, but disagreement elsewhere. Experimentally however, what is seen is an agreement over a wide range, but with a pronounced deviation on approaching the SRF. If, out of sentimental attachment to the lumped-element theory, we say that the inductance is constant, then it appears that the self-capacitance starts to decline when the external capacitance is reduced to the point at which it becomes comparable to the self-capacitance. It is as though there is a component of capacitance or inductance that only comes into existence when a shunt impedance is connected to the coil.

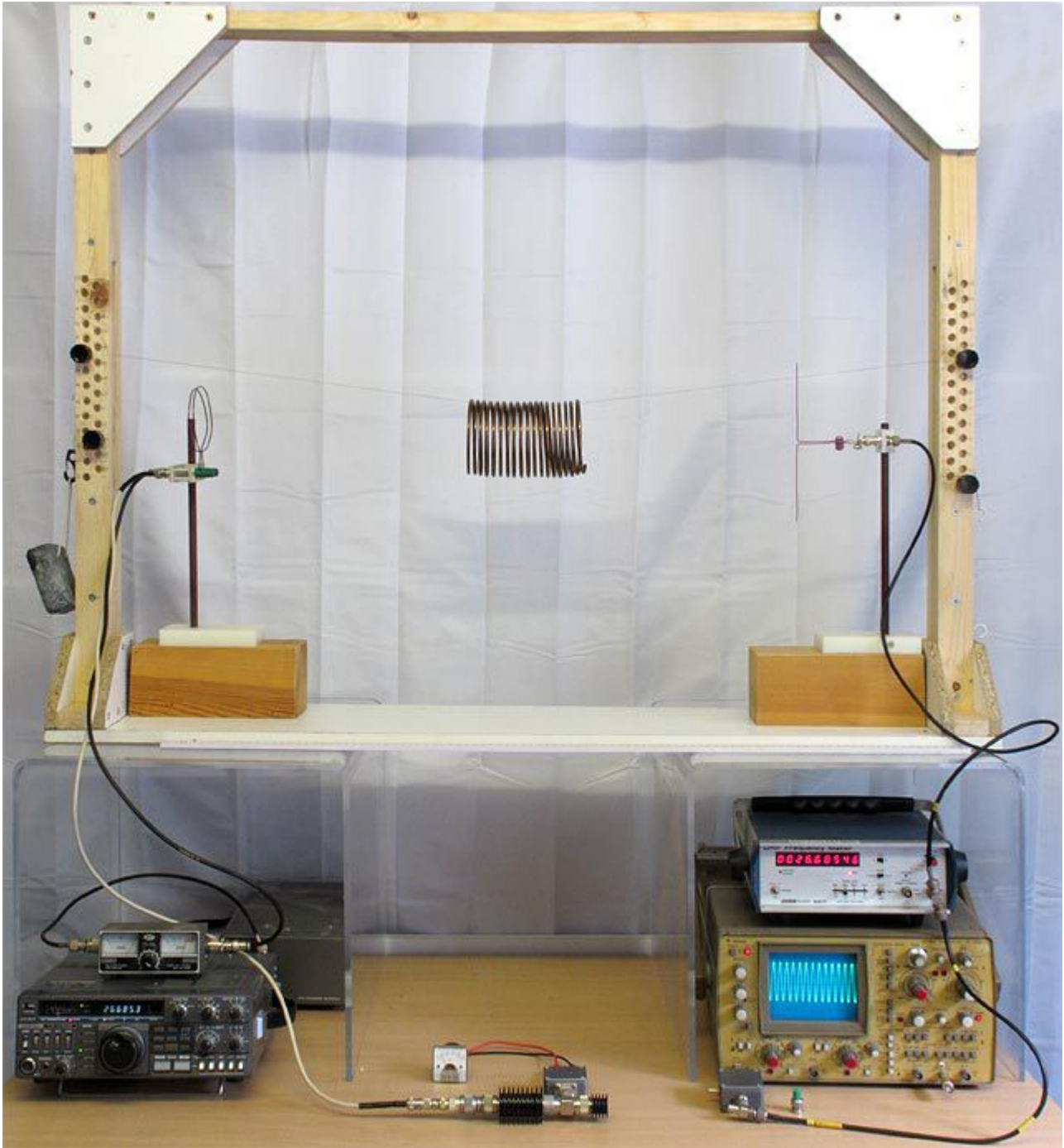
One way to look at what might be happening is to note that, with a large resonating capacitance connected, the current distribution along the length of the coil wire is relatively uniform. With a small external capacitance (or no capacitance) however, there will be current nodes associated with the ends of the wire, and the current distribution will have its peak half-way along the coil.

Inductance is a dynamic phenomenon, it doesn't exist in the absence of current, and so as the current distribution becomes non-uniform, some inductance must disappear. Thus the extrapolated SRF will increase as the resonating capacitances get smaller. This idea is corroborated, to some extent, by the observation that the deviation is greater for long coils than it is for short coils. This can be expected because the induced voltage across the ends of a short coil will give rise to an end-to-end capacitance, which will help to maintain the current as external capacitance is removed. While an explanation based on declining inductance might be useful however, it nevertheless assumes lumped-element LC parallel resonance, and this cannot account for the fact that there is a strong relationship between the SRF and the conductor length.

Theoretical difficulties aside, a problem with the ill-behaved resonance data is that it looks like an artefact. Specifically, it looks like a calibration problem associated with the jig strays and the smaller reference capacitors. No amount of careful recalibration would make it go away however; and so for some time the only viable solution was to exclude the deviant data points from the analysis by setting their fitting weights to zero. Still thinking that it was a systematic error, this led the author to try measuring the SRF of coils without connecting them to a test jig.

1.1 Scattering experiment

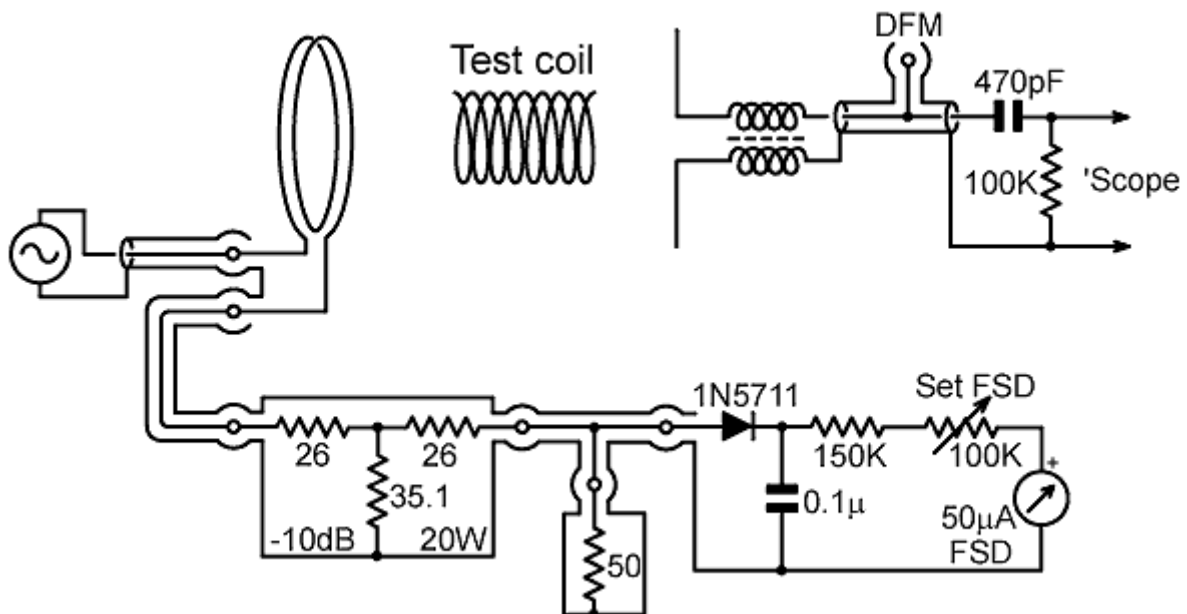
For solenoid measurements, a solution to what was thought at the time to be a calibration issue was to scatter radiation from isolated coils and detect the resultant field using a small loop or an electrometer dipole connected to an oscilloscope. An experiment using a high-powered signal source is shown in the photograph below. In that case the generator is an HF radio transmitter modified to give continuous coverage from 1.6 MHz to 30 MHz, and the induction coil is a 2-turn loop of about 90 mm diameter made from stiff wire.



In the configuration shown, a coil of copper tubing is suspended from a length of multi-strand Dyneema¹⁵ fishing line, which is tensioned by means of a lead weight. The arrangement places a negligible amount of dielectric material inside the coil, which is therefore effectively suspended in mid air. The supporting frame, antenna stands, etc., are also constructed from non-conducting materials wherever possible, to minimise eddy currents, and the coil is kept well clear of the electronic test equipment.

Of course, the coil is not strictly isolated from its environment, because it is in the near (induction) field of the radio transmitter. It is however, sufficiently isolated that the positioning of antennas and test equipment has little effect on the resonant frequency. Note also that the term 'scattering' refers to the scattering of radiation by the coil. It does not refer to the measurement of S (scattering) parameters (although an S_{21} transmission measurement using the two antennas is a very good way of finding resonances).

The electrical configuration is shown in the diagram below. Notice that the generator passes current through the induction loop to a coaxial load resistor; the point being to maintain a reasonable impedance match and thereby avoid provoking the transmitter's protection circuitry. Thus, although the power delivered to the load is in the 2 W to 10 W range, the actual radiated power is somewhat less than 100 μ W. Also observe that the arrangement constitutes a low-k transformer (and the distance between the loop and any point on the test coil is much less than one wavelength). The response of the diode detector monitoring the transmitter output is proportional to the input current. The balun on the pick-up antenna is 4-turns bifilar on a Fair-Rite FT50A-61 bead¹⁶, and the primitive high-pass filter before the oscilloscope helps to reject mains hum.



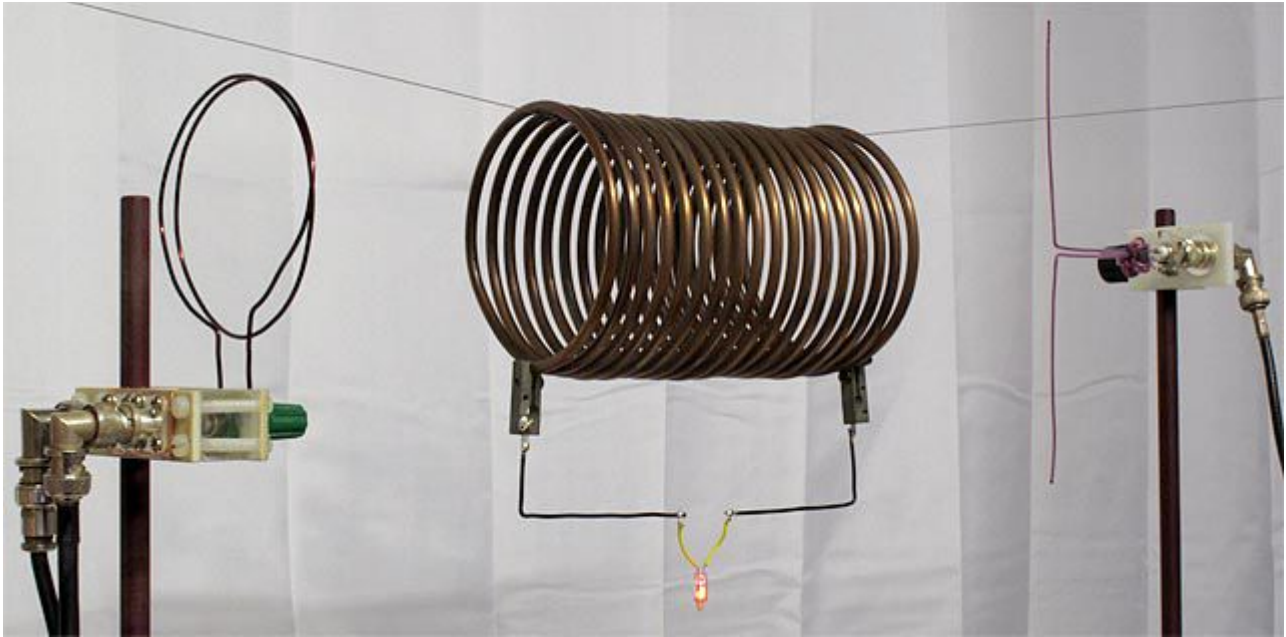
It takes several hundred microvolts at the oscilloscope input to produce a usable display, and so for the antenna separation shown (about 0.85 m) very little is seen in the absence of a test coil. With a coil in situ however; numerous scattering resonances can be detected (depending on the coil geometry and the available frequency coverage), some visible with the field sensor looking along the axis and some requiring it to be moved around to the side. One of the strongest resonances however is the fundamental SRF; which gives rise to an enormous increase in scattering cross-section, and a consequent sharp increase of several orders of magnitude in the received signal. Note that the detected signal is the superposition of incident and scattered waves, giving rise to

¹⁵ Gel-spun ultra-high molecular weight polyethylene (UHMwPE). The line shown is 0.43mm in diameter, and rated for a maximum load of 36 kg. 'Dyneema' is a registered trade mark of DSM. <http://www.dyneema.com/emea/>

¹⁶ <http://www.amidoncorp.com/specs/>

interference phenomena when investigating weak resonances; but the scattering signal at the SRF is so great that there is no ambiguity in finding the centre of the peak.

That this is a parallel resonance frequency is incidentally most easily demonstrated by connecting a neon bulb across the coil (see photograph below). A parallel LC network presents a high impedance at its terminals and so exhibits a high voltage when energised. Attaching wires to the coil, of course, shifts the resonance to lower frequency; but the shift is progressive, depending on the amount of stray capacitance and inductance added, and is not sufficiently great to confuse the assignment.



We now come to the principal observation; which is that the lowest parallel SRF of a disconnected coil occurs when the total length of wire is comparable to the free-space half-wavelength (just as it does with an end-fed wire antenna). This is most accurately true for coils with a length to diameter ratio in the 1 to 3 range. The data for the coil shown above (DWK 18T) serve to illustrate the point:

DWK 18T

Solenoid length:	$\ell = 152 \text{ mm}$
Average diameter :	$D_a = 96 \text{ mm}$ (= inside diam. + wire diam.)
length to diameter ratio:	$\ell / D_a = 1.583$
Number of turns:	$N = 18.09$
Wire (tubing) diameter:	$d = 4.7 \text{ mm}$
Winding pitch:	$p = \ell / N = 8.4 \text{ mm}$
Pitch to wire diam. ratio:	$p / d = 1.79$
Conductor length:	$\ell_w = \sqrt{(\pi D_a N)^2 + \ell^2} = 5.45793 \text{ m}$
SRF:	$f_{0s} = 26.69 \text{ MHz}$
Free-space half-wavelength:	$\lambda_0/2 = c/(2f_{0s}) = 5.61619 \text{ m}$
Apparent helical velocity factor:	$v_{hx} / c = 5.458 / 5.616 = 0.972$

From this, the principal resonance mechanism can be deduced. Waves travel along the helix and reflect from the impedance discontinuities that occur at the ends of the wire. The strong scattering resonance at the fundamental SRF corresponds to the standing-wave pattern that builds up when a single round trip brings the wave back to its starting point in phase with itself. The apparent average phase velocity moreover, despite interaction with the fields from adjacent turns and

possible end effects, is not greatly different from c for the shapes of coil found to give best Q in radio filter applications; which implies that the wave is intimately associated with the guiding wire, at least at the SRF¹⁷.

More information about the nature of the travelling wave can be had by using dipoles for both source and receiver; with cables brought straight-out at the back and choked-off with baluns. With the test coil removed, and an uncluttered working area, it can be shown that there is a minimum in the direct signal when the two dipoles are at right-angles. When the coil is introduced however, with its axis along the path between the antennas, there is no-longer a minimum when the dipoles are crossed, particularly on approaching and going above the SRF. Hence an observation that will come as no surprise to those who work with helical antennas¹⁸; which is that the coil converts linearly polarised radiation into circularly polarised radiation. By sampling the electric field while looking along the axis, we see an advancing wave with a rotating electric vector; i.e., the axial component of the propagating wave travels along the helix with its electric vector substantially perpendicular to the axis.

In truth, there is nothing novel or controversial about the scattering experiment as described so far. The association between self-resonance and wire length has been easily observable since the invention of the grid-dip oscillator (GDO) in the 1920s, it was known to both Howe and Medhurst, and was actually studied in detail by Paul Drude in 1902 (next section). There is also theory that can account for the observed velocity factors in disconnected coils, at least approximately. What is of interest is the way in which the information sheds light on the relationship between self-capacitance and the transmission-line resonance.

The scattering experiment shows that the principal SRF of air-cored solenoids occurs when the wire length is in the vicinity of $\lambda_0/2$. This is particularly true when the overall shape is chosen to give optimal Q . What Medhurst's study shows however, is that the $\lambda/2$ rule only applies when the coil is long and thin. Specifically, for the solenoid shapes typically used in radio applications (ℓ/D in the 1 to 2 range), the self-capacitance deduced from regression analysis predicts the SRF at a frequency that is too low in comparison to that of the disconnected coil. This does not imply, incidentally, that self capacitance is a useless conception. It is still the appropriate modelling parameter for conventional parallel LC resonators, because it correctly describes the circuit behaviour whenever the minimum padding capacitance is greater than C_L (which is usually the case). When parallel resonance data are acquired over a wide frequency range however; the points (as has been shown previously) are seen to veer away from the regression line at high frequencies as the shunt impedance is removed and the $\lambda/2$ wire-length resonance is approached.

17 Note however that there is a certain sleight of hand using the average coil diameter. We expect the current density to be greatest on the inside of the wire at high frequencies. If we use the inner diameter (91.3 mm) for the calculation, we get a conductor length of 5.191 m and a helical velocity factor of 0.924. The true value is somewhere between 0.924 and 0.972, but such subtleties make no difference to the resonance assignment.

18 **Antennas for all applications**, John D Kraus and Ronald J Marhefka, 3rd international edition 2003, McGraw-Hill. ISBN 0-07-123201-X. Chapter 8. The helical antenna, axial and other modes.

1.2 Conductor length vs. SRF

A systematic study of solenoid self-resonance was published by the German physicist Paul Drude¹⁹ in 1902. Drude made measurements on a large number of coils, both with and without coil formers, and collected data covering a wide range of length-to-diameter ratios. RF excitation of reasonably narrow bandwidth was achieved by means of an induction loop with a variable resonating capacitor, which was driven by an induction coil and a Tesla transformer with both primary and secondary spark gaps. Resonance was detected by holding an electrodeless low-pressure sodium-vapour discharge tube near to the coil. Accurate frequency measurement methods had not been developed at the time, but the operating wavelength of the exciter loop in each instance was determined to an accuracy of somewhat better than 1% by using a parallel-wire transmission line with a moveable shorting strap, resonance of the line being indicated by placing the discharge tube at the voltage anti-node.

Drude was able to characterise his coils in a surprisingly simple way by defining a function, f , as the ratio of the self-resonant half-wavelength to the wire length. He chose this definition because it gives $f=1$ for a straight piece of wire. The symbol f is nowadays always used to mean 'frequency' in an electrical context; but before we change it, note that in the previous section we have already defined 'apparent helical velocity factor' as the ratio $\ell_w/(\lambda_0/2)$. Drude's f is the reciprocal of that, which means that it is the apparent refractive index for a wave travelling along the helix. Hence we will use the symbol n_{hx} , defined as:

$$n_{\text{hx}} = \frac{\lambda_0}{2 \ell_w} = \text{apparent refractive index for helical propagation (Drude's } f\text{)}.$$

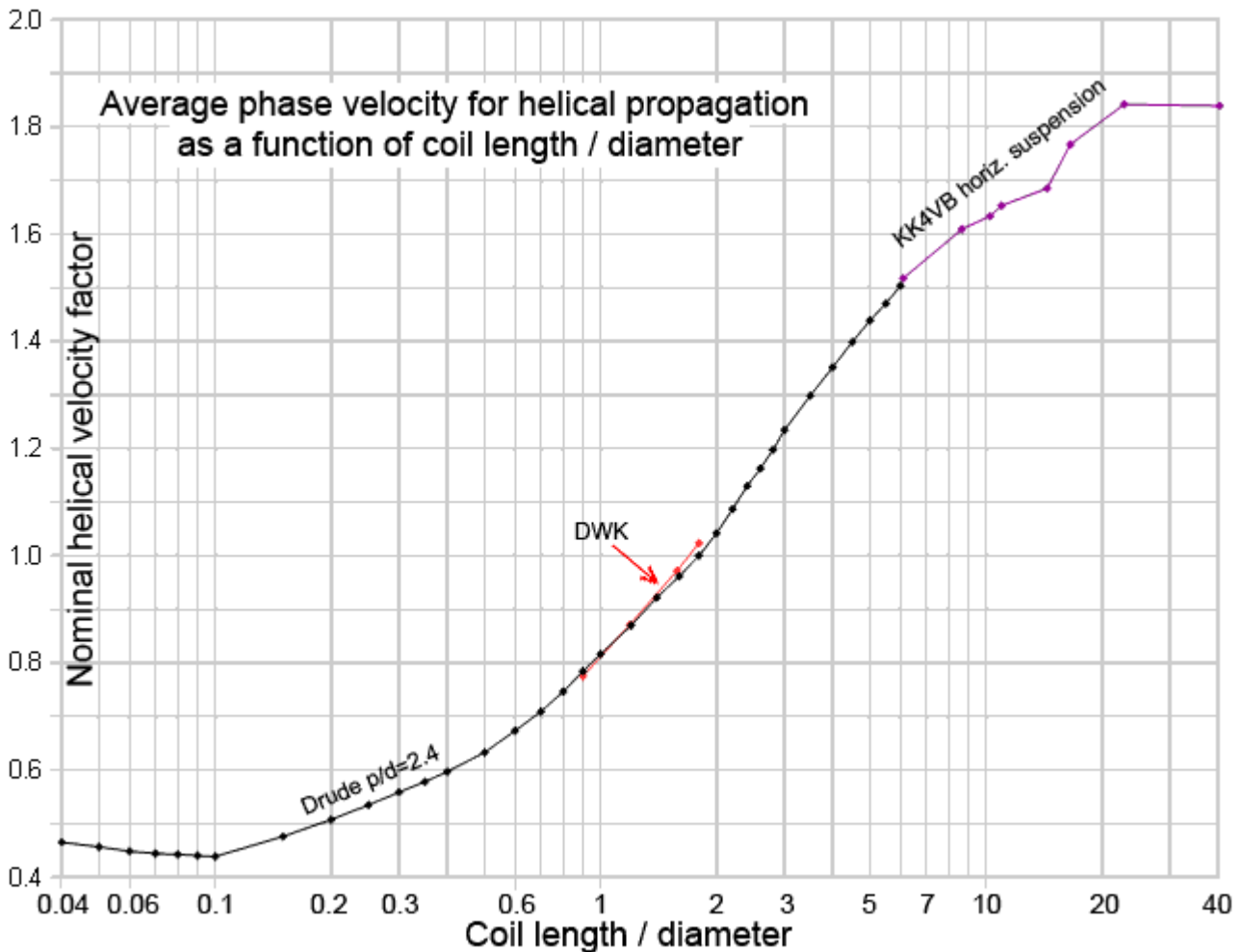
Note however, that Drude made no mention of the possible dynamics of wave propagation in coils, and was interested in explaining his results in terms of inductance and capacitance.

Drude's principal solid core materials were wood and ebonite (hard rubber), neither of which are of much interest to modern engineers. His coreless coils however were made by using twine to bind cotton-covered copper wire into helices, and for those he made series of measurements at three different pitch-to-diameter ratios. For the two smaller p/d ratios, the turns were compressed until they were held apart by the wire insulation, and in these cases, the self-resonant frequencies are reduced by the effect of the dielectric. For the largest p/d ratio however (2.4), there was enough space between the turns to render the dielectric effect fairly negligible. That the amount of dielectric present had little effect is demonstrated by the fact that some new measurements, made using the scattering method described in the previous section, agree very closely with Drude's data.

Drude recorded resonance data for his coils over a length/diameter range from 0.04 to 6. In addition to that, Alex Pettit (KK4VB) has made supplementary measurements²⁰ covering the range from 6 to 40, using an induction loop and an impedance analyser. The results are shown in the graph below, with the data plotted as nominal (i.e., apparent) helical velocity factors (i.e., $1/n_{\text{hx}}$, which is the reciprocal of Drude's f)

¹⁹ **Zur construction von Teslatransformatoren. Schwingungsdauer und Selbstinduction von Drahtspulen** (On the construction of Tesla transformers: Period of oscillation and self-inductance of the coil). P Drude, 1902, Ann. Phys. 314 (10) p293-339, 314 (11) p590-610. English translation by D W Knight and R S Weaver, 2015, available from: <https://www.researchgate.net/publication/301624796>

²⁰ http://g3ynh.info/zdocs/magnetics/appendix/kk4vb_srf.html



Apparent velocity factor for air-cored solenoids at the first SRF. Note that Drude, working in 1902, smoothed his data by sketching a curve between the scattered points and then reading the smoothed values back from the graph paper. This method is likely to introduce artefacts, and such is the most probable explanation for some obvious kinks in the curve. Alex's data (KK4VB) have not been smoothed and show experimental scatter (note that it is extremely difficult to make good measurements on very long or very short coils). The segment marked DWK relates to measurements made on self-supporting thick-wire coils, on the author's scattering jig, in order to confirm that Drude's $p/D = 2.4$ measurements are largely free from the dielectric effects.

The curve obtained has the appearance of a sigmoid with a long-coil limit possibly somewhere in the region of $v_{hx}=2c$. This is broadly consistent with (approximate) helical waveguide theories (see section 1.7) but it is *not* consistent with self-capacitance measurements which, as we will see, always show a long-coil asymptotic limit of $v_{hx}=c$. What we have found therefore is that coils measured open-circuit have an SRF much higher than that predicted by extrapolation measurements. This, of course, explains the discovery that data veer-away from the Howe-method regression line as the external capacitance becomes very small, the point being that the coil is crossing over from in-circuit to open-circuit behaviour. We will return to this matter in section 10.

1.3 Single-conductor transmission-line

In order to understand the transmission-line-like behaviour of coils, and also to reassure ourselves that it is consistent with (rather than contradictory to) the familiar lumped-element model; it is helpful to understand the relationship between the physical and electrical parameters of a conventional line and the equivalent parameters of a coil. It is also necessary to clarify the relationship between equivalent line-length and conductor length.

The input impedance of a lossless transmission line can be expressed as follows²¹:

$$\mathbf{Z} = \frac{R_0 [\mathbf{Z}_T + \mathbf{j} R_0 \tan(2\pi \ell_{TL}/\lambda)]}{[R_0 + \mathbf{j} \mathbf{Z}_T \tan(2\pi \ell_{TL}/\lambda)]}$$

Where R_0 is the characteristic resistance²², \mathbf{Z}_T is the impedance at the far-end of the line (the termination), ℓ_{TL} is the physical length of the line, and λ is the wavelength in the propagation medium provided by the line.

Now, if we terminate the line with a short-circuit, the terms involving \mathbf{Z}_T in both numerator and denominator vanish, and we are left with:

$$\mathbf{Z} = \mathbf{j} R_0 \tan\left(\frac{2\pi \ell_{TL}}{\lambda}\right)$$

which says that the shorted lossless line is purely reactive, with a reactance:

$$X = R_0 \tan\left(\frac{2\pi \ell_{TL}}{\lambda}\right)$$

Also, noting that 2π radians corresponds to 360° , and that the tangent of an angle is positive between 0° and 90° , we can see that X will be positive provided that ℓ_{TL}/λ is less than $1/4$, i.e.: when $0 < \ell_{TL} < \lambda/4$ the short-circuited line has an inductive reactance. Also; when $\ell_{TL} \rightarrow \lambda/4$, $X \rightarrow \infty$, i.e.; the line has a parallel-type self-resonance when its physical length is $\lambda/4$ (λ being the *electrical* wavelength, not necessarily the free-space wavelength). Thus the line and the coil are so far qualitatively similar, except that the lowest parallel SRF of the line occurs when its electrical length is $\lambda/4$, whereas the SRF of the coil occurs when the conductor length is $\lambda/2$. This little conundrum however immediately evaporates when we note that the line is a go-and-return circuit. In other words, the conductor length of a transmission line is twice its physical length, i.e.; $\ell_w = 2\ell_{TL}$. So now we can write the shorted transmission-line reactance as:

$$X = R_0 \tan\left(\frac{\pi \ell_w}{\lambda}\right) \dots\dots\dots (1.2)$$

so that when $\ell_w < \lambda/2$ the impedance presented at the terminals is inductive and when $\ell_w \rightarrow \lambda/2$, $X \rightarrow \infty$.

Notice, incidentally, that the quantity inside the tangent bracket is the electrical length of the transmission line in radians. Recall also that for small angles, the tangent converges with the angle, i.e., as $\theta \rightarrow 0$, $\tan\theta \rightarrow \theta$. Thus, since $\lambda = v_p/f$ (phase velocity / frequency), the reactance of the short-circuited transmission-line input at low frequencies becomes:

21 See for example: **Transmission lines for digital and communications networks**, R E Matlack, 1969, McGraw-Hill, LCCN 68-30561. p48, equation (2-77).

22 Generally called the 'characteristic impedance', but real for a lossless line and so referred to here as a 'resistance'.

$$X = 2\pi f \frac{R_0 \ell_{TL}}{v_p}$$

i.e., since the reactance is inductive:

$$X_L = 2\pi f \frac{R_0 \ell_w}{2v_p}$$

This has the same form as the lumped-element formula for inductive reactance; i.e., we find that:

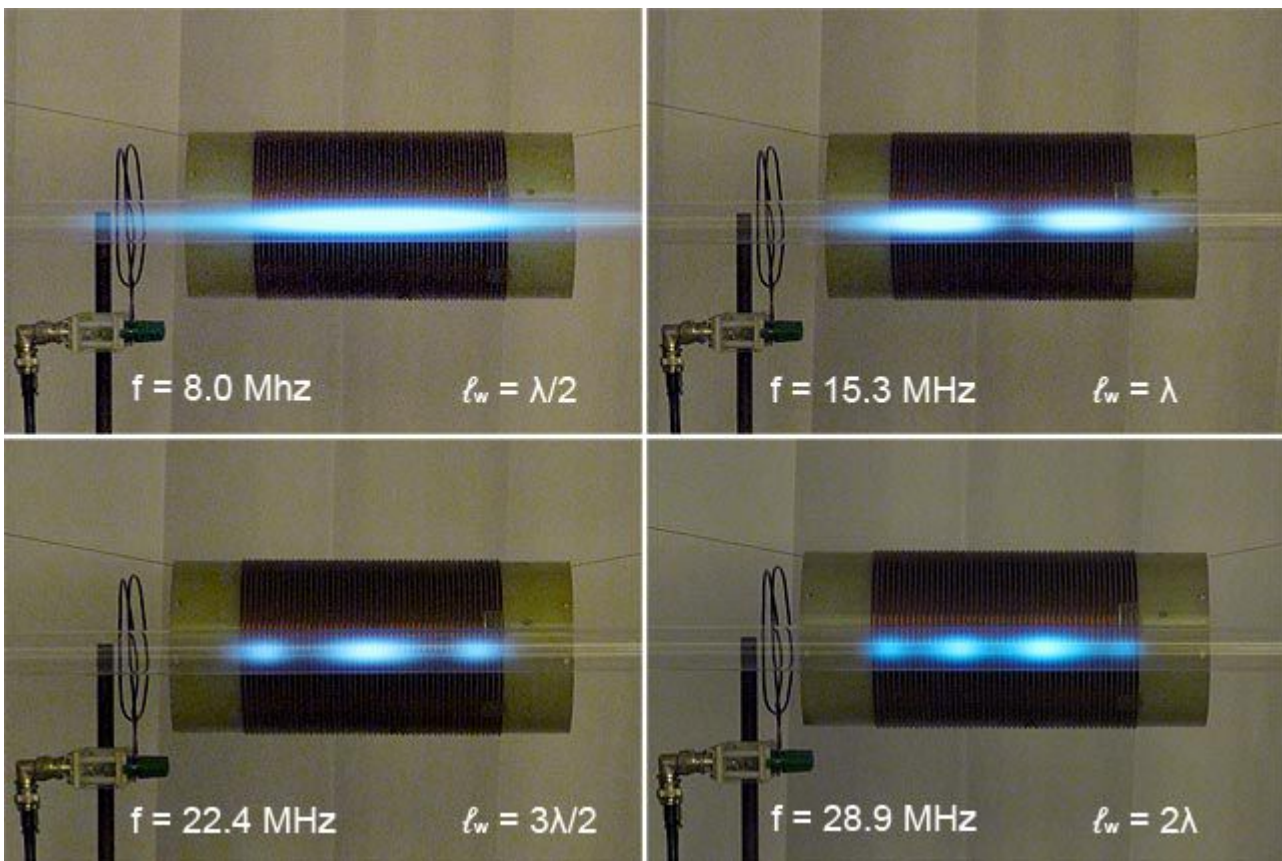
$$L = \frac{R_0 \ell_w}{2v_p} \tag{1.3}$$

Unfortunately, we must be circumspect about applying this relationship analytically because, according to widely accepted helical transmission line models, R_0 and v_p are frequency-dependent (the line is dispersive). It does show however that the inductance of a coil is related to the conductor length. Also, it might be the case that the theory that has been widely assumed to apply will prove to be in need of modification in the case of coils having a relatively uniform current distribution along the helix, in which event the simple formula above might prove to be useful in that special (but somewhat important) case. We will return to this matter in section **11**.

Those who have worked with VHF and UHF antennas will, of course, know that an adjustable length of short-circuited transmission line can be used as a variable inductor. Such a device is sometimes called a 'trombone', by analogy to the musical instrument. The trombone however, continues to be useful at frequencies above the $\lambda/4$ ($\ell_w = \lambda/2$) resonance, because its input reactance alternates between inductive and capacitive as the frequency is increased. A crossover occurs each time there is a resonance; and resonances occur at intervals of $\ell_w = m\lambda/2$ ($m = 1, 2, 3, \dots$), alternating between high input impedance (parallel type, m odd) and low input impedance (series type, m even).

The lumped-element representation of resonator as an inductance in parallel with a capacitance would have us believe that there is only one resonance when we use a wound inductor instead of a transmission-line stub. This idea is oddly persuasive, but it arises from a confusion between the idealised analytical circuit element and an actual practical coil. In fact, the only relationship between the two is that the inductive circuit-element can be used to represent a coil that is being operated well below its SRF. The coil, on the other hand, can always be represented as a transmission line, albeit in general a dispersive one; and qualitatively it exhibits the same series of resonances as a conventional line terminated by a short-circuit.

The standing-wave patterns that occur on a short-circuited transmission line should be familiar to anyone who has studied radio theory. A solenoid coil also exhibits a pattern of standing waves as we step through the sequence of $m\lambda/2$ resonances, and in the following set of photographs, these are made visible by using a strong excitation and placing a mercury-vapour gas discharge tube close to the coil. The electric field produced by the coil ionises the gas, and a changing pattern of voltage nodes is seen as m is increased.



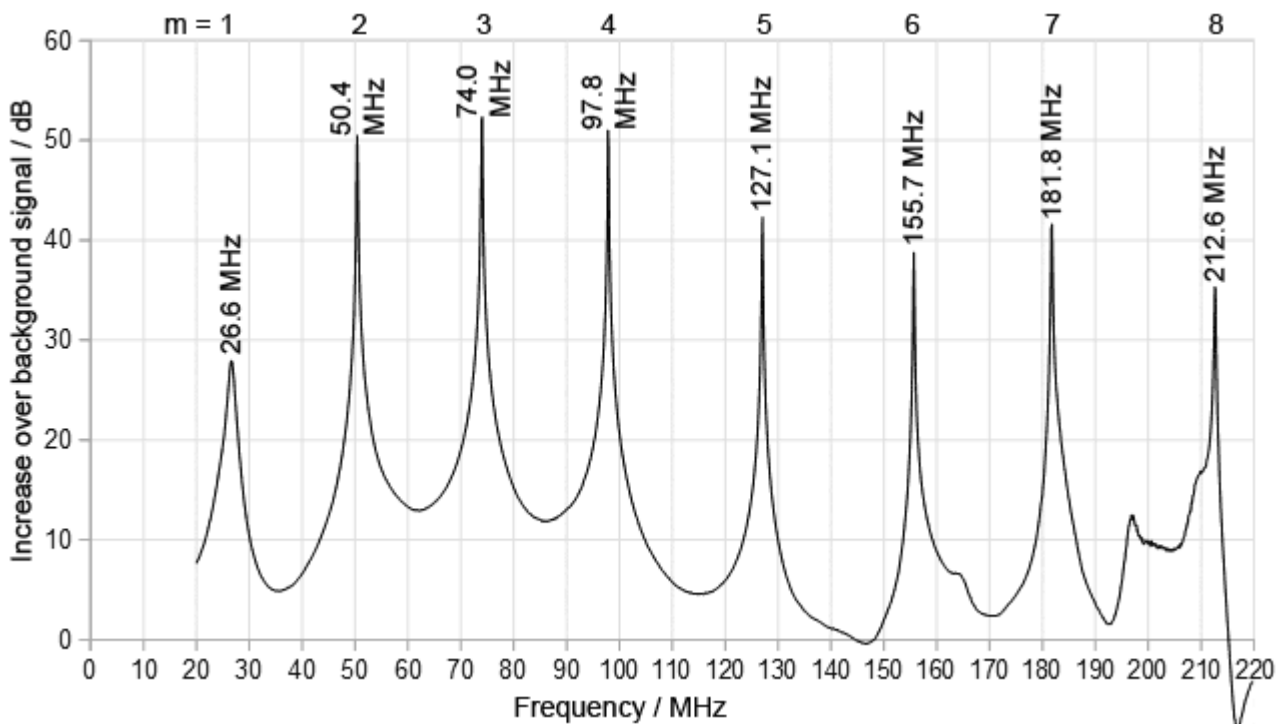
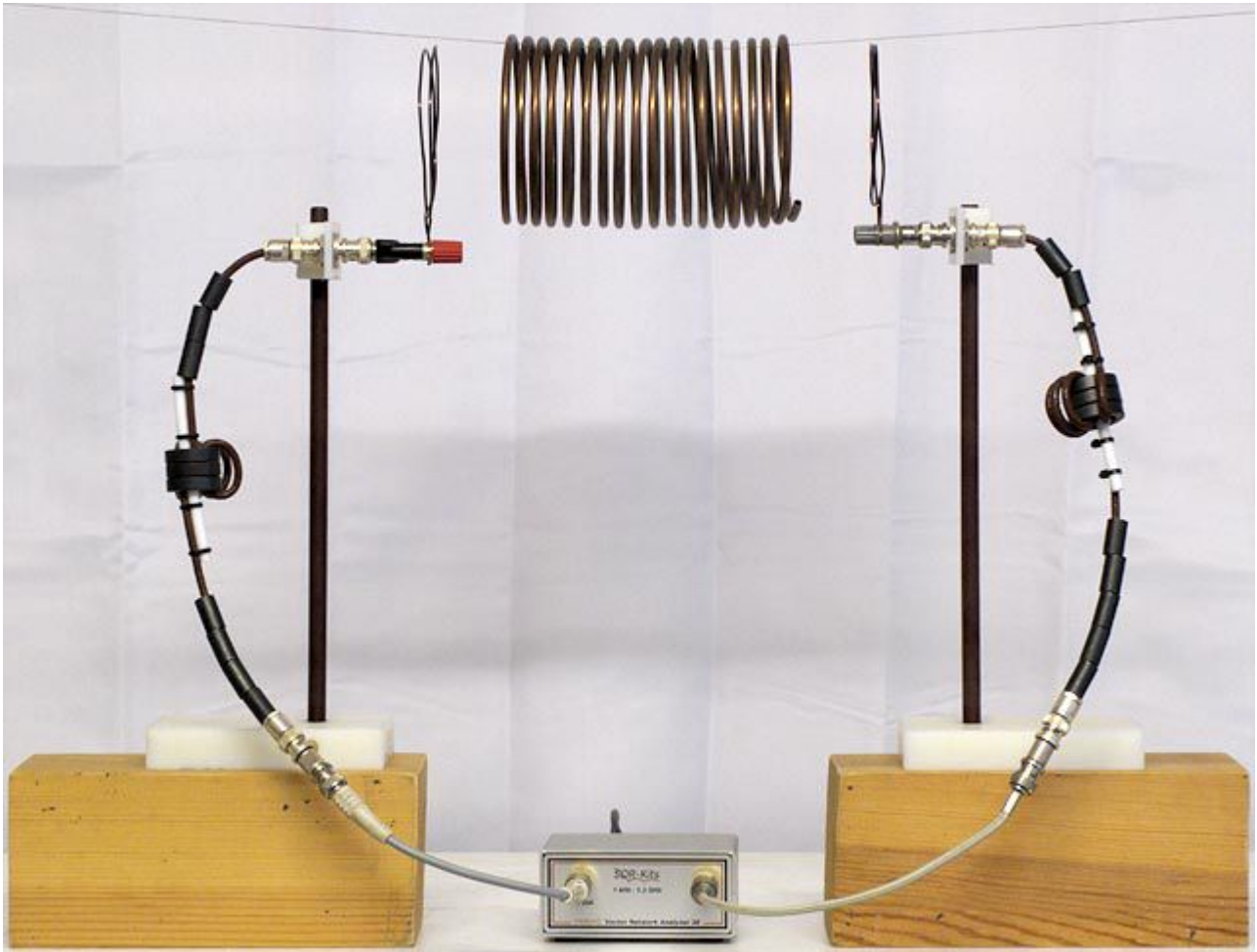
The node pattern is not obviously reminiscent of the textbook parallel-conductor-line discussion, but it takes a little mental juggling to see the analogy. Bear in mind that the gas discharge tube is mainly sampling the electric field strength of a wave that travels along the helical conductor with its electric vector almost perpendicular to the solenoid axis. Also, by viewing the coil side-on, we are essentially looking into the terminals of the equivalent parallel-conductor line (the terminals being the two ends of the coil).

At the fundamental SRF, a wave makes a single round-trip before it gets back into phase with itself. No cancellation occurs, and so we see the gas ionised all along the coil, with some sprawl at the ends due to fringe-field effects. At the higher-order resonance frequencies however, waves undergo one or more cycles on a go-and-return trip, the points of reversal are fixed at or near the ends, and we see the superposition of all waves that satisfy the imposed conditions. Hence there are points along the coil axis at which electric-field cancellation occurs (i.e., voltage nodes).

Note incidentally, that by saying that the coil is a dispersive transmission line, we mean that the velocity factor for wave propagation changes with frequency. This means that the high-order resonances do not occur at exact integer multiples of the fundamental SRF. Hence they are referred to as 'overtones' rather than 'harmonics'.

The illustrations on the following page show a transmission measurement obtained by placing a coil between two loop antennas connected to a network analyser²³. The coil is the large 18.1 turn copper-tubing solenoid discussed earlier (DWK 18T). The first eight $m\lambda/2$ conductor-length resonances can be seen on the interval between 20 MHz and 220 MHz.

²³ DG8SAQ VNWA3E. http://sdr-kits.net/VNWA3_Description.html.



$m\lambda/2$ conductor-length resonances (of coil DWK 18T). Resolution is 100 kHz (2000 data points spanning 200 MHz). The use of unun (common-mode) chokes in the lines to and from the network analyser reduces capacitive loading by the antennas and helps to minimise background artefacts (i.e., system resonances).

1.4 Normal-mode antennas and Tesla coils

The fundamental quarter-wave transmission-line resonance of the isolated coil is not the only type of quarter-wave resonance of which a helical conductor is capable. The other type of resonance occurs when the coil is mounted above an infinite ground plane. In that case, the conductor really is $\lambda/4$ in length (as opposed to $\lambda/2$ for the isolated coil) because the missing part is provided by the ground plane according to the 'ground reflection' or 'ground mirror' effect.

The resonant behaviour is illustrated by the inductively-loaded vertical antenna shown on the right. This antenna works from about 1.7 MHz to 2.5 MHz (in its fundamental resonance mode), its resonating capacitance (for a resistive input impedance at the base) being adjusted by means of a telescopic whip at the top. It falls into the category of extremely electrically short antennas (ca. 0.01λ), and so might be expected to be beyond the folkloric design principle that a normal-mode loaded-vertical is a quarter-wave antenna with part of its conductor wound around a stick. As the coil parameters illustrate however, its conductor length is very close to $\lambda_0/4$ in the 160m band, with an average velocity factor of 1.023, (assuming that the close turn-spacing forces the effective coil diameter to the inner diameter, and neglecting end effects). There is however, a considerable element of coincidence in this result, because the large length/diameter ratio (≈ 9.3) forces the velocity factor up (as we saw in section 1.2), but the fibre-glass coil former and the capacitance of the telescopic whip force it down.

The antenna is shown operating at 1.84 MHz, with a neon lamp soldered to the tip (only one terminal connected) and a 6W fluorescent tube mounted near the top of the coil by means of an acrylic clamp. The glow-discharges in the gas tubes demonstrate the voltage magnifying effect (the antenna works on the same principle as a Tesla coil²⁴). The coil parameters are given in the table below.



²⁴ **System of Transmission of Electrical Energy**, N Tesla, US Pat. No. 645 576, March 1900. p3, lines 58-64: "The length of the thin-wire coil . . . should be approximately one quarter of the wave length . . ."

Operating frequency:	1.84 MHz ($\lambda_0 = 162.9$ m)
Physical antenna height (adjusted for 1.84 MHz):	1.45 m
Solenoid length:	$\ell = 236$ mm
No. of turns:	$N = 507$
wire diameter:	$d = 0.45$ mm
Coil inner diam.:	25.4 mm
	$\ell/D = 9.29$ (based on inner diam.)
Coil conductor length at inner diam.:	$\ell_w = \sqrt{[(\pi DN)^2 + \ell^2]} = 40.46$ m
Total conductor length (assuming strong proximity effect):	$40.46 + 1.45 - 0.236 = 41.67$ m
Apparent average velocity factor:	1.023

The lowest self-resonance in the presence of a ground-plane occurs at approximately half the frequency of the parallel-resonant SRF. It cannot however be excited in the absence of a ground plane because it is the fundamental series self-resonance; i.e., a generator can only deliver energy to an impedance, and so a counterpoise is required to complete the circuit if the coil is to be series-driven. Note however, that it is possible to excite multiple-internal-reflection resonances at approximate sub-multiples of the SRF²⁵ (sometimes called sub-harmonics). One of these will be close to the lowest series resonance, but it will have a different field pattern.

The much misunderstood 'ground mirror' effect can incidentally be explained as the attainment of a limiting value when extending the transmission-line length. Using the scattering method of section 1.1 for example, it is easily shown that if a short length of wire is attached to one end of the coil, the resonant frequency drops. The frequency-shift occurs because the sharp impedance discontinuity (the reflection point) at the coil terminal is abolished and replaced by the discontinuity at the end of the wire. If progressively longer pieces of wire are added, the frequency continues to drop in a predictable manner ($v \approx c$), but the Q also diminishes as the added conductor becomes the principal resonator. When the added conductor length becomes comparable to the coil conductor-length however, the half-wave resonance of the total conductor becomes strong again and, of course, now peaks at around half the frequency of the isolated coil SRF. The now so-called quarter-wave resonance remains at this frequency if the length of the added conductor is further increased.

This transmission-line extension effect, although not identified as such, was observed by Drude in his 1902 study of coil resonance²⁶. He noted that when 'capacitance' is added to one end of an isolated coil, such as by the connection of a conducting sphere, the period of oscillation is increased but *'this increase is always smaller than twice the period of the coil with free ends'*.

²⁵ **Radio Frequency Transistors**. Norn Dye and Helge Granberg (Motorola). Butterworth-Heinemann 1993. ISBN 0-7506-9059-3. See p142

²⁶ **Drude 1902. On the construction of Tesla transformers**. Already cited in section 1.2. p337-338. Also, p 609, Summary of results, point no. 7.

1.5 Helical resonators

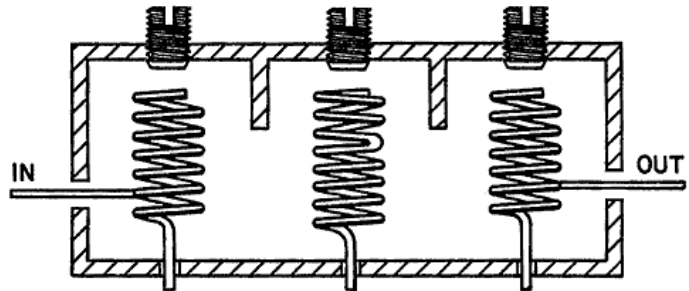
Another example of the use of solenoids in the series (ground-plane) self-resonant mode is given by the helical filter²⁷, a type of bandpass filter often used at VHF or UHF. Such filters consist of an array of coils, all grounded at one end and typically coupled by means of apertures in the shielding between them. In this configuration, and assuming that the resonator is a simple helix, the coils resonate when the conductor length is

$$\ell_w = (2m+1)\lambda/4, \quad m = 0, 1, 2, \dots$$

with the $m=0$ (i.e., $\lambda/4$) choice usually being preferred. λ of course refers to electrical wavelength, the relationship between it and free-space wavelength λ_0 being modified by the screening cavity and tuning arrangements.

What is interesting about the helical resonator for the present discussion is that it can be given a lumped-element representation for the purposes of simulation, but its behaviour can only be explained by treating it as a transmission line. In other words, it tells us that the lumped-element theory contains no information about the physics of the solenoid inductor.

The point is illustrated by the semi-diagrammatic drawing shown below, which is taken from Peter Vizmuller's patent for the folded helical resonator²⁸. A lumped-element model can be obtained notionally by resonating the coils using the capacitances to the cavity walls and adjusting screws, and by representing the coupling as a mixture of the mutual inductances between the parts of the coils carrying most current (the grounded ends) and the capacitances between the parts of the coils having the highest voltages relative to ground (the open-circuit ends). So far, so good, but now notice that the middle resonator has its winding-direction reversed part-way along its length. It is Vizmuller's discovery, and the basis of his invention, that the reversal, for a given total conductor length, makes practically no difference to the $\lambda/4$ resonance. The lumped-component theory however, would have us expecting that the large negative mutual inductance between the two sections would cancel much of the overall inductance of the coil and send the resonance to much higher frequency.



What actually happens in Vizmuller's folded resonator, is that the higher-order harmonic behaviour is altered. An important modification is obtained, for example, when the line-length ratio of the two sections is 3:1; i.e., the winding direction is reversed for $1/4$ of the total length. In that case, the $3\lambda/4$ resonance is suppressed (and replaced by a resonance at $4\times$ the fundamental). This makes the folded resonator useful (for example) for filtering the output of push-pull amplifiers (which cancel even-order harmonics, but produce an abundance of odd-order harmonics, especially the 3rd).

A study of Tesla transformers using the folded-helix topology has been carried out by Richard Craven²⁹.

27 **Filters with helical and folded helical resonators.** Peter Vizmuller. Artech House 1987, ISBN 0-89006-244-7.

28 **Folded-over helical resonator.** Peter Vizmuller (Motorola Inc.). US Pat. # 4422058, 1983.

29 **A study of secondary winding designs for the two-coil Tesla transformer,** Richard M Craven, PhD thesis, Loughborough University, 2014. <https://dspace.lboro.ac.uk/dspace-jspui/handle/2134/14375>

1.6 Helical waveguide models overview

A theoretical analysis that is generally assumed to come close to describing the high-frequency behaviour of solenoids is that given by Schelkunoff for the sheet-helix model first proposed in 1926 by Franz Ollendorff³⁰. Schelkunoff's extended derivation is outlined in J. R. Pierce's classic work on the travelling-wave tube^{31 32} and elsewhere^{33 34 35}. The theory has also been augmented to include the effects of inner and outer coaxial conducting cylinders^{36 37}; and Poritsky et al³⁸ perform a derivation including inner and outer Faraday shields and inner and outer magnetic cores.

A sheet-helix (also called a 'sheath helix') is notionally constructed by winding a helix with an infinitesimal conducting filament, then adding more identical filamentary helices in the gap between turns, parallel to the first, until the gap is completely filled. The filaments are connected together at the two ends of the winding. The resulting structure is essentially a current-sheet solenoid, except that the isolation of the filaments ensures that conduction can only take place in the helical direction.

The case of interest for the purpose of inductor modelling is that in which the circumference of the coil is small in comparison to wavelength, so that the field patterns are radially symmetric (the Kraus T_0 mode³⁹ or 'delay-line' mode). For coils of many turns, this model is still appropriate at frequencies well above the fundamental SRF. The system supports a hybrid of two modes for electromagnetic propagation: one being associated with a plane wave, the 'slow-wave', travelling along the coil axis; the other being associated with a wave travelling along the helical conductor. Note that the two waves are not physically distinguishable. The overall field pattern is given by their superposition. They represent two ways in which radiation can traverse the coil, and since they must always remain in lock-step, the ratio of their phase velocities is given by the conductor length per unit coil length.

Ramo et al. liken the propagation environment for the axial slow-wave (in an actual coil, rather than in a sheet-helix) to the situation within a disk-loaded waveguide⁴⁰. The wave passes a series of slits, each of which leads to a short-circuited transmission-line stub, the resulting inductive loading causing a reduction in phase velocity. The series of Hertzian loops let into the walls of the

-
- 30 **Die Grundlagen der Hochfrequenztechnik** [Foundations of high-frequency technology], Franz Ollendorff, Springer Verlag 1926. p79-87 **Das dynamische Feld der mehrwindigen Spule** [Dynamic field of multi-turn coils]. [Ollendorff 1926].
- 31 **Theory of the Beam-Type TWT**. J R Pierce. Proc. IRE. Feb. 1947. p111-123. See Appendix B, p121-123, "**Propagation of a wave along a helix**", which gives Schelkunoff's derivation of propagation parameters for the Ollendorff helix.
- 32 **Travelling Wave Tubes**. J R Pierce. Bell System Technical Journal [<http://bstj.bell-labs.com/>], 1950: 29(1) p1-59, 29(2) p189-250, 29(3) p390-460, 29(4) p608-671. See esp. Ch 3 (p20) and Appendix 2 (p56).
- 33 **RF Coils, Helical Resonators and Voltage Magnification by Coherent Spatial Modes**, K L and J F Corum, Microwave Review, Sept 2001 p36-45.
- 34 **Multiple Resonances in RF Coils and the Failure of Lumped Inductance Models**. K L Corum, P V Pesavento, J F Corum. 6th International Tesla Symposium 2006.
- 35 **Fields and Waves in Communication Electronics**. S Ramo, J R Whinnery and T Van Duzer. Wiley 1994. ISBN 0-471-58551-3. Section 9.8: The idealized helix and other slow-wave structures.
- 36 **Some wave properties of helical conductors**, J H Bryant, Elec. Comm. 31(1) 1954. Considers the free coil case and also the effects of inner and outer coaxial conducting cylinders.
- 37 **Coaxial Line with Helical Inner Conductor**. W Sichak. Proc. IRE. Aug. 1954. p1315-1319. Correction Feb. 1955, p148. Reprinted in: Electrical Communication 32(1), March 1955. p62-67.
- 38 **Field Theory of Wave Propagation ALong Coils**. H Poritsky, P A Abetti, R P Jerrard. Power Apparatus and Systems, Part III, Trans. of the AIEE. 72(2), Oct. 1953. p930-939.
- 39 **Antennas for all applications**, J D Kraus and R J Marhefka. 3rd edition, 2003, Mc Graw-Hill. ISBN 0-07-123201-X. Section 8.8, p251-252.
- 40 **Fields and Waves in Communication Electronics**. [cited earlier] Section 9.9: Surface guiding.

misnamed 'cavity' magnetron have an analogous effect^{41 42}. The additional complication in the solenoid lies in the varying relative dominance of the axial and helical processes.

The difficulty is that of finding an overall quantitative theory. The sheet-helix model is often assumed to be definitive because it underlies the invention of the TWT. It has also successfully explained why the voltage magnification that occurs in Tesla coils is much greater than the lumped-element approach predicts. Thus Sichak⁴³ and the Corum brothers⁴⁴ have been emphatic in stating that the model is general, and in particular that it can be applied in the lumped-element limit (i.e., by inserting the sheet-helix results for R_0 and v_{hx} into equation 1.3). There are some caveats however, and the output of models using the theory should be treated with caution.

The sheet-helix theory is a theory based on what happens in the middle region of an infinitely long solenoid. It lacks fringing-field corrections (cf. Nagaoka's coefficient) and so can only be argued to pass to the lumped theory for very long coils. Even then however, its accuracy for predicting inductance is poor in comparison to the conventional magnetic approach. This limitation must be at least partly attributed to artificial constraints inherent in the model. Hence corrections for the difference between the sheet-helix and an actual helical wire are needed, and these are not the same as the corrections used with the current-sheet model.

A further difficulty however is that the elevated helical phase-velocities associated with trading between the helical wave and the axial slow-wave might actually be absent in coils exchanging current with an external circuit. A velocity-limiting effect certainly occurs in helical lines having an outer coaxial shield (although slow-waves are still produced), and it might be that in-circuit and free-coil measurements differ for analogous reasons. If that is so, then the free-coil helical-waveguide approach will remain appropriate for open circuit systems (subject to short-coil corrections that have yet to be obtained), but it will not apply unmodified to the matter of self-capacitance. Much of this article will be concerned with these issues.

A more realistic helical transmission-line model, known as the 'tape helix', was introduced by Samuel Sensiper in 1951^{45 46}. This is similar to the sheet-helix (zero current perpendicular to the helix direction), but allows for an inter-turn gap and so produces additional (usually minor) terms to account for axial periodicity. With regard to velocity factors however, the results for the lowest axially-symmetric (delay-line) mode are generally similar to those of the sheet-helix. A general treatment of the tape helix, including the facility to model the presence of an external coaxial conducting cylinder, is given by Louis Stark⁴⁷.

The earliest theoretical study of wave propagation on helical conductors, based on a single perfectly conducting filament, was published by H C Pocklington⁴⁸ in 1897. Approximate solutions predicted that the phase velocity of the axial wave would approach c at low frequencies, and the helical velocity would fall to c at high frequencies. Thus Pocklington appears to have established the basic physical situation, but the later sheet and tape-helix models are considered to be more accurate.

41 **The Magnetron as a Generator of Centimeter Waves**. J B Fisk, H D Hagstrum, P L Hartman. Bell System Technical Journal. Vol. 25(2), April 1946. See fig. 22.

42 **Technical and Military Imperatives: A Radar History of World War II**. Louis Brown. 1999. Taylor and Francis. ISBN13: 978-0-7503-0659-1. See Ch. 4. Resonant Magnetron: p153, p409.

43 **Sichak 1955** (cited above). Page 1317 in Proc. IRE or p64 in Elec. Comm. "The standard formula for the inductance of a long solenoid can be obtained by treating the solenoid as a short length of short-circuited line and using [the sheet-helix expressions for characteristic impedance and phase velocity]."

44 **Corum & Corum, 2001** (cited above). Passage to lumped elements, p41.

45 **EM Wave Propagation on Helical Conductors**, S Sensiper, Tech. Report No. 194, May 1951, MIT Research Lab. of Electronics. <http://dspace.mit.edu/bitstream/handle/1721.1/4865/RLE-TR-194-04734124.pdf>

46 **Electromagnetic Wave Propagation on Helical Structures (a Review and Survey of Recent Progress)**, Samuel Sensiper, Proc. IRE, Vol. 43 (Feb. 1955) p149-161.

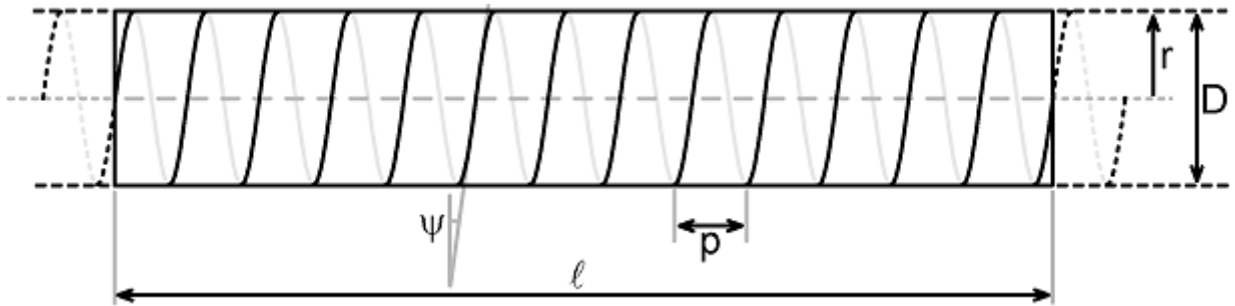
47 **Lower modes of a concentric line having a helical inner conductor**. L Stark, J. Appl. Phys. 25(9), 1954. p1155-1162.

48 **Electrical oscillations in wires**, H C Pocklington, Proc. Camb. Phil. Soc. (9), jct. 1897, p324-332.

1.7 Velocity-factor for a finite free helix

Despite the large number of papers on helical-waveguide theory, one of the best ways to get acquainted with the subject in relation to RF inductors is via Ollendorff's original derivation⁴⁹. The reason is that much of the later commentary is concerned with travelling-wave tubes and helically-wound coaxial cables, in which case, the primary interest is satisfied by considering an infinitely long coil. Ollendorff, on the other hand, defined the problem using an infinitely long coil, but then adapted it by considering a section of the coil of length ℓ . This gives a considerable simplification in applying the method to practical inductors; but it means that the model has no fringe-fields and therefore cannot provide an accurate description of coils of small ℓ/D ratio. Further simplification is also necessary in order to make the problem mathematically tractable. This is obtained by defining the winding as a perfectly conducting current-sheet (no gap fields, no losses), and by constraining the current to flow only in the direction of the helix (no current density perpendicular to the helix direction). Only the radially-symmetric (T_0 or 'delay-line') mode is considered, i.e., it is assumed that the circumference of the solenoid is small in comparison to wavelength.

The helix parameters are defined in the illustration below (the notation used in this article is not the same as Ollendorff's).



The various resonant frequencies of a length of transmission line can, of course, be calculated from the physical dimensions and an appropriate velocity factor. In this case however, the velocity factor for axial propagation turns out to be a function of frequency (the transmission line is found to be dispersive) and so instead of solving for it directly, Ollendorff produced an expression for finding the sequence of overtone resonances.

$$\frac{2\pi f}{c} = \sqrt{\frac{J_0(\mathbf{j}x) H_0^{(1)}(\mathbf{j}x)}{J_1(\mathbf{j}x) H_1^{(1)}(\mathbf{j}x)}} \frac{2m\pi}{2\ell} \frac{p}{2\pi r}, \quad m = 1, 2, 3, \dots \quad (1.4)$$

where $x = m\frac{\pi}{2} \frac{D}{\ell}$, and m is the overtone number (putting $m=1$ corresponds to the first SRF).

The quantities within the square root are Bessel (J_n) and Hankel (H_n) functions of the first kind of zero and first order, with purely imaginary arguments. This square-root of a combination of Bessel functions crops up in all subsequent derivations of helix waveguide properties, including the small pitch-angle limiting case of Sensiper's tape helix, and so we will give it the symbol $W(x)$ and refer to it as 'Ollendorff's function'. Also note that, while some commentators persist in writing it as above, it is a real quantity and can be converted to a function of a real argument by using standard Bessel function identities:

⁴⁹ Ollendorff 1926, already cited. For a rough working translation of the article 'The dynamic field of multi-turn coils', contact the author (see title page of this article).

$$J_0(\mathbf{j}x) = I_0(x) \quad (\text{Dwight}^{50} \text{ p195, 813.1})$$

$$J_1(\mathbf{j}x) = \mathbf{j} I_1(x) \quad (\text{Dwight p195, 813.2})$$

$$H_0^{(1)}(\mathbf{j}x) = -\mathbf{j} \frac{2}{\pi} K_0(x) \quad (\text{Dwight p197, 817.2})$$

$$H_1^{(1)}(\mathbf{j}x) = -\frac{2}{\pi} K_1(x) \quad (\text{Dwight p197, 817.5})$$

Where I_n and K_n are modified Bessel functions of the first and second kind. Thus, noting the cancellations that occur, and that $\mathbf{j}^2 = -1$:

$$W(x) = \sqrt{\frac{J_0(\mathbf{j}x) H_0^{(1)}(\mathbf{j}x)}{J_1(\mathbf{j}x) H_1^{(1)}(\mathbf{j}x)}} = \sqrt{\frac{I_0(x) K_0(x)}{I_1(x) K_1(x)}} \quad \text{Ollendorff's function} \quad (1.5)$$

The modified Bessel functions are built-in functions in spreadsheets such as Open Office.

Now recalling that $c = f \lambda_0$, we can write equation (1.4) as:

$$\frac{2\pi}{\lambda_0} = W(x) \frac{2\pi m}{2\ell} \frac{p}{2\pi r} \quad (1.6)$$

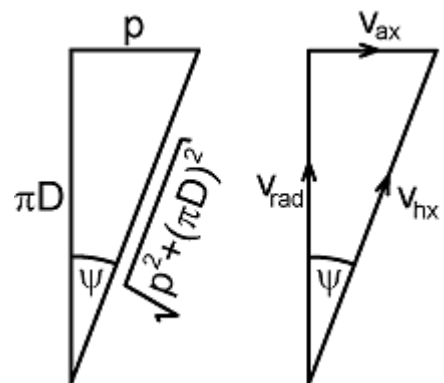
but notice that $2\ell/m$ is the axial wavelength of the standing-wave at resonance; and this being an electrical wavelength, is related to the axial phase velocity via $v_{ax} = f \lambda_{ax}$. Thus:

$$\frac{2\ell}{m \lambda_0} = \frac{\lambda_{ax}}{\lambda_0} = \frac{v_{ax}}{c} = W(x) \frac{p}{2\pi r} \quad \text{Axial velocity factor.} \quad (1.7)$$

Also notice however that $p/2\pi r = p/\pi D = \tan \psi$, where ψ is the pitch angle; and recall that $\tan \psi = \sin \psi / \cos \psi$. Thus we can write:

$$\frac{v_{ax}}{c} \cdot \frac{1}{\sin \psi} = W(x) \frac{1}{\cos \psi}$$

Now referring to the diagram on the right, and noting that the axial and helical propagation processes constitute a single hybrid mode, it can be seen that:



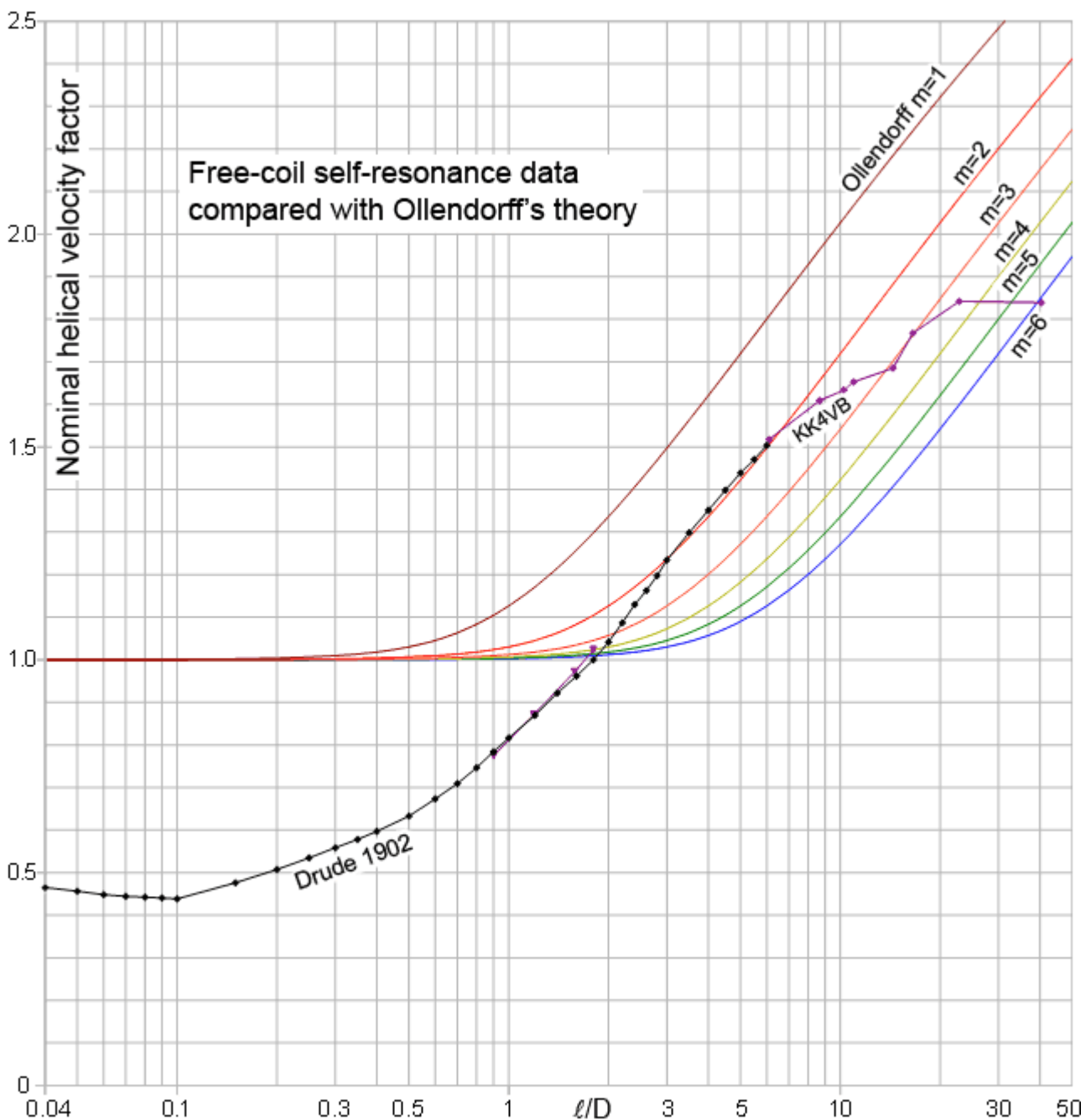
$$\sin \psi = \frac{v_{ax}}{v_{hx}}$$

and using this as a substitution gives:

$$\frac{v_{hx}}{c} = \frac{W(x)}{\cos \psi} \quad , \quad \text{where} \quad x = m \frac{\pi}{2} \frac{D}{\ell} \quad \text{Helical velocity factor.} \quad (1.8)$$

For small pitch angles, i.e., coils of many turns and typical radio coils, $\cos\psi$ is close to 1 and can usually be neglected. Thus the mysterious combination of Bessel functions that appears everywhere in helical waveguide theory is the uncorrected free-coil radial (i.e., circumferential) velocity factor, which can be used as an approximation for the helical velocity factor when the pitch-angle is small.

Most discussions of helical waveguide theory show Ollendorff's function plotted against a composite parameter which is a function of f , D and p . Here however, we will start by showing it plotted against ℓ/D for differing values of m . This, as shown in the graph below, is particularly illuminating when compared with Drude's air-dielectric coil data and the supplementary measurements by Alex Pettit (KK4VB) (as introduced in section 1.2). This is exactly the kind of data that Ollendorff was trying to explain, and while it might appear at first glance that he has not done that, in reality he has achieved a brilliant success. It all comes down to recognising the significance of the dispersion parameter m .



Electromagnetic phenomena are scaleable. Consequently, when a dispersion effect is linked to the dimensions of a structure, that effect will scale with the structure. Thus Ollendorff cannot directly state the variation of phase-velocity with frequency, but when solving for a particular frequency associated with a dimensional resonance, he can state a set of frequencies associated with the overtones of that resonance. Now if we transform that information to make it dimensionless, i.e., we represent it as velocity factor vs. ℓ/D , we lose all knowledge of specific frequencies, but instead obtain a set of choices along a dispersion co-ordinate m .

The obvious choice when comparing the theory with fundamental SRF data is to put $m=1$. We should not expect this to agree with our data however, for several reasons, the first of which is that there are no fringe-field corrections.

We can see from the graph that the dispersion effect is associated with superluminal helical phase velocity, and that this phenomenon does not occur in short coils. Thus we can deduce that there will be no superluminal velocity in the end regions of a truncated coil, and we can assume that the lengths of the two fringe-field regions will each be comparable to the coil radius. Thus one of the effects of applying an end correction to the theory will be to shift the set of dispersion contours to the right along the ℓ/D axis. It so happens that the parameter m does just that, and if we set it to 1.9 it produces a curve that coincides with Drude's data from about $\ell/D=3$ to $\ell/D=5$. Broadly, at this stage, we can say that the apparent superluminal helical phase velocity needed to account for Drude's and Alex's measurements is confirmed by Ollendorff's theory.

There is however another effect apparent in Alex's data ($\ell/D=6$ to $\ell/D=40$), which is the flattening-off of the phase-velocity profile in very long coils. This is a second-order effect, but a rather noticeable one, and it has several possible causes:

- 1) The superluminal effect is easily disturbed by changes in the current profile; and so a change in gradient might be something that the model fails to reproduce because the conduction-current is constrained to flow only in the helix direction. In the next few sections, it will be demonstrated that the superluminal phase velocity is easily abolished by perturbations in the coil current, and so any model shortcomings in this respect are likely to have some influence in regions in which the velocity is elevated.
- 2) Since Alex's measurements were made using a single stretchable coil, they might be affected by a constantly increasing SRF as ℓ/D increases. The measured frequencies however only ranged from 64 MHz to 78 MHz, while it requires an approximate doubling of frequency to traverse a whole number distance in the m co-ordinate. Thus while the frequency increase might account for some of the flattening, it is not sufficient to produce the whole effect. It should also be noted that this idea is not a strictly correct interpretation of Ollendorff's theory. The contours tell us that if we know one overtone, we can find the series, and not that a curve for a single value of m can cross contours. That constraint might break down however on consideration of small pitch-angle limiting behaviour.
- 3) The helical phase velocity as given by equation (1.8) is strictly Ollendorff's function divided by $\cos\psi$. Thus, the theoretical curve plotted contains the assumption that $\cos\psi=1$. It follows that the vertical axis for the graph is actually velocity factor divided by $\cos\psi$; which means that strictly the measurements should also be corrected by dividing by $\cos\psi$. It will turn out that this adjustment is not negligible for some of Alex's data, but we must hold off from applying theoretical corrections until we have finished developing the theory, and so we will leave this matter until section 11.
- 4) Apart from Ollendorff's model, there is a perfectly good physical reason for expecting that the the helical phase velocity will eventually fall back to c in the limit that the coil becomes very long. This is because as the coil is stretched out, it becomes more like a straight wire in free space. This is also particularly true if the pitch-angle is allowed to increase as the coil is elongated. The resonance of a straight wire cannot be excited by an induction loop perpendicular to it, but propagation along the wire at $v\approx c$ is nevertheless the limiting behaviour as the response disappears.

Some readers might be wondering, at this point, why we are so concerned with the superluminal region when there is a gross and obvious discrepancy for the smaller ℓ/D ratios. The reason however is that the basic explanation for the latter is straightforward and somewhat mundane. Ollendorff's model produces a phase velocity, whereas the actual data are apparent phase velocities computed using the conductor-length and the SRF. Thus the apparent velocities are roughly realistic for longer coils, but there is an induced axial electric-field that must give rise to an end-to-end capacitance in shorter coils. Thus the SRF is that of a short-circuited transmission-line apparently terminated in a static capacitance. This will be lower than the SRF that would occur in the absence of the axial-field, giving the impression that the phase velocity is reduced. Thus, as ℓ/D becomes smaller, the apparent velocity factor crosses the $v/c=1$ line. To model this effect, we require a way of calculating the axial-field capacitance, and a way of determining the characteristic resistance (impedance) of the helical transmission-line so that its input reactance at the SRF can be obtained. The transmission-line equation will then provide the electrical length, and thus the phase velocity by comparison with the actual length (see section 11). We might also turn this observation on its head however, and say that since Ollendorff has shown us that the true helical phase velocity will be c in shorter coils, then Drude's and other short-coil measurements contain information on the axial-field capacitance.

Interestingly, the balance between the axial-field effect and the superluminal effect means that free coil SRF measurements give an apparent phase velocity $v_{hx}=c$ when the ℓ/D ratio is about the same as the golden ratio⁵¹ (1.618 . . .). This also happens to be roughly the point at which the Q of radio coils is maximised. This coincidence (if it is a coincidence) is responsible for the observation that the SRF of a radio inductor (actually the free-coil value, not a value predicted from in-circuit measurements) occurs when the length of the wire is approximately $\lambda_0/2$.

Simple fringe-field correction

In addition to making the measurements shown earlier, Alex also made a set of long coil measurements in which he recorded the fundamental and the first and second overtone resonances⁵² (i.e., $m=1, 2$ and 3). In the following graph, these are shown compared with the m contours produced by Ollendorff's function (1.5) with a single empirical parameter included in an attempt to correct for the fringe-fields. The correction is applied to the argument of the modified Bessel functions thus:

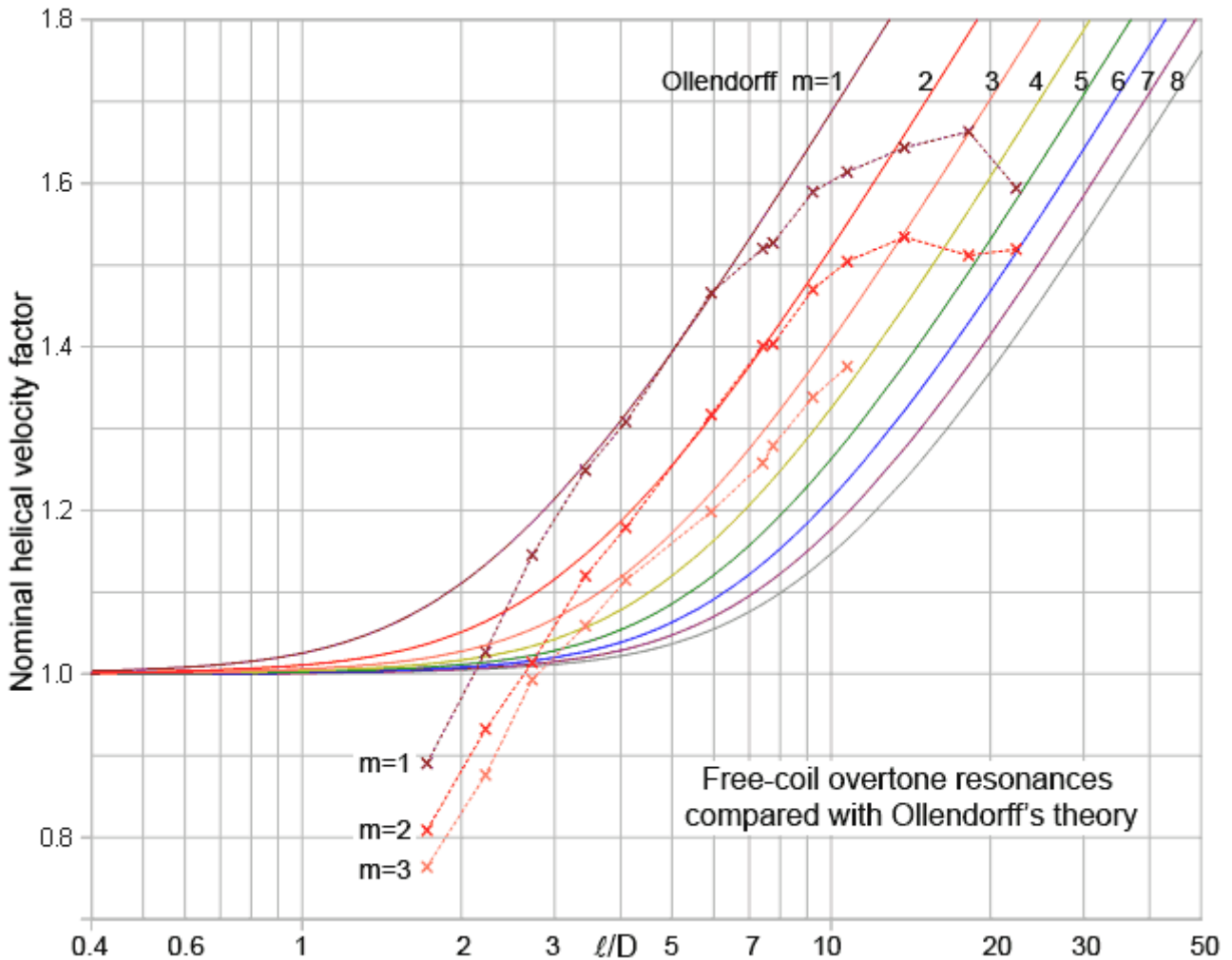
$$x = (m + k_{fr}) \frac{\pi}{2} \frac{D}{\ell} \quad (1.9)$$

There are two obvious ways in which we might apply a basic correction; one being the multiplication of the whole argument by a constant, which shifts the set of contours along the horizontal axis; and the other being the addition of a constant to the overtone number, which produces a shift that dies-out as m becomes large. The latter method, with $k_{fr}=1.15$ seems to reproduce the spacing between the three experimental velocity factor curves rather well. This method however, can only be used when $v_{hx}/c > 1$, and when we come to apply a general fringe-field correction, it will be done in a different way.

To make a complete model for the free coil, of course, we also need to correct for the axial electric-field capacitance primarily affecting short coils, and we need to correct for the flattening-off of velocity factor that occurs when the coil is long.

51 https://en.wikipedia.org/wiki/Golden_ratio $\phi = (1 + \sqrt{5})/2$

52 http://g3ynh.info/zdocs/magnetics/appendix/kk4vb_srf.html



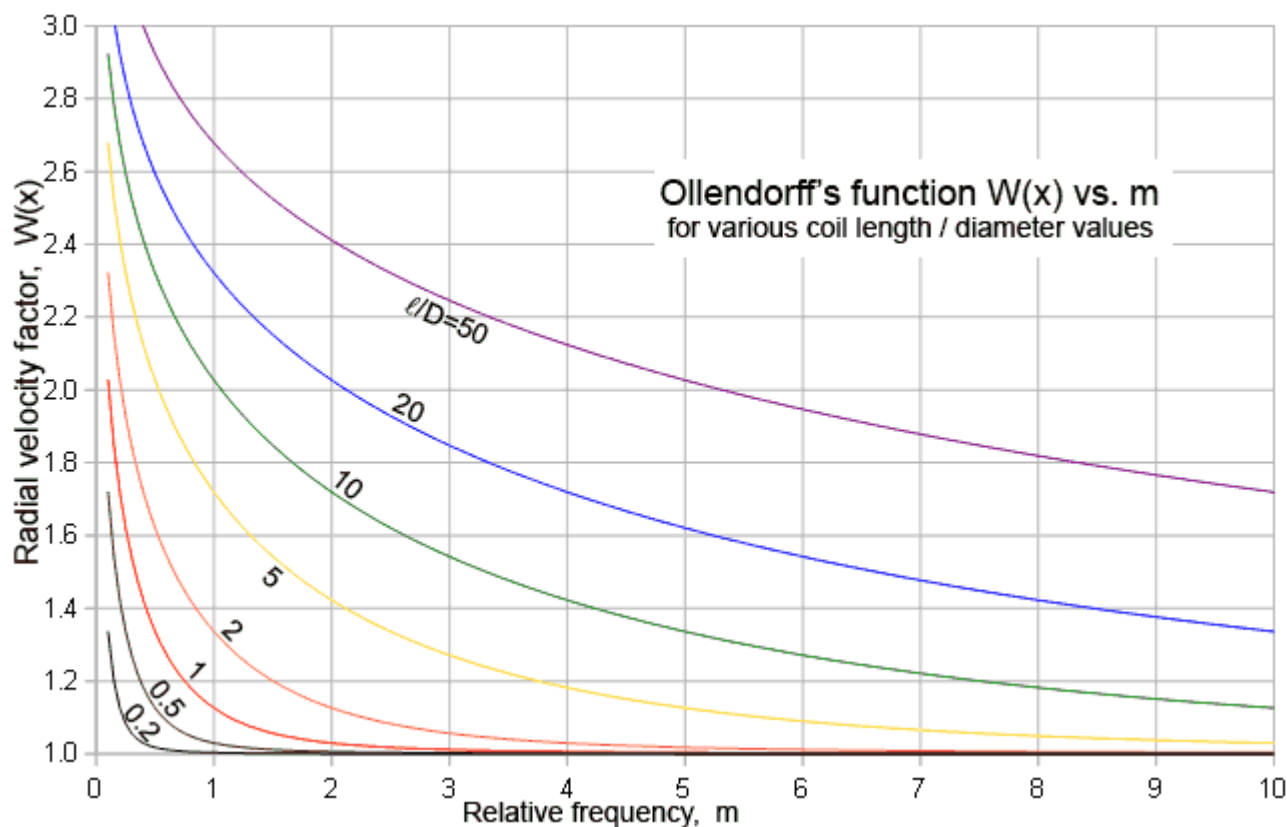
Overtone series measurements made by Alex Pettit using a single stretchable coil. Note that for $l/D < 5$, the coil was supported on a polyethylene rod. This causes the apparent velocity factors to come out somewhat too low, the effect diminishing as the coil becomes longer. For $l/D > 5$ the coil was suspended vertically from one end. This gives a much better fit until the measured velocity factors begin to flatten-off. The data are not smoothed and therefore show considerable scatter, and the drop-off is exacerbated because pitch-angle correction has not been applied.

An Open Office Basic macro routine for calculating Ollendorff's function using the built-in Bessel functions is given in the box below.

```
Function OLLENDF(byval x as double) as double
' Calculates Ollendorff's function. D W Knight. Version 1.00, 2016-03-16
Dim I0 as double, I1 as double, K0 as double, K1 as double
Dim oFA as Object
oFA = createUNOService("com.sun.star.sheet.FunctionAccess")
I0 = oFA.callFunction( "Besseli", array(x, 0) )
K0 = oFA.callFunction( "Besselk", array(x, 0) )
I1 = oFA.callFunction( "Besseli", array(x, 1) )
K1 = oFA.callFunction( "Besselk", array(x, 1) )
OLLENDF = sqr( I0*K0/(I1*K1) )
end function
```

Decline of velocity factor with frequency

Note that in visualising Ollendorff's theory in terms of v_{hx} vs. ℓ/D , as we have done in the preceding discussion, there is a danger of giving a false impression. The theory implies that long coils will show an elevated v_{hx} at relatively low frequencies, but that this will tail-off as the frequency increases. Hence, if we pick a particular value of ℓ/D , increasing the frequency by following a line of increasing m results in a decline in phase velocity. The graph below shows the effect



That the helical phase velocity in a long coil is high at low frequencies and decays asymptotically towards c as the frequency is increased was demonstrated experimentally by C C Cutler⁵³ in 1948, using a scaled-up model of a travelling-wave-tube helix. Cutler also noted a fairly good agreement between field measurements and the helix waveguide model at high frequencies, but at low frequencies there was a need to shift the model curve towards higher frequency. This observation provides some justification for the empirical correction used in (1.9), which is to the effect that the amount of adjustment applied needs to die-off as the frequency is increased.

53 **Experimental determination of helical-wave properties.** C C Cutler, Proc. IRE Feb. 1948, p230-233. See p232, Fig 4. and observation 4.

1.8 Velocity factor for an infinite free helix

After Ollendorff had published his solution for the solenoid resonance problem, there was an upsurge in interest in applying his method to the problem of the infinite helix. To do so abolishes the length parameter and replaces it with a transmission-line parameter called the radial wavenumber⁵⁴. This approach quickly became ubiquitous, to the extent that Ollendorff's original solution was largely forgotten, and subsequent applications of the theory to truncated helices have the problem formulated in this somewhat unintuitive way. Still, it is necessary to explore this approach fairly thoroughly, because it is the source of some formulae that have found wide application in the field of self-resonance and self-capacitance calculation.

Note that attenuation is not considered. Following Schelkunoff⁵⁵, we give the radial wavenumber the symbol γ and define it in the expression:

$$\gamma^2 = \beta^2 - \beta_0^2 \quad (1.10)$$

where β is the axial phase constant, defined as:

$$\beta = \frac{2\pi}{\lambda_{\text{ax}}} = \frac{\omega}{v_{\text{ax}}}, \quad \text{where } \omega = 2\pi f$$

and β_0 is (by analogy) the 'free space phase constant':

$$\beta_0 = \frac{2\pi}{\lambda_0} = \frac{\omega}{c}$$

The axial velocity factor is then:

$$\frac{v_{\text{ax}}}{c} = \frac{\beta_0}{\beta}$$

and a little rearrangement of (1.10) gives it as:

$$\frac{v_{\text{ax}}}{c} = \frac{1}{\sqrt{1 + \left(\frac{\gamma}{\beta_0}\right)^2}} \quad (1.11)$$

where the single unknown γ needs to be determined from the coil parameters. Now bearing in mind that γ is measured in [radians / unit length], we multiply it by the coil radius ($D/2$) to make it dimensionless and then use it as the argument in Ollendorff's formula (1.6). To see this substitution in action, recall that in section 1.7 the Bessel function argument was given as:

$$x = m \frac{\pi}{\ell} \frac{D}{2}$$

this now changes to:

⁵⁴ A wavenumber is a frequency measured in cycles per unit length or radians per unit length.

⁵⁵ See Pierce 1947, **Theory of the beam-type TWT** (already cited in section 1.6), Appendix B, **Propagation of a wave along a helix**.

$$x = \gamma \frac{D}{2} \quad (1.12)$$

and we have to make the substitution: $m\pi/\ell \rightarrow \gamma$ throughout. We can now rewrite equation (1.6) with all instances of $m\pi/\ell$ thus replaced, and bearing in mind that $p/\pi D = \tan\psi$, we end up with:

$$\beta_0 = \frac{2\pi}{\lambda_0} = W(\gamma D/2) \gamma \tan\psi \quad (1.13)$$

Ollendorff's formula now becomes a transcendental equation for γ , which is to say that it gives no direct algebraic solution, but we can nevertheless find γ for a given set of coil parameters by a process of trial and error. Those parameters are incidentally the coil diameter (or radius), the pitch (or pitch angle) and the frequency (or free-space wavelength).

Now if we multiply both sides of (1.13) by $D/2$, replace instances of $\gamma D/2$ with x and rearrange, the problem is put into the generalised form:

$$\frac{2\pi}{\lambda_0} \frac{D}{2} \frac{1}{\tan\psi} = x W(x) \quad (1.14)$$

There are numerous ways in which the left-hand side of this expression can be rearranged, but for the time being, we will simply regard it as a generic function of three unique variables $U(f, D, p)$. Thus:

$$U(f, D, p) = x W(x) \quad (1.14a)$$

The need to solve this equation has caused some difficulty in the past; but as problems requiring an iterative solution go, this is probably one of the most well behaved. The reason is that the radial velocity factor $W(x)$ usually remains fairly close to 1, and so the best first estimate for x in any iteration process is U .

The un-optimised Open Office Basic macro routine shown below accepts an input value of $U \geq 0.013$ and returns x to within $\pm 0.000\,000\,001$.

```
Function GetOlex(byval u as double) as double
' Solves Ollendorf's function for u = x W(x) and returns x.
' Calls function Ollendf(x). v 1.00, D W Knight, 2016-03-21.
Dim u1 as double, x as double, diff as double, shift as double, n as integer
if u < 0.013 then exit function
n = 0
x = u
do
  u1 = x*ollendf(x)
  diff = u - u1
  shift = diff/2
  x = x + shift
  n = n + 1
loop until abs(diff) < 1E-9 or n > 255
Getolex = x
end function
```

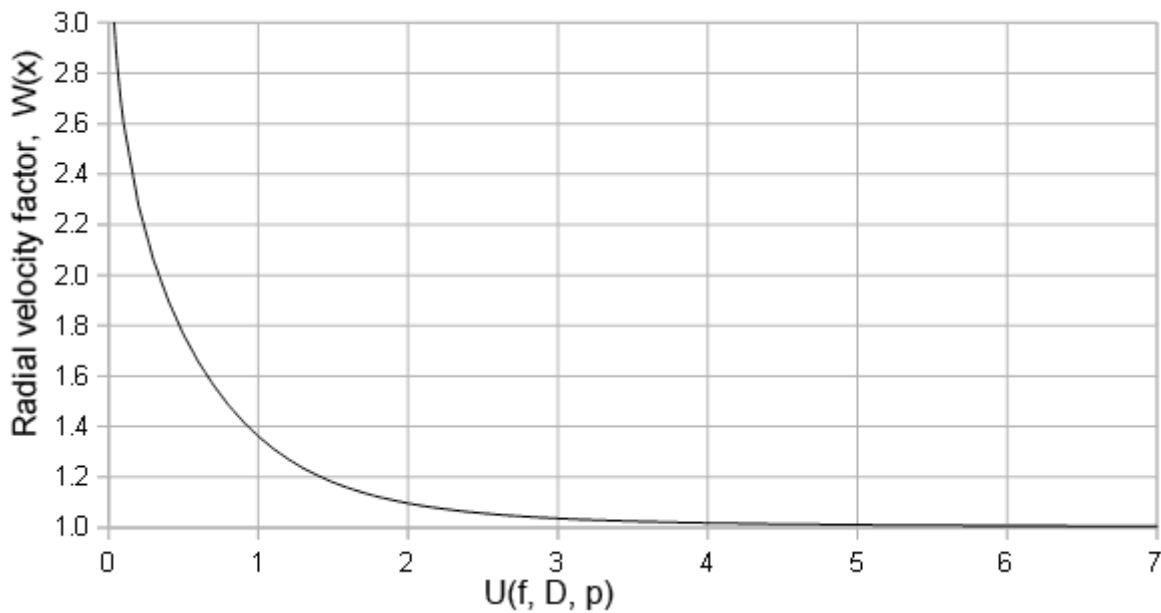
Now, having a way of solving for $x = \gamma D/2$, we can collect various definitions of the composite parameter U by inspection of (1.13), (1.14) and (1.14a). Thus:

$$U(f, D, p) = \beta_0 \frac{D}{2} \frac{1}{\tan \psi} = \frac{2\pi}{\lambda_0} \frac{D}{2} \frac{\pi D}{p} = x W(x) \quad , \quad \text{etc.} \quad (1.15)$$

Also, we note that by rearranging (1.13), the radial velocity factor can be written:

$$W(x) = \frac{\beta_0}{\gamma \tan \psi}$$

These two identities are the horizontal and vertical coordinates of the graph below, which occurs in practically every paper on the subject of helical waveguide theory.



This graph is effectively a version of the graph of $W(x)$ vs. m , shown at the end of section 1.7.

Using this formulation, we can find the self-resonances of finite-length coils by feeding the determined parameter $x = \gamma D/2$ back into equation (1.11). To do this, note that $v_{ax} = f \lambda_{ax}$, and that the λ_{ax} is some multiple of the coil length. For an ungrounded free-coil resonator:

$$\lambda_{ax} = \frac{2\ell}{m} \quad , \quad \text{where } m = 1, 2, 3, \dots$$

and for a free coil grounded at one end

$$\lambda_{ax} = \frac{4\ell}{2m+1} \quad , \quad \text{where } m = 0, 1, 2, \dots$$

For the ungrounded free-coil case, for example, we take equation (1.11) and apply the substitutions $\beta_0 = 2\pi f_0/c$ and $\gamma = 2x/D$, which gives:

$$\frac{v_{ax}}{c} = \frac{1}{\sqrt{1 + \left(\frac{2xc}{D2\pi f_0}\right)^2}}$$

Substituting $v_{ax} = f_0 2\ell / m$ and squaring then gives:

$$\left(\frac{f_0 2\ell}{mc}\right)^2 = \frac{1}{1 + \left(\frac{2xc}{D2\pi f_0}\right)^2}$$

i.e.:

$$\left(\frac{f_0 2\ell}{mc}\right)^2 \left(1 + \left(\frac{2xc}{D2\pi f_0}\right)^2\right) = 1$$

Multiplying-out and cancelling gives:

$$\left(\frac{f_0 2\ell}{mc}\right)^2 + \left(\frac{2\ell x}{m\pi D}\right)^2 = 1$$

which can be solved for f_0 thus:

$$f_0 = \frac{cm}{2\ell} \sqrt{1 - \left(\frac{2\ell x}{m\pi D}\right)^2}$$

A more interesting version is obtained however if we multiply $m/2\ell$ into the square root:

$$f_0 = c \sqrt{\left(\frac{m}{2\ell}\right)^2 - \left(\frac{x}{\pi D}\right)^2} \quad (1.16)$$

Now recall that, in the Ollendorff formulation of the problem, the Bessel function argument was given as:

$$x = m \frac{\pi}{\ell} \frac{D}{2}$$

Which means that, in that particular case:

$$\frac{m}{2\ell} = \frac{x}{\pi D}$$

Should this be used as a substitution in (1.16), either way round, the result is $f_0=0$. This is the trivial solution to the sheet-helix problem. It is valid, but somewhat useless except that it gives us a check on the derivation of (1.16).

Kandoian & Sichak

Prior to the time when electronic computers were accessible to engineers and researchers, the fact that the radial wavenumber γ had to be obtained by solution of a transcendental equation gave rise to the need for an approximate formula. That was provided by Kandoian and Sichak^{56 57} as a means for estimating the height (i.e., length) of coils used in helically-wound $\frac{1}{4}$ -wave vertical antennas. The formula however is based on the unmodified Schelkunoff version of sheet-helix theory, and so can be applied both to grounded and ungrounded free coils. Hence it is common practice to write it as an expression for axial velocity factor:

$$\frac{v_{ax}}{c} = \frac{1}{\sqrt{1 + 20 \left(\frac{D}{p}\right)^{2.5} \left(\frac{D}{\lambda_0}\right)^{0.5}}} \quad \text{Kandoian - Sichak formula.} \quad (1.17)$$

For those familiar with the original, one notational difference is that it uses turns-per-unit-length; but since that is the same as the reciprocal of the pitch distance, i.e., $1/p$, we use the latter here.

Now comparing the formula with equation (1.11), we can see that an empirical solution for γ is given in the form:

$$\left(\frac{\gamma}{\beta_0}\right)^2 = \left(\frac{\gamma \lambda_0}{2\pi}\right)^2 = 20 \left(\frac{D}{p}\right)^{2.5} \left(\frac{D}{\lambda_0}\right)^{0.5}$$

and using (1.12) as a substitution (i.e., $\gamma=2x/D$) we get:

$$\left(\frac{x \lambda_0}{\pi D}\right)^2 = 20 \left(\frac{D}{p}\right)^{2.5} \left(\frac{D}{\lambda_0}\right)^{0.5}$$

which can be rearranged to give:

$$x = \sqrt{20} \pi \left(\frac{D}{\lambda_0} \frac{D}{p}\right)^{1.25} \quad (1.18)$$

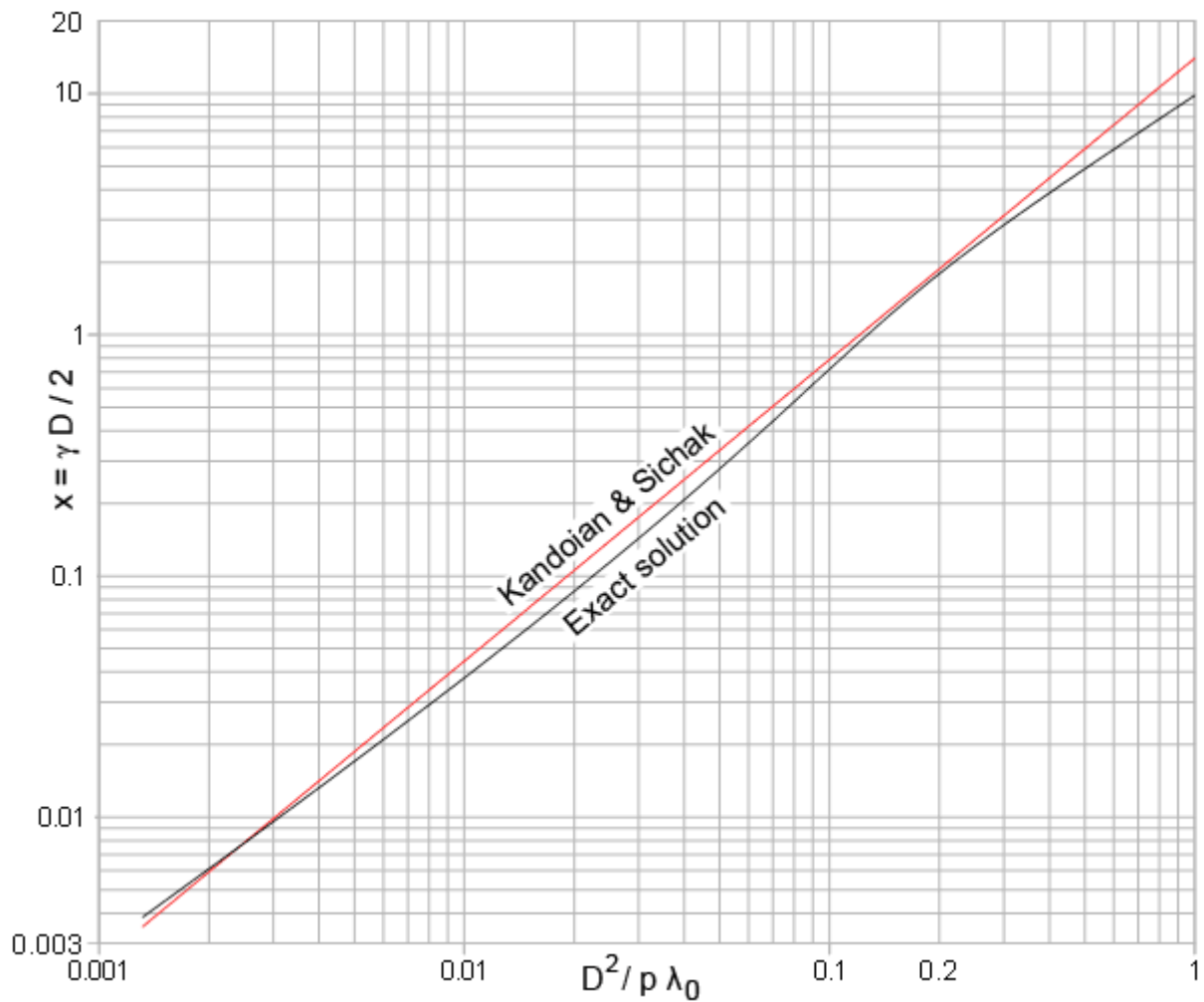
Note incidentally, that M is used instead of x in the original documents. In the various versions of the K&S article, this is shown plotted against $D^2/p\lambda_0$, another non-intuitive composite parameter, but by inspection of equation (1.15), we can see that:

$$\frac{D^2}{p\lambda_0} = \frac{U(f, D, p)}{\pi^2} \quad (1.19)$$

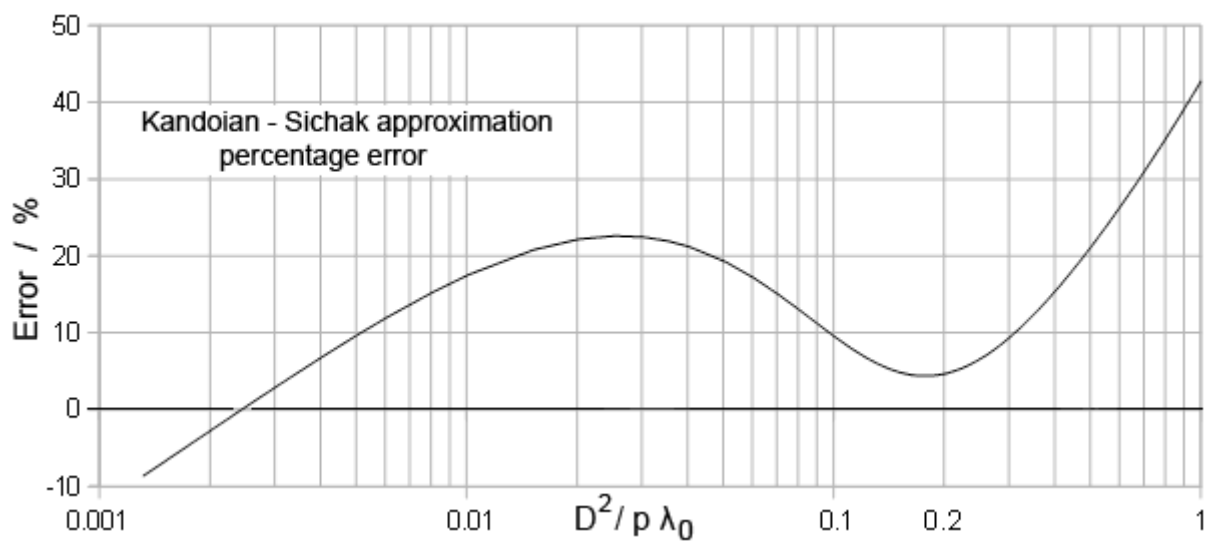
Here however, we plot both the K&S approximation for x , and the exact value obtained by solving equation (1.14a); and perhaps more to the point, we also plot the percentage difference.

56 **Wide-frequency-range tuned helical antennas and circuits**, A G Kandoian and W Sichak, Elec. Comm, Dec 1953, vol. 30(4), p294-299. + errata, Elec. comm 31(1), p49. Also published in Convention record of the IRE, 1953, National Convention, Part 2 - Antennas and communication, p42-47. See equation (3).

57 **Reference Data for Radio Engineers**, ITT corp. 4th edition 1956. p682-687. See equation (19).



Kandoian & Sichak approximation for $x = \gamma D / 2$ (radial wavenumber \times coil radius) compared to exact solution of equation (1.14a). The approximation is claimed to be valid up to $D^2 / \rho \lambda_0 = 0.2$. The actual percentage error is shown in the graph below.



It must be understood, of course, that prior to digital computers it was the norm to use approximate methods, and the K&S formula was fairly well optimised for calculation using log tables. As we can see, it is rather inaccurate; but Ollendorff's theory is also inaccurate in its basic form through lack of fringe and axial field corrections, and whether or not a secondary source of error is fatal depends on how it combines with other errors. To investigate that, we can compare it with both Ollendorff's theory and free-coil resonance data, by converting it into an expression for helical velocity factor. To do so we can neglect the unit term in the square-root argument of equation (1.17), so that we have:

$$\frac{v_{ax}}{c} = \frac{\lambda_{ax}}{\lambda_0} = \frac{1}{\sqrt{20 \left(\frac{D}{p}\right)^{2.5} \left(\frac{D}{\lambda_0}\right)^{0.5}}} \quad (1.20)$$

This additional approximation is used by Kandoian and Sichak themselves, and it can be justified on the basis that the remaining term is $\gg 1$ when the pitch is small, because the axial velocity is then much less than the helical velocity.

What we want to get out of this is the helical velocity factor as a function of ℓ/D , and since we have good data for ungrounded free coils resonating at the fundamental SRF, we can specify the case with $\lambda_{hx} = 2\ell_w/m$ so that:

$$\frac{v_{hx}}{c} = \frac{\lambda_{hx}}{\lambda_0} = \frac{2\ell_w}{m\lambda_0}, \quad m=1$$

How to extract this quantity from (1.20) is not exactly obvious, but the trick is to start by raising the whole thing to the power of 4. Thus:

$$\left(\frac{\lambda_{ax}}{\lambda_0}\right)^4 = \frac{1}{20^2 \left(\frac{D}{p}\right)^5 \frac{D}{\lambda_0}} = \frac{p^5 \lambda_0}{20^2 D^5 D}$$

i.e.;

$$\frac{1}{\lambda_0} = \left(\frac{p^5}{20^2 D^6 \lambda_{ax}^4}\right)^{0.2}$$

Now observe that the length of the coil is the number of turns multiplied by the pitch, i.e., $\ell = Np$, so $p = \ell/N$. Thus:

$$\frac{1}{\lambda_0} = \left(\frac{\ell^5}{20^2 (ND)^5 D \lambda_{ax}^4}\right)^{0.2}$$

Also, to a good approximation for coils of small pitch angle, $\ell_w = \pi DN$, so that $ND = \ell_w/\pi$. Hence:

$$\frac{1}{\lambda_0} = \frac{\pi}{\ell_w} \left(\frac{\ell^5}{20^2 D \lambda_{ax}^4}\right)^{0.2}$$

i.e.;

$$\frac{2 \ell_w}{\lambda_0} = \frac{v_{hx}}{c} = 2 \pi \left(\frac{\ell^5}{20^2 D \lambda_{ax}^4} \right)^{0.2}$$

and finally noting that for $m=1$, $\lambda_{ax}=2\ell$, this leaves us with:

$$\frac{v_{hx}}{c} = 2 \pi \left(\frac{\ell}{20^2 D 2^4} \right)^{0.2} = \frac{2 \pi}{(20^2 2^4)^{0.2}} \cdot \left(\frac{\ell}{D} \right)^{0.2}$$

Which can also be written:

$$\frac{v_{hx}}{c} = \frac{2 \pi}{80^{0.4}} \left(\frac{\ell}{D} \right)^{0.2} = 1.088789 \left(\frac{\ell}{D} \right)^{0.2} \quad (1.21)$$

This is plotted on the following graph for comparison with Ollendorff's theory ($m=1$) and combined free-coil SRF data (i.e., Data from Drude, DWK and Alex Pettit plotted as a single curve and averaged in the case of duplicate measurements).

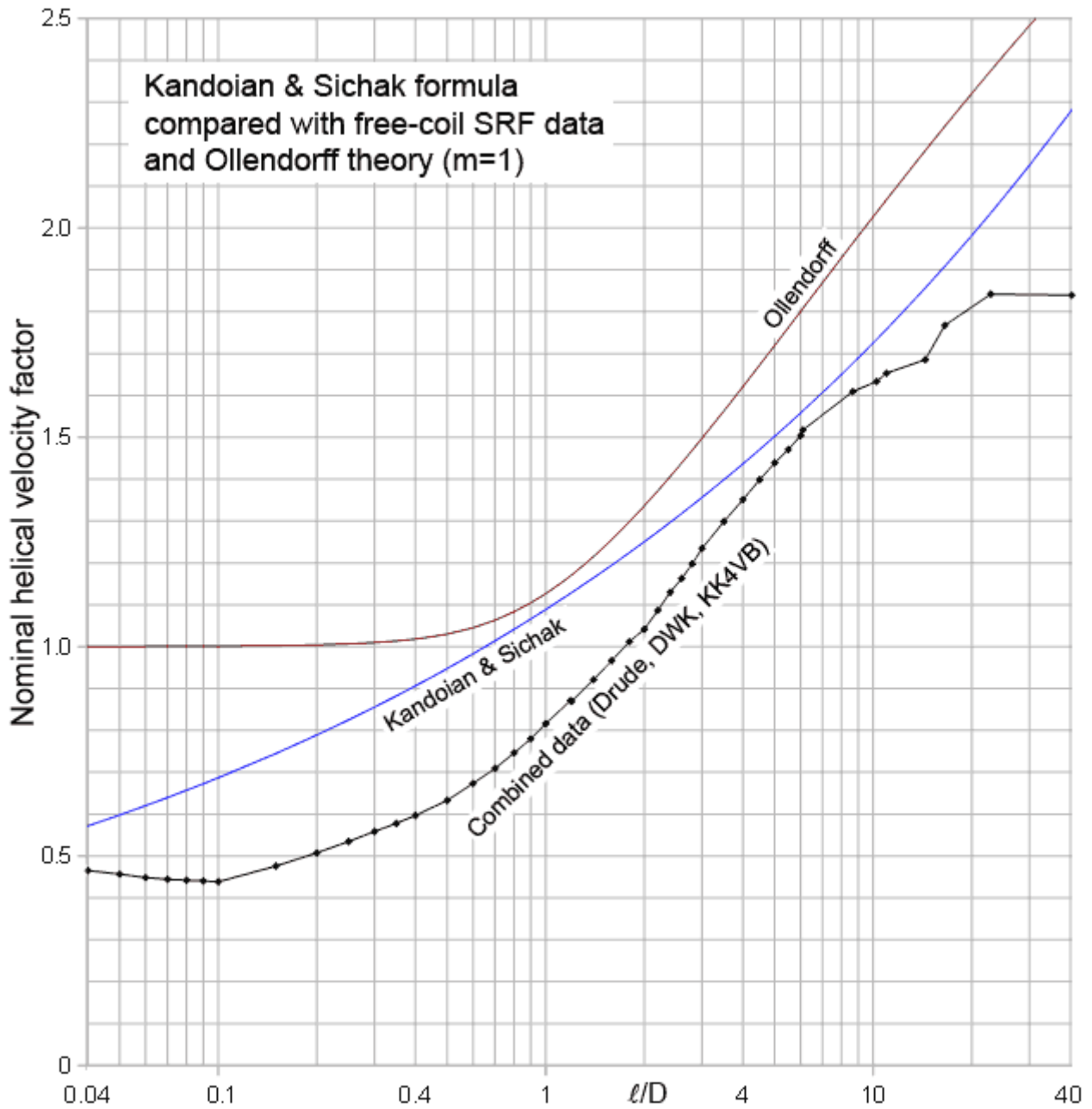
What we find is somewhat surprising. So many approximations have been piled into the formula that it has lost all knowledge of asymptotes, inflection and gradient; but by what appears to be a pure fluke, it falls considerably closer to the data than the Ollendorff curve. Particularly, in the ℓ/D range from about 3 to 15, fairly typical of HF antenna loading coils and Tesla coils, it is actually not a bad approximation. Thus it would have offered fair guidance to engineers trying to fettle such devices, which of course must account for its long-standing success. Note incidentally, that the numerical constant and the exponent in equation (1.21) are empirical parameters derived from fitting choices made by Kandoian and Sichak. Adjusting them can give an improvement, although the curve remains a poor fit overall and has no merit as a candidate for the purpose of data reduction.

The derivation given above is similar to a derivation given in a study of self-resonance and self capacitance by Miranda and Pichorim⁵⁸. Those authors apply the K&S formula to the prediction of fundamental and overtone self-resonance calculation for half-wave and quarter-wave resonators, with fair results. A comparison between the formula and the self-capacitance data of Medhurst however is problematic due to an incorrect resonance assignment. We will investigate Medhurst's work in great detail over the course of the next few sections, and demonstrate that free coil resonance formulae such as K&S cannot be applied to the self-capacitance problem (see section 10).

The K&S formula, useful though it has been over the years, is obsolete in the age of digital computers. It has also become a source of misdirection in some quarters, because it has come to be referred-to as an 'exact' solution to to the coil self-resonance problem. This belief is traceable to an unfortunate choice of words in the last sentence prior to equation (2) in the K&S 1953 helical antennas paper, the troublesome statement being: "The exact expression for [the helical velocity factor] is . . .". What they actually meant is that 'what follows is exactly the same as the theory given by Schelkunoff (which is not in itself exact), prior to our making an approximation to it'. The ambiguity is further compounded by two errors in the sentence that immediately follows. This is written: "The approximation in figure 2 is obtained by neglecting (1) in comparison to other

⁵⁸ **Self-resonant frequencies of air-core single-layer solenoid coils calculated by a simple method.** C M de Miranda and S F Pichorim, Electrical Engineering, March 2014. DOI: 10.1007/s00202-014-0312-3.

factors."; but what it should say is "The approximation in figure 2 is obtained by neglecting the term 1 in comparison to the other terms in equations (1) and (2)." The lack of clarity seems to cause people to ignore the sentence, thereby making the K&S formula 'exact' according to some commentators⁵⁹.



⁵⁹ The 2009 website publication of the DAE formula (section 5) attracted correspondence admonishing the author for failing to realise that an 'exact solution' to the problem already existed.

2.0 Self-capacitance

As we must conclude from preliminary discussion, despite the sometimes confusing evidence, the reactance of a coil is only strictly defined by a transmission-line model. For purposes of circuit design however, it is well known that a coil behaves approximately as a lumped inductance in parallel with a fixed capacitance on a large interval between very low frequencies and the fundamental SRF. Hence the logical starting point for a general expression for self-capacitance is to use the electrical resonance formula as an asymptotically-correct bridge, linking the low-frequency inductance (derived from magnetics) to the SRF (related to the conductor length).

As will be demonstrated later, when the apparent self-resonance frequencies of coils are calculated from extrapolated self-capacitance measurements, the data indicate that the wire is physically one half-wavelength long at the long-coil limit. Given that a strong resonance also occurs when $\lambda/4$ of wire is connected at one end to an infinite ground-plane however, it might not be immediately obvious why the $\lambda/2$ conductor-length resonance is active in this case. The 'self-capacitance' however is a way of representing the propagation-delay for a wave travelling along the wire, and for a parallel resonance to occur, the wave must traverse the coil twice in a go-and-return journey. Self-capacitance is also a hypothetical contributor to the impedance measured at the terminals of the coil, as opposed to a contributor to the impedance measured between one end of the coil and a ground plane. Hence it should be understood that, while some impedance measuring devices are earthed at one of the test terminals, and some are not, they all produce substantially the same result for measurements made by direct (two terminal) connection to device under test. It should be noted that several authors have not resolved this issue, and have consequently interpreted their data incorrectly. Verifying that taking the ground connection on and off makes barely any difference to a coil shunted by an impedance of magnitude smaller than that of its self-capacitance is advisable⁶⁰.

2.1 Propagation of uncertainty from SRF to self-capacitance

In deriving an expression for coil self-capacitance from the conductor length, it is useful to be aware of the way in which any uncertainty in the relationship between conductor length and SRF will be transmitted into the calculated value of self-capacitance. A particular reason for wanting that information is that there is often a discrepancy of a few % in the assumption that the electrical length of the winding wire is identical to the physical length. Furthermore, a given percentage uncertainty in SRF does not translate into the same percentage uncertainty in self-capacitance.

When we represent the coil as a lumped inductance (L) in parallel with a lumped self-capacitance (C_L), the self-resonant frequency is given by the electrical resonance formula⁶¹:

$$f_{0s} = \frac{1}{2\pi\sqrt{L C_L}} \quad (2.1)$$

The self capacitance is then, by rearrangement:

$$C_L = \frac{1}{(2\pi f_{0s})^2 L}$$

⁶⁰ Stray capacitance will change a little, but that's the only noticeable effect until the shunt impedance starts to approach an open circuit. Making self-capacitance measurements without using a ground connection is best however (see method used in section 10), because then the actual $\lambda/2$ resonance occurs at the point at which the shunt is removed.

⁶¹ This assumes zero losses, i.e., the relationship is accurate for high Q coils.

The uncertainty in C_L due to the uncertainty in f_{0s} (using the standard rule for propagation of uncertainties), is given by the rate of change of C_L with respect to f_{0s} multiplied by the uncertainty in f_{0s} . The rate of change is obtained by differentiation (strictly partial differentiation because there is another variable L that we assume to be a constant), and in this case it involves a simple application of the standard formula:

$$\frac{\partial(ax^n)}{\partial x} = a n x^{n-1} \quad (\text{where, for the present case, } n = -2)$$

Thus:

$$\frac{\partial C_L}{\partial f_{0s}} = -\frac{1}{2\pi^2 L f_{0s}^3}$$

If the uncertainty in C_L is δC_L , and the uncertainty in f_{0s} is δf_{0s} , then:

$$\delta C_L = \frac{-\delta f_{0s}}{2\pi^2 L f_{0s}^3}$$

This relationship relates to absolute uncertainties (i.e., the uncertainty is in the same units as the quantity to which it relates), whereas relative uncertainty is often more informative (i.e, uncertainty expressed as a proportion of the determined quantity). We can however obtain the relationship between the proportionate uncertainties (i.e., $\delta C_L/C_L$ and $\delta f_{0s}/f_{0s}$) by using equation (2.1) to substitute for f_{0s}^2 in the expression above. Multiplying numerator and denominator by $2C_L$ gives:

$$\delta C_L = \frac{-2\delta f_{0s} C_L}{4\pi^2 L C_L f_{0s}^3}$$

but $4\pi^2 L C_L = 1/f_{0s}^2$, thus:

$$\frac{\delta C_L}{C_L} = -2 \frac{\delta f_{0s}}{f_{0s}}$$

When uncertainties are given as standard deviations, it is of course the magnitude of this expression that interests us (we do not care about the minus sign, which simply says that an increase in SRF is associated with a reduction in self-capacitance). What we find therefore is that the proportionate (or percentage) uncertainty in the self capacitance, as determined from the SRF, is twice the proportionate uncertainty in the SRF. This might not seem to bode well for our intention to derive self-capacitance from conductor length; but generally, the ability to calculate a small capacitance (typically a few pF) to within a few % constitutes a good first-order estimation procedure. Thus the fact that the error in self-capacitance, due to error in the assumption that SRF is dictated by physical conductor length, is twice the error in predicted SRF is not particularly serious.

2.2 Self-capacitance derived from the conductor-length

The length of wire in a helical coil is given by:

$$\ell_w = \frac{2\pi r N}{\cos \psi} \quad (2.2)$$

where r is the effective solenoid radius, N is the number of turns, and ψ is the pitch angle. At the extrapolated SRF (as will emerge from physical data):

$$\ell_w = \lambda/2$$

where $\lambda = v/f$; v being the apparent velocity of light in the surrounding medium. v is given by:

$$v = \frac{1}{\sqrt{\mu \epsilon}} = \frac{1}{\sqrt{\mu_0 \mu_r \epsilon_0 \epsilon_r}}$$

and for a self-supporting coil in air or vacuum (neglecting the effects of the helical propagation environment), $\lambda = \lambda_0$ and:

$$v = c = \frac{1}{\sqrt{\mu_0 \epsilon_0}}$$

Hence, at the SRF, at least to a first-order approximation:

$$\ell_w = \frac{1}{2 f_{0s} \sqrt{\mu \epsilon}}$$

Using this in (2.2) gives:

$$\frac{2 r N}{\cos \psi} = \frac{1}{2 \pi f_{0s} \sqrt{\mu \epsilon}} \quad (2.3)$$

At this point it might seem logical to substitute for $2\pi f_{0s}$ using the electrical resonance formula (2.1), but to do so will not result in an equality. This problem arises because of a hidden generalisation in eliminating f_{0s} . Equation (2.1) defines the relationship between L and C_L only at the extrapolated SRF, whereas we want the relationship to hold from DC to the SRF, and we want it to capture any changes in wave propagation that might result from connecting the coil to a circuit. This implies that the self-capacitance is not strictly a constant, it might even change in the presence of a shunt impedance, and so it cannot be defined as a constant. Hence we need an additional parameter, which is as yet unquantified, but which might prove to be a function of coil geometry, or frequency, or load impedance, or perhaps all of those. It is analogous to a relative permittivity, and so we will include it with the permittivity and permeability factors. It is also analogous to Nagaoka's coefficient (the fringing magnetic field correction for the current-sheet solenoid), and so we will call it k_E (electric correction factor). Hence, substituting (2.1) into (2.3) and restoring equality by including k_E :

$$\frac{2 r N}{\cos \psi} = \sqrt{\frac{L C_L}{\mu \epsilon k_E}}$$

Squaring both sides then gives:

$$\frac{4r^2N^2}{\cos^2\psi} = \frac{LC_L}{\mu\epsilon k_E}$$

Hence:

$$C_L = \frac{\mu\epsilon 4r^2N^2k_E}{L\cos^2\psi} \quad (2.4)$$

The equivalent lumped inductance of a solenoid can be written⁶²:

$$L = \mu \frac{\pi r^2}{\ell} N^2 k_H \quad (2.5)$$

where k_H is an aggregation of correction factors that is typically within 2% of Nagaoka's coefficient (k_L) for coils of small pitch angle, and is assumed to be equal to k_L in the current-sheet approximation. Substituting (2.5) into (2.4) gives:

$$C_L = \frac{4\mu\epsilon r^2 N^2 \ell k_E}{\mu\pi r^2 N^2 k_H \cos^2\psi}$$

i.e.;

$$C_L = \frac{4\epsilon}{\pi} \ell \frac{k_E}{k_H} \frac{1}{\cos^2\psi} \quad (2.6)$$

From which we note that this representation finds the self capacitance to be independent of the number of turns. For a self-supporting coil in air, it becomes:

$$C_L = \frac{4\epsilon_0}{\pi} \ell \frac{k_E}{k_H} \frac{1}{\cos^2\psi} \quad , \quad \text{where} \quad \frac{4\epsilon_0}{\pi} = 11.27350207 \text{ pF/m}$$

The coefficient k_E , of course, remains to be determined. Also, we should note that Nagaoka's coefficient and the various other small corrections that make-up k_H are defined purely in terms of static magnetic fields. k_H is therefore (at least in principle) at liberty to change as the phase-shift over the length of the coil increases. That means that any apparent frequency-independence of self-capacitance is dependent on the way in which the effects of phase-shift either scale with coil geometry, or cancel due to complementary variations in the electric and magnetic coefficients.

62 **Solenoid inductance calculation.** D W Knight. <http://g3ynh.info/zdocs/magnetics/> . See section 12,

3. Medhurst's formula

The most widely cited study of solenoid self-capacitance is that reported by R G Medhurst⁶³. The intended remit of that work however, was probably not as wide as is generally assumed. Medhurst engaged in a study of the AC resistance of solenoids with a view to producing formulae and tables for the prediction of Q. In order to do that, he needed to correct his measurements for the effect of self-capacitance, and it was his original intention to use the theory of A J Palermo (to be discussed in section 6) for that purpose. Palermo gives a formula based on the hypothesis that the self-capacitance can be deduced by considering the capacitance between adjacent turns. Medhurst soon ran into difficulties with that approach; and so was forced to "find out whether Palermo's formula did in fact agree with experiment". He concluded that the data supporting Palermo's theory were suspect; and fell only a little short of accusing Palermo of scientific fraud.

Medhurst's solution to the dearth of believable theory was to make self-capacitance measurements on a large number of test coils, all of which were wound on solid polystyrene rods. He then corrected the data for strays and fitted them to the following regression formula:

$\frac{C_L}{D} = 0.1126 \frac{\ell}{D} + 0.08 + 0.27 \sqrt{\frac{D}{\ell}} \quad [\text{pF} / \text{cm}]$	Medhurst's Formula
---	--------------------

The first thing to notice here is that the coefficient 0.1126 is $4\epsilon_0/\pi$ in pF/cm with an error in the last digit as occurs when the value of c is taken to be 300 M m/s (instead of 299 792 458 m/s, which is now the standard value). As Medhurst stated in his paper: "The first numerical factor follows from Nagaoka's inductance formula for long coils and the experimental fact that the self-resonant wavelength for long coils equals twice the length of the winding". In other words; he employed a derivation somewhat akin to that which led us to equation (2.6), but using the long current-sheet approximation ($k_L=1$), and without encountering the $1/\cos^2\psi$ factor. The latter omission is of no consequence however, because Medhurst was aware that self-capacitance is substantially independent of turn-spacing provided that the coil has plenty of turns. He therefore chose to keep the number of turns per unit length high to eliminate pitch effects, and thus worked in the regime where $\cos^2\psi \rightarrow 1$.

Medhurst's formula can, of course, be put into the form of equation (2.6), and it is instructive to do so. We start by multiplying throughout by D, restoring natural constants to their proper identities, and converting to SI units by multiplying by 10^{-12} to get rid of the p in pF, and multiplying by 100 to get rid of the c in /cm. This gives:

$$C_L = \frac{4\epsilon_0 \ell}{\pi} + 8 \times 10^{-12} D + 27 \times 10^{-12} D \sqrt{\frac{D}{\ell}} \quad [\text{Farads}]$$

Now, factoring $4\epsilon_0 \ell/\pi$ from each of the terms we get:

$$C_L = \frac{4\epsilon_0 \ell}{\pi} \left[1 + \frac{8 \times 10^{-12} \pi}{4\epsilon_0} (D/\ell) + \frac{27 \times 10^{-12} \pi}{4\epsilon_0} (D/\ell)^{\frac{3}{2}} \right]$$

which, after re-enumerating the empirical constants (and avoiding the introduction of rounding error by retaining more significant figures than is justified), gives:

$$C_L = \frac{4\epsilon_0 \ell}{\pi} \left[1 + 0.7096 (D/\ell) + 2.395 (D/\ell)^{3/2} \right] \quad [\text{Farads}] \quad (3.1)$$

⁶³ Medhurst 1947. Reference given earlier

Comparing this with equation (2.6), shows that Medhurst has given us the coefficient k_E / k_H as:

$$\frac{k_E}{k_H} = [1 + 0.7096(D/\ell) + 2.395(D/\ell)^{3/2}]$$

We will not however accept Medhurst's formula as it stands, there being several shortcomings that need to be addressed.

Repeat of Medhurst's data analysis

The first issue is that, in 1947, carrying out a least-squares fitting procedure on any sizeable dataset could amount to several days of work. Consequently, Medhurst's statistical investigation is minimal. He does however report his data; which, although not in raw form, are nevertheless as adjusted prior to fitting. Hence we can repeat the analysis.

Writing equation (3.1) with undefined empirical coefficients we have:

$$C_L = \frac{4\varepsilon_0}{\pi} \ell [1 + k_1(D/\ell) + k_2(D/\ell)^{3/2}]$$

Dividing both sides by $(4\varepsilon_0/\pi)D$ gives:

$$\frac{C_L/D}{4\varepsilon_0/\pi} = (\ell/D) [1 + k_1(D/\ell) + k_2(D/\ell)^{3/2}]$$

Multiplying ℓ/D into the right-most bracket gives:

$$\frac{C_L/D}{4\varepsilon_0/\pi} = (\ell/D) + k_1 + k_2(\ell/D)^{-1/2}$$

and subtracting (ℓ/D) from each side gives:

$$\frac{C_L/D}{4\varepsilon_0/\pi} - (\ell/D) = k_1 + k_2(\ell/D)^{-1/2}$$

This is a straight-line graph of the form $y=a+bx$, with:

$$y = \frac{C_L/D}{4\varepsilon_0/\pi} - (\ell/D)$$

Notice here that the derivative $\partial y/\partial(C_L/D)$ is a constant. Hence there is no non-linear scaling of uncertainties to contend with in this case.

Medhurst reports his adjusted data as a table of C_L/D vs. ℓ/D . What he actually measured in each case however, was capacitance in the range of about 1 pF to 10 pF. Hence we should note that the uncertainty of a C_L/D value is probably best expressed as a percentage common to the whole dataset. It transpires however, that the regression line for Medhurst's function does not lie particularly close to the data for low C_L/D values when realistically weighted. The problem is that

the choice of polynomial is not optimal, and needs artificial weighting in order to force it on to the lower asymptote. Thus, assuming for purely pragmatic reasons that all of Medhurst's data have equal uncertainties, a simple least-squares fit⁶⁴ returns the following information:

$$k_1 = 0.824903 \pm 0.089$$

$$k_2 = 2.328995 \pm 0.073$$

$$\sigma_{CL} = 3.6 D \text{ pF}$$

the latter statistic meaning that a value for C_L computed from the formula below has a standard deviation in pF of 3.6 times the coil diameter in metres. Hence, Medhurst's formula, in its best state of optimisation is:

$C_L = \frac{4\epsilon_0}{\pi} \ell [1 + 0.8249(D/\ell) + 2.329(D/\ell)^{3/2}]$ [Farads]	$D/2 \gg p$	3.2 Medhurst refitted
--	-------------	---------------------------------

Our best estimate for the coefficient k_E/k_H using Medhurst's data and choice of fitting function is therefore:

$\frac{k_E}{k_H} = [1 + 0.8249(D/\ell) + 2.329(D/\ell)^{3/2}]$	Solid polystyrene former	3.3
--	--------------------------	------------

Equation (3.2) describes the data fairly well, but the pattern of residuals (observed minus calculated) is not random and, as mentioned above, the weighting required in order to obtain it is not realistic. This indicates that a different choice of fitting function will give a better result (i.e., a smaller standard-deviation of fit). There is however no point in pursuing this matter until we have solved the riddle of the missing dielectric constant.

4. Coil-former dielectric

All of Medhurst's coils were wound on solid polystyrene rods. No matter whether we subscribe to the 'capacitance-between-adjacent-turns' hypothesis, or to a transmission-line theory; even the most cursory consideration of the fields involved will tell us that the dielectric constant of the coil-former must appear in any expression for self-capacitance. In fact, it is odd that Medhurst did not raise this matter, especially since he did briefly consider the issue of dielectric losses in determining R_{ac} . If he accepted that the dielectric was penetrated by the electric field, then why did he assume that it would not affect the capacitance?

A clue to the conundrum can be had by plotting Medhurst's formula and comparing it against two lines: one being the long-coil asymptote for the case where the effective permittivity is the same as that of air, i.e.;

$$\frac{C_L}{D} = \frac{4\epsilon_0}{\pi} (\ell/D)$$

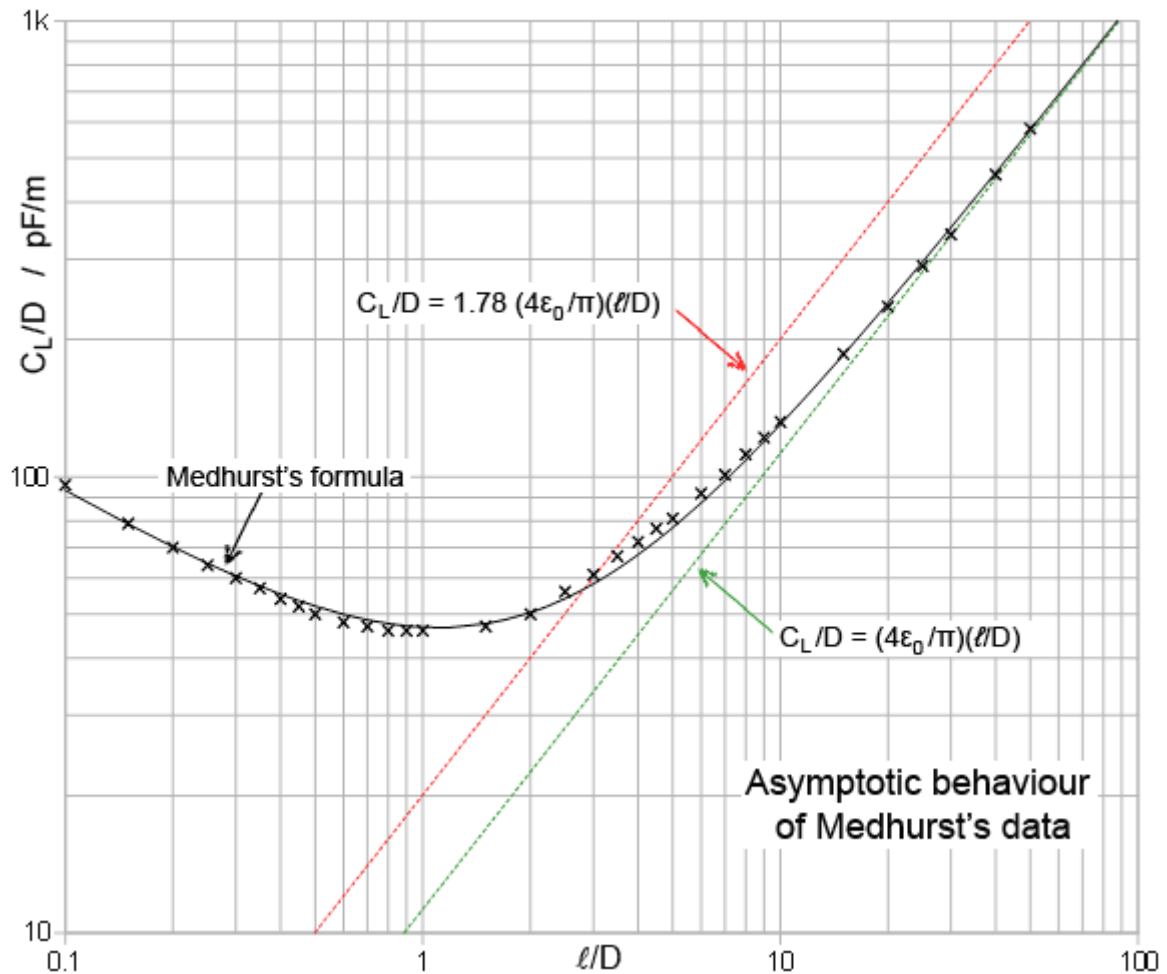
the other being the the long-coil asymptote for the case where the effective permittivity is the average of that of the coil former and the surrounding air. Medhurst made all of his measurements

⁶⁴ See worksheet: **Medhurst.ods**, sheet 1, downloadable from <http://www.g3ynh.info/zdocs/magnetics/appendix/self-res.html>

at frequencies in the range 460 kHz to 25 MHz. The dielectric constant of typical polystyrene in this region of the spectrum is 2.56. Hence the average relative permittivity is: $(2.56+1)/2 = 1.78$, and the asymptotic formula in that case is:

$$\frac{C_L}{D} = 1.78 \frac{4\epsilon_0}{\pi} (\ell/D)$$

The comparison is given in the graph below, with Medhurst's adjusted data superimposed⁶⁵.

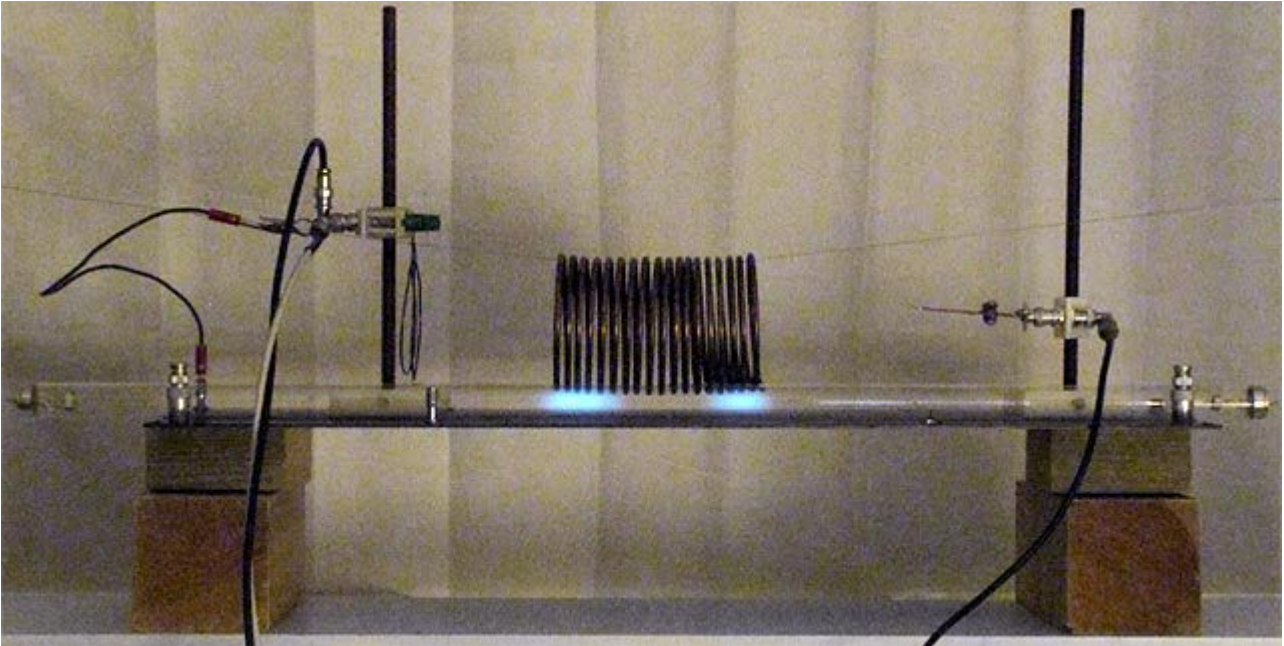


It is obvious that when the coils become long and thin, the data converge with the line corresponding to an effective relative permittivity of 1. This behaviour can be interpreted in one of two ways: *either* the coil former dielectric plays no part in determining the self-capacitance; *or* the effect of the coil former material diminishes as ℓ/D increases.

Medhurst obviously chose the first interpretation. He appears to have done so (despite having used the relationship between conductor length and SRF in deducing the asymptotic form) because he was attempting to interpret his findings according to the then prevailing wisdom: which is that self capacitance is composed of internal and external components. The internal component is the capacitance between adjacent turns, which he considered to be the minor contributor. The external component is the capacitance from the coil body to the ground plane, which he considered to be dominant. This gave him qualitative grounds for rejecting Palermo's theory, and presumably a reason for ignoring the coil former dielectric; but he seems to have decided to terminate the

⁶⁵ See worksheet: **Medhurst.ods**, sheet 2

investigation without pursuing the matter further. We can perhaps understand his lack of curiosity at this point by observing that the shortcomings of Palermo's work had practically doubled the amount of work he needed to do in order to complete his study of AC resistance, and the development of a universal formula for self-capacitance was not his objective. What is less excusable is the assumption, by several generations of engineers since then, that Medhurst's formula can be applied to all coils, rather than just to coils with solid polystyrene cores. That the self-capacitance of a coil is not due to the presence of a ground plane is demonstrated by the experiment illustrated below.



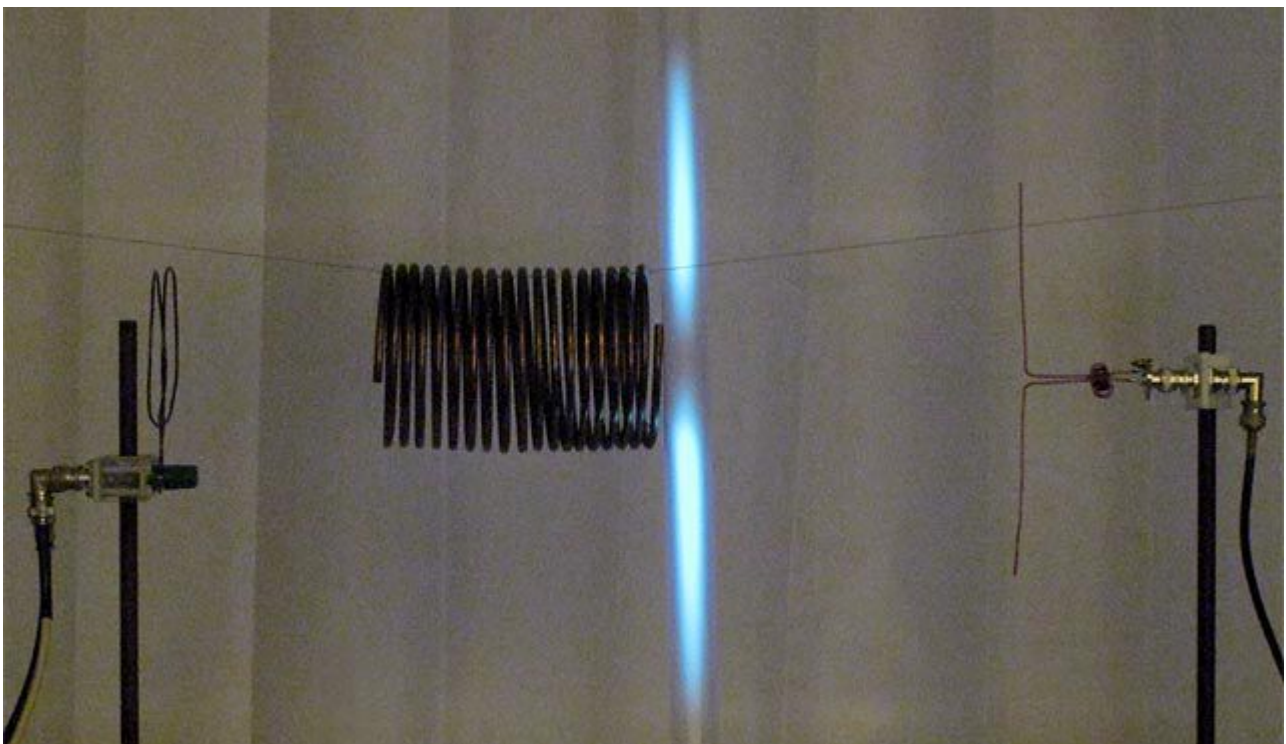
Effect of a ground plane on SRF: In this setup, the coil is suspended above an anodised aluminium plate, which is earthed to the outer shield of one of the cables connected to the induction loop. A 2 ft mercury-vapour tube (the same as was used in an earlier illustration) is laid on the plate close to the coil and parallel to the axis. At the fundamental parallel resonance frequency, the glow discharge in the tube shows that the field pattern is in accordance with a simple static capacitance in parallel with the coil. The added capacitance however, only reduces the resonant frequency from 26.7 MHz to 24.7 MHz (-7.5%), a surprisingly small change given that the ground plane is only 20 mm (0.2 coil diameters) away. Because the solenoid axis is parallel to the plate, the disposition is such as to minimise eddy currents. The principal interaction is therefore via the electric field. Using the electrical resonance formula, it is trivial to show that, if a coil is shunted by a capacitance equal to its self-capacitance, then its resonant frequency will be reduced by a factor of $1/\sqrt{2}$, i.e., a shift of -29%. Evidently, the ground plane capacitance is considerably less than the self-capacitance, and so it cannot be the principal component of the self-capacitance. Medhurst's ground-plane hypothesis therefore fails.

In this discussion, of course, we take the view that the SRF is a transmission-line resonance, in which case the disappearance of the coil-former permittivity from the long-coil asymptotic behaviour is not difficult to explain. Consider a wave travelling along the helix. In the middle region of the solenoid at least, the electric vector will be substantially perpendicular to the axis (actually, tilted by an amount equal to the pitch angle). The boundary conditions for the related sheet-helix problem also require that the electric field is continuous across the conducting wall⁶⁶, and while we will establish that this model is not appropriate here without modification, the continuity of the field is nevertheless the same. Hence the relative permittivity on the inside of the

⁶⁶ See, for example, Corum & Corum, cited earlier.

solenoid will affect wave propagation. When the circumference is small in comparison to the wavelength however, the electric field will be cylindrically symmetric. This means that the electric fields associated with wave propagation that penetrate into the interior of the solenoid from opposite sides will be almost equal and opposite. Therefore the radial fields on the inside of the solenoid will tend to cancel; the degree of cancellation being minimal when $\ell/D \ll 1$ and almost complete when $\ell/D \gg 1$.

The radial field cancellation effect is incidentally demonstrated by an ingenious experiment conducted by Lee et. al⁶⁷. These authors used an electrodeless piezoelectric sensor, transmitting its mechanical vibrations through a quartz rod to an electrical transducer outside the coil. This gives a relatively non-invasive method for sensing the field in both magnitude and direction. They confirm that the main field inside a solenoid is in the axial (induced voltage) direction and not the azimuthal (radial) direction.



Radial field pattern at the SRF: A gas discharge tube perpendicular to the coil axis mainly shows the radial field amplitude. This demonstration shows that the electric field is continuous across the solenoid wall. It also shows the axial node, which occurs because the phase-shift from turn-to-turn is small at this frequency (26.7 MHz), so that the E-field for helical propagation cancels at the axis.

It follows that self-capacitance can be conceived as the sum of two parts, although not as envisaged by Medhurst. If we define the relative permittivity external to the solenoid as ϵ_x and the relative permittivity on the inside as ϵ_i , then we need to re-derive the formula in such a way that:

$$\epsilon_r = \epsilon_x \quad \text{when } \ell/D \gg 1$$

and

$$\epsilon_r = \frac{(\epsilon_i + \epsilon_x)}{2} \quad \text{when } \ell/D \ll 1$$

⁶⁷ **Electric fields in solenoids.** S. Lee, Y Lee and I Yu., Japanese J Appl. Phys, 44(7a), 2005, 5244-5248.

i.e., for the latter case; when the diameter of the coil is large in comparison to the length, the effective permittivity tends to the average of the internal and external permittivities. It is worth noting here incidentally, that Sichak⁶⁸, in his study of helically-loaded coaxial lines, comes to the same conclusion in deriving his velocity factors.

A general first-order expression for coil self-capacitance was derived earlier as (2.4):

$$C_L = \frac{4\varepsilon}{\pi} \ell \frac{k_E}{k_H} \frac{1}{\cos^2 \psi}$$

We can still retain this general form, and satisfy the required asymptotic behaviour, by re-writing the equation as follows:

$$C_L = \frac{4\varepsilon_0}{\pi} \ell \left[\varepsilon_x + k_C \frac{(\varepsilon_x + \varepsilon_i)}{2} \right] \frac{1}{\cos^2 \psi}$$

Here the external relative permittivity ε_x has been separated from the original permittivity factor ε , and k_C is a coefficient that goes to zero when $\ell/D \gg 1$. Now factoring ε_x from the square bracket we have:

$$C_L = \frac{4\varepsilon_0 \varepsilon_x}{\pi} \ell \left[1 + \frac{k_C}{2} \left(1 + \frac{\varepsilon_i}{\varepsilon_x} \right) \right] \frac{1}{\cos^2 \psi} \quad (4.1)$$

which is in the same form as equation (3.2) (Medhurst's formula optimised) when $\varepsilon_x = 1$ and $\cos^2 \psi = 1$. Also noting that $\varepsilon_i = 2.56$ for Medhurst's data, we have an initial estimate for k_C from equation (3.3):

$$1.78 k_C = 0.8249 (D/\ell) + 2.329 (D/\ell)^{3/2}$$

i.e.,

$$k_C = 0.4634 (D/\ell) + 1.3084 (D/\ell)^{3/2}$$

68 **Coaxial Line with Helical Inner Conductor.** W Sichak. Proc. IRE. Aug. 1954. p1315-1319. Correction Feb. 1955, p148. See equations (5) and (6).

5. Empirically-corrected formula for self-capacitance

Now having the complete form for an expression for self-capacitance (at least, in as far as Medhurst's approach is valid), we can use Medhurst's data, or indeed good data from any source, to find an empirical expression for the coefficient k_C . We start by dividing both sides of equation (4.1) by D and rearranging:

$$\left[\frac{(C_L/D) \cos^2 \psi}{(\ell/D) (4 \epsilon_0/\pi) \epsilon_x} - 1 \right] \frac{2}{(1 + \epsilon_i/\epsilon_x)} = k_C \quad (5.1)$$

If Medhurst's data are used to evaluate k_C using this expression, it will be found that a roughly-straight line of negative gradient is obtained when $\log(k_C)$ is plotted against $\log(\ell/D)$. Hence, to a first approximation, there is a regression line having the form:

$$\ln(k_C) = k_1 - k_2 \ln(\ell/D)$$

We can, of course, make the gradient positive by inverting the argument of the logarithm on the right, i.e.:

$$\ln(k_C) = k_1 + k_2 \ln(D/\ell)$$

Fitting the data on this basis yields⁶⁹:

$$\ln(k_C) = 0.604 + 1.363 \ln(D/\ell)$$

Although the existence of a logarithmic relationship might be analytically significant however (see section 9); the fit, corresponding to a standard deviation of 4.7% for unit variance of an observation of unit weight ($\chi^2/\nu = 1$), is not as good as that obtained in the process of optimising Medhurst's formula (section 3). Hence a more complicated function with a greater number of adjustable parameters is needed.

Taking the exponent of the expression above gives a first approximation for k_C as:

$$k_C \approx \exp[\ln(1.83) + 1.363 \ln(D/\ell)]$$

where $\ln(1.83) = 0.604$. Hence:

$$k_C \approx 1.83 (D/\ell)^{1.363}$$

The fit can obviously be improved by replacing this with a polynomial in D/ℓ . Notice also that k_C must go to zero when ℓ/D is very large, i.e., when $D/\ell \rightarrow 0$. Hence the required polynomial has no zero-order (i.e., constant) terms. If the polynomial has a finite first-order term however, we can create a new expression with a finite zero-order term by multiplying throughout by ℓ/D ; i.e., if we have a starting expression:

$$k_C = k_1 (D/\ell) + k_2 (D/\ell)^2 + k_3 (D/\ell)^3 + \dots$$

then

⁶⁹ See worksheet: **Medhurst.ods**, sheet 3.

$$(\ell/D) k_C = k_1 + k_2 (D/\ell)^{p2-1} + k_3 (D/\ell)^{p3-1} + \dots$$

Fitting the data to an expression of this type is easily accomplished using a modified linear regression procedure, where the third and higher terms (if needed) are manually adjusted. The fact that we don't obtain uncertainties for the higher-order coefficients when we use this method doesn't matter, because we have no use for the uncertainty of a fitting parameter that is unrelated to any physical quantity. Hence we rearrange equation (5.1) so that $(\ell/D)k_C$ is the coefficient to be represented as a polynomial:

$$\left[\frac{(C_L/D) \cos^2 \psi}{(4\varepsilon_0/\pi) \varepsilon_x} - (\ell/D) \right] \frac{2}{(1 + \varepsilon_i/\varepsilon_x)} = (\ell/D) k_C \quad (5.2)$$

This expression is now taken to represent a simple polynomial of the form:

$$y = k_0 + k_1 x + k_2 x^2 + \dots$$

Note that the relationship between x and D/ℓ is yet to be decided; but by inspection of Medhurst's formula it should come as no surprise that something approaching an optimal fit is obtained when:

$$x = \sqrt{D/\ell}$$

In performing a least-squares fit, we must, of course, weight the data according to their relative uncertainties. Medhurst does not report the actual capacitances or diameters used in obtaining his table of C_L/D values, but by fitting the data initially with equal weights, it can be seen from the pattern of residuals that the largest C_L/D values have the greatest scatter. Also, the largest C_L/D values are those for long coils, and the data for long coils are least important because the long coil asymptotic behaviour is analytically defined. Hence it is reasonable to fit the data on the basis that the uncertainty in an observation is proportional to the absolute value of the observation, i.e.:

$$\delta(C_L/D) = u (C_L/D)$$

where u is a proportionate uncertainty (and $100u$ is a percentage uncertainty) common to the whole dataset. From this we can determine the uncertainty of a y value as:

$$\delta y = \frac{\partial y}{\partial (C_L/D)} \delta(C_L/D) = \frac{\partial y}{\partial (C_L/D)} u (C_L/D)$$

The derivative $\partial y/\partial(C_L/D)$ is obtained by differentiating (5.2):

$$\frac{\partial y}{\partial (C_L/D)} = \frac{\cos^2 \psi}{(4\varepsilon_0/\pi) \varepsilon_x} \frac{2}{(1 + \varepsilon_i/\varepsilon_x)}$$

Hence:

$$\delta y = u (C_L/D) \frac{\cos^2 \psi}{(4\varepsilon_0/\pi) \varepsilon_x} \frac{2}{(1 + \varepsilon_i/\varepsilon_x)}$$

which, for coils with external air dielectric and small pitch angle, reduces to:

$$\delta y = \frac{u(C_L/D)}{(4\epsilon_0/\pi)} \frac{2}{(1+\epsilon_i)}$$

The statistical weight of an observation is given by:

$$w_i = 1 / \delta y_i^2$$

and u is adjusted until the standard deviation of fit, $\sqrt{\chi^2/\nu} = 1$.

A good fit ($u = 0.021$) was obtained using the polynomial⁷⁰:

$$(\ell/D)k_c = k_0 + k_1\sqrt{D/\ell} + k_2(D/\ell)$$

where:

$$k_0 = 0.717439 \pm 0.027$$

$$k_1 = 0.933048 \pm 0.021$$

$$k_2 = 0.106$$

Thus:

$C_L = \frac{4\epsilon_0\epsilon_x}{\pi} \ell \left[1 + k_c \frac{(1+\epsilon_i/\epsilon_x)}{2} \right] \frac{1}{\cos^2 \psi} \quad \pm 2.1\%$	5.3 C_L-DAE
where $k_c = 0.717439(D/\ell) + 0.933048(D/\ell)^{3/2} + 0.106(D/\ell)^2$	

This will be referred to as the DAE (doubly-asymptotic, empirically corrected) formula for solenoid self-capacitance (generally applicable when the externally connected capacitance is $> C_L$). Note that there is little point in extending the polynomial; a standard deviation of 2.1% being about right for the data available (and the theory as it stands), and the absence of high-order terms making it reasonably safe to extrapolate.

Notice incidentally that the empirical constants have been retained to more decimal places than their uncertainties would seem to warrant. This is because, when using an empirical formula to reproduce a dataset, the best curve is always obtained by not rounding the determined coefficients (i.e., by retaining information to a few places beyond the uncertainty).

A Basic macro function for calculating self-capacitance from the DAE formula is given in the box below.

```
Function CLDAE(ff as double, ei as double, ex as double) as double
'Calculates solenoid CL/D [pF/m] using DAE formula. v1.01
'ff (form factor) is solenoid length / Diameter
Dim kc as double
kc = 0.717439/ff+0.933048*ff^-1.5 + 0.106/(ff*ff)
CLDAE = 11.27350207*ex*ff*(1+kc*(1+ei/ex)/2)
end function
```

⁷⁰ See worksheet **Medhurst.ods**, sheet 4

6. Inter-turn capacitance

A trivial investigation involving a Grid-Dip Oscillator and a set of engineer's callipers will confirm that the various resonances exhibited by a disconnected radio coil are associated with the total conductor length. It is therefore extraordinary that the self-capacitance of single-layer coils is often still attributed to the static capacitance that is presumed to exist between adjacent turns⁷¹. This warrants consideration of whether or not the inter-turn capacitance hypothesis is plausible, and whether or not it can provide insights into the properties of inductors.

The basic idea is that if we inspect a small region of a solenoid wall we see a set of wires lying parallel to each other. It is then presumed that there will be a capacitance between any chosen pair of wires; and that this capacitance can be calculated from physical dimensions. There is a small paradox inherent in the fact that every infinitesimal element of capacitance is shorted-out by a loop of wire of length $\ll \lambda$, but we will put that detail aside for the moment.

The capacitance between a parallel pair of conducting cylinders is given by Russell's formula⁷²:

$$C = \frac{\epsilon \pi h}{\ln \left[\frac{p}{d} + \sqrt{\left(\frac{p}{d}\right)^2 - 1} \right]} \quad [\text{Farads}] , \quad h \gg p , \quad h \gg d . \quad \text{Russell's formula} \quad (6.1)$$

Where h is the length of the cylinders, p is the distance from axis to axis, and d is the cylinder diameter. Note that, if the surrounding medium is air, $\epsilon = \epsilon_0$; and in old publications, $\epsilon_0 \times \pi$ is sometimes given approximately as $1/3.6$ pF/cm. Also:

$$\ln(x + \sqrt{x^2 - 1}) = \operatorname{arccosh}(x)$$

which gives rise to the compact form:

$$C = \frac{\epsilon \pi h}{\operatorname{arccosh}(p/d)} \quad [\text{Farads}] \quad (6.1a)$$

Since $\operatorname{arccosh}$ (inverse hyperbolic cosine) is a built-in function of spreadsheets and some programming languages, the latter formula is often convenient. Note that $\operatorname{arccosh}(1) = 0$, which means that the capacitance goes to infinity when the cylinders are just touching without making electrical contact.

Palermo

The 1934 paper of A J Palermo⁷³ was mentioned earlier as the source of Medhurst's frustrations. Palermo asserts that, since the voltage between adjacent turns is $1/N$ times the voltage across the whole coil, we should take the self-capacitance of the coil to be $1/N$ times the capacitance calculated using equation (6.1a). To calculate that capacitance he integrates over the whole coil (ignoring pitch angle), effectively choosing to identify $h = \pi DN$, and arrives at the formula:

71 Some authors don't even bother to give the coil ℓ/D ratio when reporting self-capacitance measurements.

72 See, for example: **Radio-Frequency Measurements by Bridge and Resonance Methods**, L. Hartshorn, Chapman & Hall, 1940 (Vol. X of "Monographs on Electrical Engineering", ed. H P Young). 3rd imp. 1942.

Ch VI, section 3: Calculation of capacitance. (Russell's formula for wires on p104).

73 **Distributed Capacity of Single-Layer Coils**, A J Palermo. Proc. IRE. Vol 22, No. 7, July 1934. p897-905.

$$C_L = \frac{\epsilon_0 \pi^2 D}{\operatorname{arccosh}(p/d)} \quad \text{Palermo's formula} \quad (6.2)$$

Relative permittivity is ignored, and there is no mention of coil-former dielectric anywhere in the paper.

Notwithstanding any doubts we might have about this approach, there is a straightforward mathematical error in the formula. The point of objection lies in the assumption that the turns overlap for the entire length of the wire; whereas there is no adjacent turn on the outside for the two turns at the ends of the coil. Hence Palermo should have taken h to be $\pi D(N-1)$, in which case he would have obtained the expression:

$$C_L = \frac{\epsilon_0 \pi^2 D(N-1)}{N \operatorname{arccosh}(p/d)} \quad \text{CT2T} \quad (6.3)$$

For the sake of working nomenclature, we will refer to this corrected version as "CT2T" (capacitance from turn to turn).

We cannot know whether Palermo started by making measurements and then derived his formula, or vice versa. It seems likely that he had at least one measurement available initially however, that of his coil No. 1. The coil was made from 2 turns of 6.24 mm diameter wire, with an average diameter of 74.7 mm and a pitch of 16.7 mm. Palermo measured the self-capacitance as 3.2 pF, and calculated 3.9 pF using an approximate version of equation (6.2). He considered this to be a "very severe test" of his formula; whereas, in view of the mathematical error, it is actually just a coincidence. Subsequent coils had turns numbers in the range of 5 to 112 however, in which case the difference between (6.2) and (6.3) is less significant.

Palermo reported a total of 19 self-capacitance measurements, 12 of which he carried out himself, and 7 of which were communicated to him by F W Grover of the National Bureau of Standards. It was in the group of measurements performed by Palermo himself that Medhurst found some of the numbers to be irreproducibly large. Later we will compare the measurements against the DAE formula and show that Medhurst was right to cry foul; but, in fact, the extent of the tampering was even greater than Medhurst had suspected.

Palermo's formula often produces values that are much too large. In such cases, he appears to have adopted the habit of adjusting the calculated value downwards and the measured value upwards in order to obtain plausible agreement⁷⁴. Since he acknowledges the help of F W Grover however, he was evidently not in a position to tamper with the NBS data; and so in that case he confined himself to writing down false calculation results. In the worst instance, his formula gives 27 pF, but he reports 12.9 pF to confer with an NBS measurement of 12.8 pF. There are other sleights of hand for those who wish to pursue the issue, but overall the paper is a travesty.

This, unfortunately, is the insalubrious basis on which the inter-turn capacitance hypothesis became part of electromagnetic folklore. What Palermo hoped to gain by promoting a defective theory is difficult to guess; but he was possibly motivated by an inability to accept failure after an early success. His formula was subsequently turned into tables and abacs to 'assist' the radio engineer; and his ideas diffused naturally into the textbooks to lie in wait for the unwary.

74 See worksheet `CL_theor_test.ods`, sheet 3.

GKMR

The 'capacitance between adjacent turns' hypothesis re-emerged in a new form in 1999, in a paper by Grandi, Kazimierczuk, Massarini and Reggiani (GKMR)⁷⁵. In the GKMR approach, the coil is considered to be equivalent to a set of wire rings. In that case, since there are $N-1$ gaps between N turns, the capacitance of an isolated coil is given by the capacitance between any pair of rings divided by $N-1$. The length of a ring is πD ; and so, using Russell's formula (6.1), and presuming the use of un-insulated wire, we have:

$$C_L = \frac{\epsilon_0 \pi^2 D}{(N-1) \ln \left[\frac{p}{d} + \sqrt{\left(\frac{p}{d}\right)^2 - 1} \right]} \quad \text{GKMR} \quad (6.4)$$

Grandi et al. support this derivation by measuring the capacitance of actual sets of wire rings. In doing so they demonstrate that the neglect of capacitance between non-adjacent turns is not important, and that the curvature of the wires does not significantly affect the validity of Russell's formula. The issue that must concern us here however, is that the wire-ring model does not have the magnetic field of the actual solenoid, and it does not consider the electromagnetic propagation that dictates the relationship between the electric and magnetic fields.

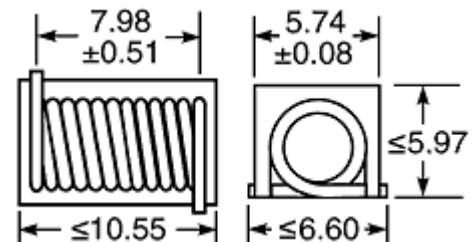
7. Comparison of self-capacitance formulae

A fair test of all of the self-capacitance theories discussed so far can be had by using data from a source with no theoretical axe to grind. Such data appear in the documentation for the Coilcraft Maxi Spring™ (132-xxSM) series of surface-mount air-core inductors⁷⁶ (pictured right), the guaranteed lower limit of SRF having been recorded to 3 decimal places. In fact these SRF data are extrapolations, made from jig measurements with finite stray capacitance, and so correspond to the pseudo-SRF calculated from the parallel combination of inductance and self-capacitance. Hence, using the published nominal inductance ($\pm 2\%$), they can be converted back to the self-capacitances they represent. What is particularly useful about this dataset is that the solenoid length ℓ and diameter D , and the wire diameter d , are constants. The only variables are the number of turns N and the pitch to wire diameter ratio p/d . Hence there is no ambiguity in deciding between theories that predict no or minimal variation in self-capacitance with turn-spacing, and those that make predictions to the contrary.



In order to test the various theories, the Coilcraft solenoid parameters were extracted from the published mechanical data as follows:

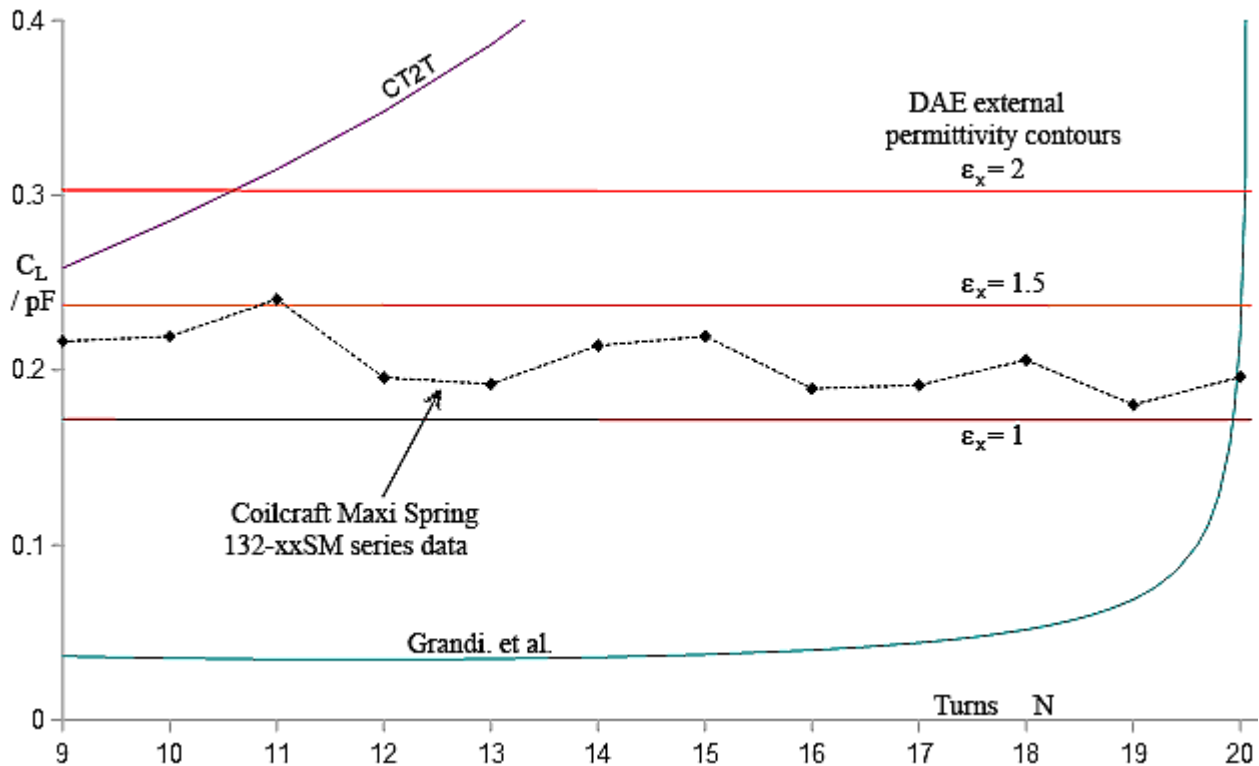
- Coil length: $\ell = 7.98 \pm 0.51$ mm
- Mean coil diam.: $D = 4.8$ mm (estimated)
- Wire diam.: $d = 0.397$ mm (estimated).



75 "Stray Capacitances of Single-Layer Solenoid Air-Core Inductors", G. Grandi, M K Kazimierczuk, A Massarini, U Reggiani. IEEE Transactions on Industry Applications, Vol 35, No. 5, Sept/Oct 1999, p1162-1168.

76 Coilcraft Maxi Spring Air Core Inductors. Document 185-1, 2003. www.coilcraft.com

Calculation results⁷⁷ are shown in the following graph:



The data are noisy, but there is obviously minimal correlation between the capacitance and the p/d ratio. Instead, the points lie slightly above the $\epsilon_x = 1$ external-permittivity contour from the DAE formula (5.3). The fact that the DAE prediction is a little low is explicable on several counts: Firstly, the experimental capacitances are calculated from the guaranteed minimum pseudo-SRF, and so correspond to a guaranteed 'no-greater-than' value. Secondly, each of the coils has a tight-fitting rectangular plastic cover, which touches the cylinder at three points around the circumference (see illustration given earlier). Thirdly, the coils have short connecting leads and so have slightly more wire than the helix parameters suggest.

The curve labelled "CT2T" is produced by the corrected version of Palermo's formula (6.3). The uncorrected version (6.2) is even worse and falls nowhere close to the data shown. The curve labelled "Grandi et al." is produced by the GKMR formula (6.4). The inter-turn-capacitance theories bear no resemblance to the data series, but all are capable of matching a single measurement by deliberate or accidental choice of turn-spacing. In the case of the GKMR formula, the turns need to be very close together in order for the coincidence to occur.

Interestingly, the theoretical work of Grandi et al. was supported by a single measurement on an actual coil, this having the very low p/d ratio of 1.02. The coil was wound using 16 turns of 10 mm diameter wire (presumably tubing), with a pitch of 10.2 mm maintained by using "plastic spacers" present for about 10% of the turn length. The type of plastic and its dielectric constant were not reported⁷⁸. The mean coil diameter D was 326 mm, and its length (Np) was 163.2 mm. The inductance of the coil was measured to be 82.3 μH at 10 kHz, and its (pseudo) SRF was 5.1 MHz, giving the self capacitance as:

⁷⁷ See worksheet: **CL_theor_test.ods**, sheet 2.

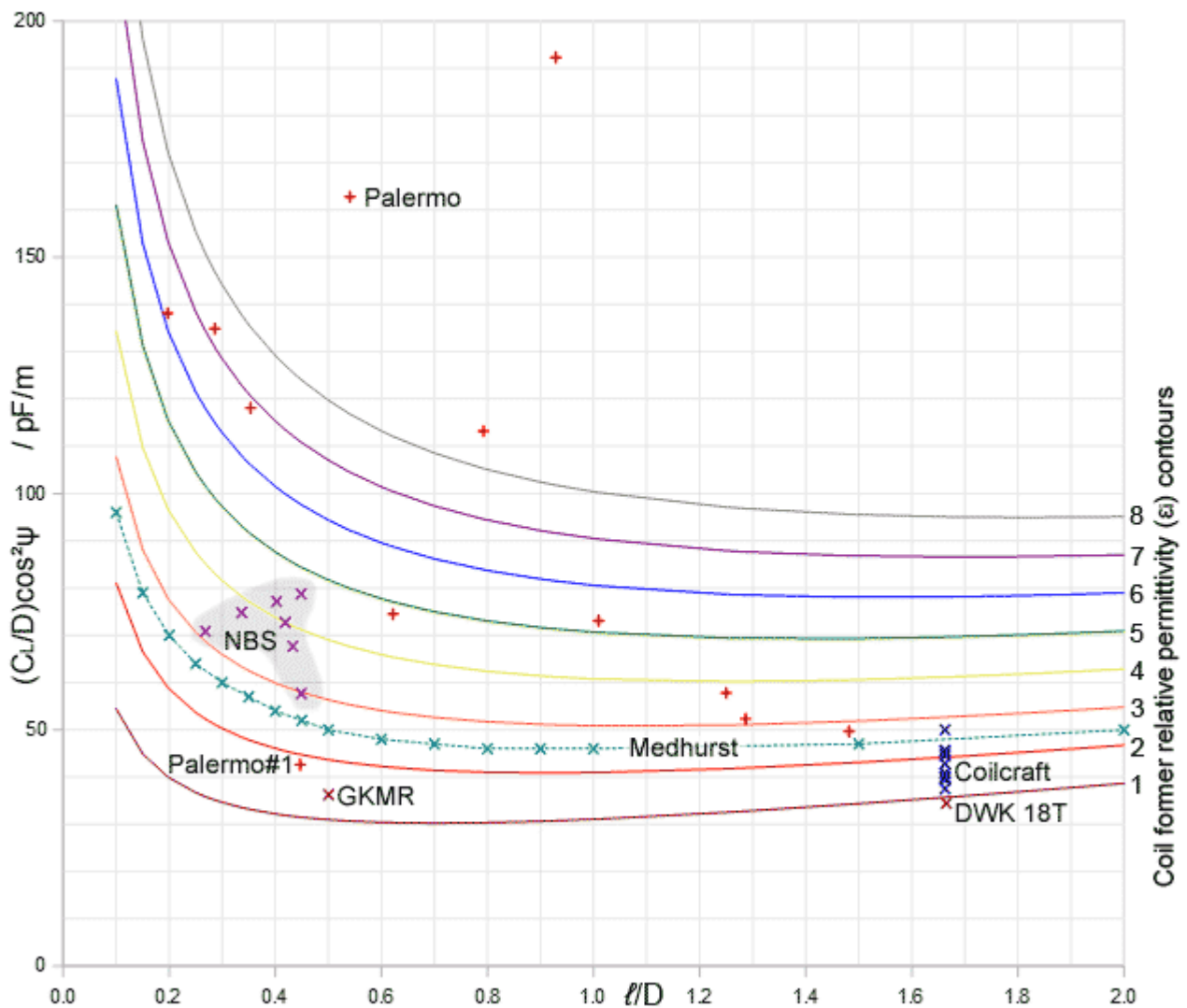
⁷⁸ The thickness and coverage suggest insulating tape.

$$C_L = \frac{1}{(2\pi f_{os})^2 L} = 11.83 \text{ pF}$$

Equation (6.4) (GKMR) predicts the capacitance to be 9.51 pF, and Grandi et al. argue that the higher value in practice is due primarily to the effect of the plastic spacers, and to a lesser extent to approximations used in the derivation of their formula. It seems curious however, given that the coil was robust enough to be self-supporting and that the spacers were bound to affect the capacitance, that the helix had to be compressed to the point where spacers were needed before the sole reported measurement was made.

The DAE formula (5.3) predicts the capacitance of the GKMR test coil to be 10.1 pF in the absence of dielectric materials. The DAE prediction, of course, is not greatly affected by turn spacing.

Of the self-capacitance prediction methods considered so far, all except the transmission-line related DAE approach have now failed. Hence it is interesting to compare the data discussed so far against a set of coil-former permittivity contours generated by the DAE formula⁷⁹. The data are shown plotted below as $(C_L/D) \cos^2\psi$ vs. l/D .



79 See worksheet: [CL_theor_test.ods](#), sheet 1.

The most arresting feature of the graph is the enormous scatter in the 'measurements' performed by Palermo. The six points above the curve for $\epsilon_i = 6$ are those that Medhurst suspected to be fake, and it is difficult to fault that conclusion; but the measurements falling below $\epsilon_i = 4$ might possibly be genuine. The result for Palermo's coil No. 1 lies above the $\epsilon_i = 1$ contour, even though the wire was thick enough to be self-supporting; but there might have been dielectric supporting material present during the measurement, and no details of any stray capacitance and lead corrections were given. His formula however predicts a value higher than his measurement, and he might simply have adjusted the result upwards.

The measurements supplied to Palermo by the NBS all fall in a tight group, despite the coils having turns numbers between 5 and 112. The situation, between the contours for $\epsilon_i = 3$ and $\epsilon_i = 5$, is consistent with the then (1934) standard practice of winding test inductors on wooden cylinders.

The measurement for the author's large air test coil⁸⁰ (DWK 18T) falls close to the $\epsilon_i = 1$ contour when either the inner or the average coil diameter is used. This is not a cheat, and neither was this measurement used in determining the empirical coefficients.

The remaining data have been discussed previously, and all lie above the $\epsilon_i = 1$ contour due (either arguably or reportedly) to the presence of dielectric material, or due to the measurement being an upper limit, or due to any uncorrected effects of connecting the coil to a measuring jig.

In summary, it is fair to say that theories that attempt to attribute the self-capacitance of single-layer solenoids to the inter-turn capacitance are wrong. In Palermo's case, the problem lies firstly in the assumption that a single wire can behave like two wires lying parallel, and secondly that the resulting capacitance should be divided by N . Logically, his theory is no better than a guess; which happens to work roughly for some coils, but has no actual predictive power.

The GKMR theory however is more plausible and challenges us to explain why it fails. A coil of wire is not a short-circuit at high frequencies. It can sustain a voltage across its terminals, and the current that flows is controlled by the resistive, inductive and capacitive elements of its impedance. If we cut the solenoid wall parallel to the axis and flatten it out, we will have a set of N parallel wires with $N-1$ gaps, and the capacitance of this structure is easily calculated. Why then is it not the self-capacitance of the coil?

The fallacy lies in the assumption that, since the coil can be modelled electrically as a set of lumped components, then the lumped components must have an independent existence within the coil. In fact, it is not even rigorous to assume that the resistance is independent of the reactance, but at least the error in that case is small provided that the Q is high. The GKMR theory fails because the reactive elements are primarily aspects an energy storage mechanism associated with the particular geometry of the helix. Cutting the coil open destroys the inductance, and thereby disrupts the all-important relationship between the electric and magnetic fields.

From the relationship between conductor length and self resonance, and from the ability of the coil to emit circularly polarised radiation when excited by linearly polarised radiation; we infer the existence of an electromagnetic wave propagating along the helix, and presume it to be a major reservoir of stored energy giving rise to the reactance. The overall field surrounding the coil will be the superposition of the fields from the individual turns. In this, the overall electric field will be at a maximum in a direction perpendicular to the wires and parallel to the pitch direction, i.e., it will be tilted away from being perpendicular to the coil axis by an amount equal to the pitch angle. If we cut the coil open lengthwise, the helical waveguide will cease to function, the structure will turn into a capacitor, and the principal direction of the electric field will switch to point parallel to the axis. It is this difference in the principal field directions between the static capacitance model and

the actual coil that causes the inter-turn capacitance hypothesis to fail.

It is conceivable however, that although a major part of the energy is stored in a propagating wave, the inter-turn capacitance might still exist as a parasitic component. In that case, we would need to include the GKMR capacitance in the total self-capacitance, and in correcting the DAE formula using actual data we might have missed a systematic offset. Fortunately, no such offset is evident, as can be seen by re-examining the graph comparing Coilcraft data and theory that was given earlier. When the spacing between turns is large, the GKMR formula predicts a small capacitance that is nearly independent of N . It is only when the gap between turns starts to close that the GKMR capacitance suddenly shoots up, but there is no corresponding trend in the data.

It was suggested by Medhurst, that the fact that the capacitance does not increase asymptotically when the gap between turns closes is due to the *proximity effect*; i.e., due to the tendency for the current streams in adjacent turns to repel each other when they are very nearly in phase. The proximity effect would indeed modify the asymptotic behaviour, but it does not explain the complete absence of observable effect.

We are drawn to the conclusion that the most prominent feature of the inter-turn capacitance hypothesis is that it consistently fails to explain any aspect of self-capacitance. This takes us back to an observation made at the beginning of this section, which is that the idea is paradoxical. If we draw a line between two points situated on adjacent turns, there will always be a loop of conductor connecting those points; and in the regime in which the concept of self-capacitance is valid (i.e., well below the SRF) the length of that loop will be small in comparison to the wavelength. Hence the inter-turn capacitance is shorted-out until the frequency becomes relatively high, an awkward fact that does not bode well for the derivation of a constant static capacitance by that method. This does not mean that there will be no 'adjacent turns' effect however, it is just that it will make a minor contribution.

8. Tubular coil formers

Medhurst was either wise or fortunate in his decision to wind his test coils on solid rods all made from the same material. Had he chosen to use tubes, or a variety of dielectrics, he would not have been able to fit his short-coil data successfully. That this is true is easily demonstrated by setting up the scattering experiment described in section 1.1. When cylindrical blocks of dielectric material are inserted into air solenoids suspended on the jig, a substantial reduction of the SRF occurs.

Most coil-formers used in practice are, of course, tubular. This gives us the problem of how to determine ϵ_i , which will be some weighted average of the permittivities of the solid dielectric and the air inside. Another issue is that of determining the fringe-field corrections for turns close to the ends of the coil (especially since the coil former permittivity only makes a substantial contribution to the self-capacitance of short coils). Unfortunately however, there is little in the way of quantitative information on the effect of discontinuous internal dielectrics. The best we will do here therefore, is to posit a first-order correction that is reasonably realistic.

Long coil correction

It seems likely that ignoring the effect of pitch angle will not cause any significant error. We will also ignore end effects, not because they will be negligible, but because there is no simple way of dealing with them. Under those conditions, for the case of a wave propagating along the helix, we only have to consider fields perpendicular to the solenoid axis. We will also restrict ourselves to the case in which the circumference of the cylinder is short in comparison to the wavelength, which means that there will be negligible phase shift from one turn to the next. Thus the electric field is radially symmetric, and its strength is at a maximum at the conducting wall and zero at the axis. Deducing the actual decay law however is no easy matter, and so we will make the crude first-order assumption that the decay will be roughly linear.

We now need to define the problem in such a way that dielectric close to the conducting wall has more effect than dielectric close to the coil axis. This can be done by considering the area under the curve of relative field strength vs. relative radius divided into regions having different dielectric constants. We will then assume that the average dielectric constant is weighted according to the relative areas in the two regions. This is a simple integration problem, so simple in fact that calculus is not needed.

In most practical situations, the medium in the hollow part of the cylinder will be the same as that outside the coil (i.e., air usually). Hence the inner medium is taken to have a dielectric constant ϵ_x . The coil-former tube is made from a material having a dielectric constant ϵ_f , and the tube has a relative wall thickness w .

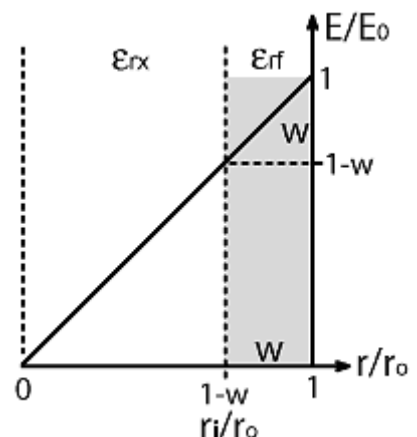
The total area under the curve is $\frac{1}{2}$. The area in the region having a dielectric constant ϵ_x is $(1-w)^2/2$. The area in the region having a dielectric constant ϵ_f is:

$$\frac{1 - (1-w)^2}{2}$$

Hence:

$$\epsilon_i = \epsilon_x (1-w)^2 + \epsilon_f [1 - (1-w)^2]$$

If r_o is the outside radius of the coil former, and r_i is the inside radius of the coil former, then:



$$1 - w = \frac{r_i}{r_o}$$

Hence:

$$\epsilon_i = \epsilon_x \left(\frac{r_i}{r_o} \right)^2 + \epsilon_f \left[1 - \left(\frac{r_i}{r_o} \right)^2 \right] \quad (8.1)$$

Note that in determining the internal permittivity in this way, it is assumed that there is no difference between r_o and the effective radius of the coil. Since the effective radius tends towards the inner solenoid radius (average radius - wire radius) at high-frequencies, this approximation is unlikely to cause a large error. In the current-sheet approximation, of course, the effective radius is the same as r_o by definition.

When using equation (5.3) to calculate self-capacitance, the internal permittivity parameter required is ϵ_i/ϵ_x . Hence, equation (8.1) can be conveniently rewritten:

$$\frac{\epsilon_i}{\epsilon_x} = \left(\frac{r_i}{r_o} \right)^2 + \frac{\epsilon_f}{\epsilon_x} \left[1 - \left(\frac{r_i}{r_o} \right)^2 \right] \quad (8.2)$$

It must be stressed that this is a very crude correction, which is offered strictly on the basis that any correction is better than no correction at all. As has been pointed out by Tuck Choy⁸¹, a simple volume-fraction averaging approach such as this will produce an upper bound for the effective permittivity, and will therefore tend to exaggerate the coil-former effect (he gives some suggestions as to how the estimate might be improved).

A volume averaging method for determining the effect of external dielectric support rods is given by Wallett and Qureshi⁸².

Short coil correction

As we will see in the next section, the coil also has an end-to-end capacitance arising from the induced axial field. Thus, for short coils in particular, the effect of the dielectric on the end-to-end capacitance will need to be taken into account and added to the long coil correction. Fortunately however, the internal axial electric field is fairly uniform⁸³ and an area weighting should be sufficient in that case.

81 **On the effects of dielectric or permeable formers on the inductance and self-capacitance of solenoids.** Tuck Choy 2015. Available from: <http://g3ynh.info/zdocs/magnetics/appendix/self-res.html>

82 **Review of slow-wave structures.** T M Wallett and A H Qureshi. Nasa Technical Memorandum 106639. 1994. <http://ntrs.nasa.gov/archive/nasa/casi.ntrs.nasa.gov/19940030764.pdf>
See page 2.

83 See, for example: **A visual demonstration of the electric field of a coil carrying a time-varying current**, F S Chute and F E Vermeulen, IEEE Trans. on Education, E24(4), Nov. 1981. This gives a tutorial on coil fields and also an ingenious demonstration of the electric field by means of resistive paper and temperature-sensitive liquid crystal material.

9. Axial induced electric-field capacitance

The analysis of Medhurst's data tells us that, in addition to the dynamic transmission-line capacitance, which is essentially a representation of time delay, there is also a substantial component that is so-far only accounted-for by the empirical correction. Since it has been demonstrated that this component has little or nothing to do with inter-turn capacitance, it becomes obvious that it must be associated with the voltage that develops across the ends of the coil. This is also apparent from the fact that the empirical correction makes little contribution in the long coil limit, but a large contribution when the coil is short. Isolating this apparently static component is of interest because it will lead to alternative self-capacitance formulae; and it will provide us with a starting point for the modelling of free-coil self-resonant behaviour.

Interestingly, it is feasible to invoke a notionally-static capacitance in order to account for self-capacitance in full. If we treat the end turns as electrodes, what we have is a capacitor stuffed with a special type of dielectric that, according to recent parlance, can be classified as a "metamaterial". An ordinary dielectric acquires its properties by virtue of the scattering of radiation from the atoms and molecules within; the emergent radiation being the superposition of the incident and scattered waves. A metamaterial, on the other hand, acquires its properties by the scattering of radiation from engineered structures. In the present case, we have a wire helix, which sustains an electric field and therefore has some dielectric quality. This medium is, of course, dispersive; but its permittivity will not change rapidly with frequency provided that we keep well away from the SRF. Thus, at low frequencies, we might usefully assume it to have a dielectric 'constant'. To derive an expression for that quantity is not straightforward, but we can at least see what the experimental data have to say about it.

The model in this case is a capacitor with parallel wire-ring electrodes; the wire diameter being d , the electrode separation being ℓ (i.e., the overall length of the coil), and the electrode circumference being πD . To the relative permittivity of the intervening metamaterial, averaged over all space, we will assign the symbol ϵ_h (h for helix). Thus, using Russell's formula (6.1a) we have:

$$C_{ee} = \frac{\epsilon_0 \epsilon_h \pi^2 D}{\operatorname{arccosh}(\ell/d)} \quad [\text{Farads}] \quad , \quad (9.1)$$

Now, since we do not know ϵ_h , we can simply set it to 1 and see how the result compares against some actual measurements⁸⁴. As can be seen from the table below, the formula produces plausible but somewhat low estimates of the self-capacitances of air-cored coils.

Coil	ℓ/D	D / mm	C_L Meas. / pF	C_{ee} / pF, $\epsilon_h = 1$	C_{ee} / D / pF/m	$\epsilon_h = C_L / C_{ee}$
Palermo No. 1	0.45	74.7	3.2	2.76	37.0	1.16
GKMR	0.50	326	11.83	8.18	25.1	1.45
DWK 18T	1.58	91.3	3.15	2.01	21.0	1.54
Coilcraft 132-xxSM series	1.66	4.8	0.205 (mean)	0.114	23.7	1.80

It is surprising that advocates of the fully-static origin of self-capacitance have never discovered this simple formula. Had they done so it would have given good service, being more accurate than any of the inter-turn capacitance theories, and actually better than Medhurst's formula when the coil is short and has no core. Also, there is some indication of scalability, as can be seen from the value of

⁸⁴ Worksheet: [CL_axial-field.ods](#), sheet 1.

C_{ee}/D obtained.

The end-to-end capacitance obtained by treating the two end turns as a pair of wire rings of course suggests itself as a candidate for the axial-field component. This approach was used by Chute and Vermeulen⁸⁵; but it produces a first-order dependence of self-capacitance on the wire diameter that is not evident in the experimental data. From a practical point-of-view also, it forces us to include a parameter that is not needed and is often not reported.

The axial field is induced because there is requirement (i.e., a boundary condition) that the circumferential electric field induced by the time-alternating axial magnetic field must be completely cancelled in the helix direction at the conducting surface (assuming a perfect conductor). Thus the axial field is related to the overall field dynamics and is not strongly influenced by the wire thickness. Instead, we know to a good first-order approximation, that the total self-capacitance is a function of ℓ/D even when the coil is short, and so we must expect the axial component to have the same dependence.

So let us see if we can reverse-engineer the axial-field capacitance from the data. To do that we can separate the solenoid self-capacitance into two components thus:

$$C_L = C_T + C_E$$

where C_T is the capacitance representing the time delay for a wave travelling along the helix, and C_E is the axial electric-field component defined in such a way that $C_E \rightarrow 0$ as $\ell/D \rightarrow \infty$.

Assuming that the external medium is air, we know from Medhurst's data, that the helical phase velocity tends towards c as $\ell/D \rightarrow \infty$ (see section 4). This is actually at odds with Drude's data for the resonances of disconnected coils, a matter to which we will turn our attention in section 10, but it is nonetheless true. Consequently, an expression for C_T is given by setting k_E to 1 in equation (2.6). It lacks any provision to account for coil-former dielectric however, and so we will start by considering only the air-cored case. Also, we will presume that the magnetic-field inhomogeneity parameter is well-approximated by Nagaoka's coefficient (k_L), in which case we have:

$$C_T = \frac{4\epsilon}{\pi} \frac{\ell}{k_L \cos^2 \psi}$$

and for coils with closely-spaced turns:

$$C_T = \frac{4\epsilon}{\pi} \frac{\ell}{k_L} \tag{9.2}$$

Now observe that, if we put $\epsilon_i = \epsilon_x = 1$ into the DAE formula (5.3), we have a curve that corresponds to Medhurst's empirical data corrected back to air core.

$$C_L = \frac{4\epsilon_0}{\pi} \ell (1 + k_c) \tag{9.3}$$

Certainly there is an assumption inherent in the way in which the effect of the polystyrene former was removed, but it is not unrealistic. Thus we have tentative a way of isolating C_E .

So now, to find an expression for C_E , we might imagine a virtual electrode structure that will allow us to model the difference between the long-coil and the short-coil field as a static capacitance. This is just something to account for the distribution of electric field lines extending

85 **On the self-capacitance of solenoidal coils.** F S Chute and F E Vermeulen. Canadian Elec. Eng. J., Vol 7(2), 1982, p31-37. See equations (16) - (19) and associated discussion.

from one end of the coil to the other when the radial field is taken away. As mentioned before; such an origin suggests that it will not look like the capacitance between the two ends when the middle of the coil is removed; because phenomena related to external impedance (and concerning fields that extend some distance from the coil) will not be greatly affected by the diameter of the wire. We should also note that when the length to diameter ratio (ℓ/D) of a solenoid goes to zero, the first turn is superimposed upon the last, and the self-capacitance due to end-effects will tend towards infinity. That certainly is where the data for short coils appear to be heading, and we should look for a first order dependence on ℓ/D that agrees.

It turns out that if we try to model the capacitance as being due to a set of plates, then the resulting curve does not fit the data. Beyond that however, there are various possibilities reminiscent of Russell's formula (6.1 or 6.1a), one of which is:

$$C_L = C_T + \frac{k_A \epsilon_0 \pi^2 D}{\operatorname{arccosh}(1 + \ell/D)} \quad (9.4)$$

where the empirical coefficient $k_A = 0.2308$. Compared against 150 points calculated from the DAE formula (8.3), logarithmically spaced over a ℓ/D range from 0.1 to 100, this gives a standard deviation of fit of 1.29 pF/m in the calculation of C_L/D . Bearing in mind that the DAE formula involves assumptions and has a standard deviation of fit of 2.1%, this means that the the two curves are statistically indistinguishable; i.e., given some physically reasonable way of removing the effect of the coil-former dielectric, (8.4) should fit Medhurst's data just as well as the DAE formula⁸⁶

Another formula, which gives an even better fit is:

$$C_L = C_T + \frac{4 \epsilon_0 D}{\ln(1 + \pi^2 \ell/D)} \quad (9.5)$$

i.e.,

$$\frac{C_L}{D} = \frac{4 \epsilon_0}{\pi} \left[\frac{(\ell/D)}{k_L} + \frac{\pi}{\ln(1 + \pi^2 \ell/D)} \right] \quad (9.6)$$

Over the same data ranges as before, this gives an SD of fit of 1 pF/m. This curve is shown on the graph below for comparison with the DAE curve with $\epsilon_i = 1$ (dotted). Shown also are the separate components C_T and C_E . Note that, although this curve has no empirical parameters, it is still empirical. It is also just as good as the DAE formula for air-cored coils, but lacks any correction for coil-former dielectric.

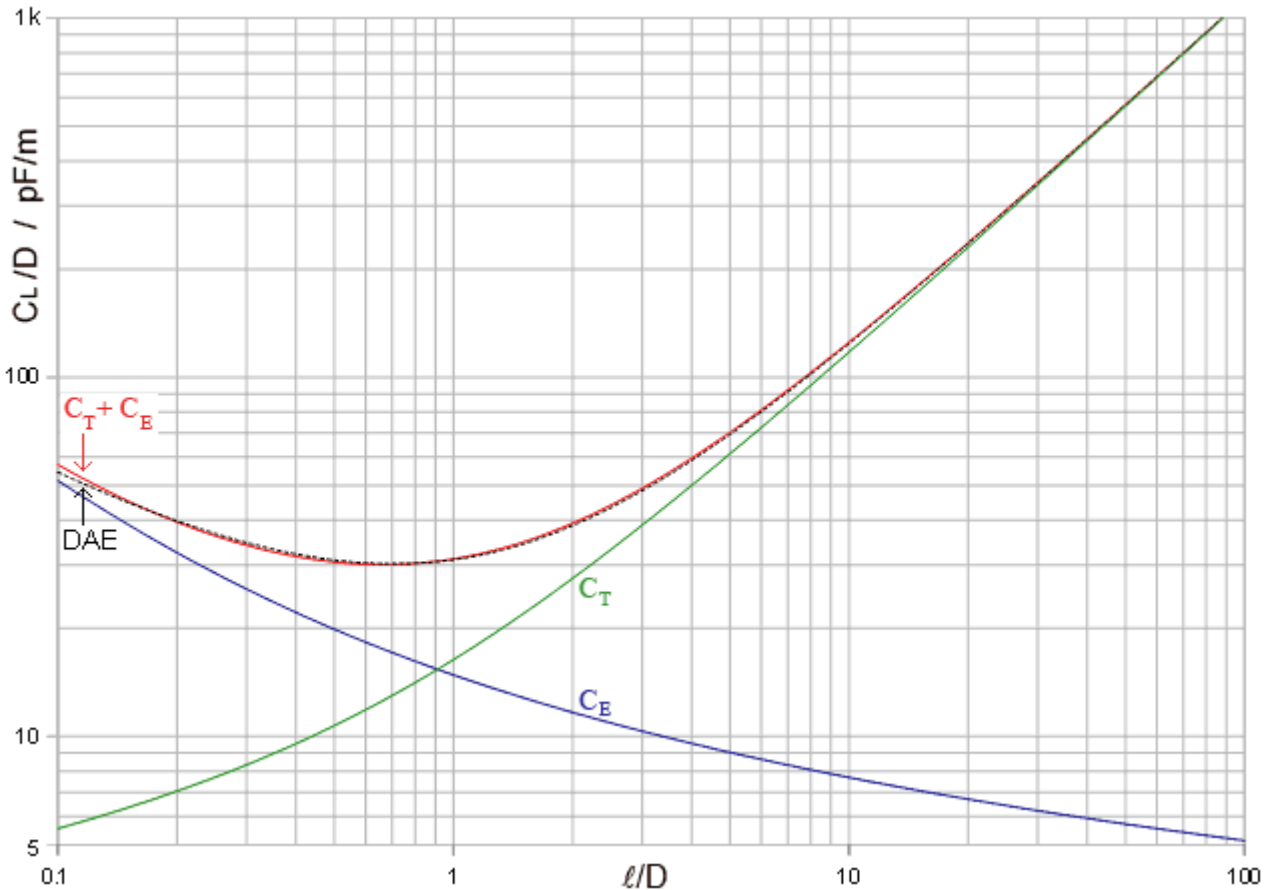
From equation (9.5), the axial-field capacitance is proportional to the coil diameter and can be written as:

$$\frac{C_E}{D} = \frac{4 \epsilon_0}{\ln(1 + \pi^2 \ell/D)} \quad (9.7)$$

While the transmission-line delay capacitance per unit diameter, on the assumption that $v_{hx}=c$, is by definition:

$$\frac{C_T}{D} = \frac{4 \epsilon_0 (\ell/D)}{\pi k_L} \quad (9.8)$$

Note that (9.8) grows with ℓ/D , while (9.7) diminishes, leading to a curve of roughly parabolic appearance (on a logarithmic scale) when the two are added. Both formulae are of course scaleable to account for the immersion of the coil in homogeneous media of any dielectric constant, simply by multiplying ϵ_0 by ϵ_r , but they lack any provision for dealing with coil former dielectric or thick wire insulation.



Self capacitance represented as the sum of a time-delay component and an induced electric-field component. The time delay component is curved because Nagaoka's coefficient is required to convert it into a capacitance via the resonance formula.

Correction for internal dielectric

Equations (9.6) - (9.8) lack any provision for dealing with coils having a difference between the internal and external dielectric constant, i.e., coils wound on formers. Such correction needs to be applied to the transmission-line and induced-field parts separately, but it is likely that the same approach as was used in section 4 will also work here to a good first-order approximation, i.e., the effective relative permittivity will be: $\epsilon_r = \epsilon_x$ when $\ell/D \gg 1$ and $\epsilon_r = (\epsilon_i + \epsilon_x)/2$ when $\ell/D \ll 1$ (subscripts i and x being for 'internal' and 'external'), with a simple weighting to bridge the two extremes. On this basis, the general form of an expression for self-capacitance was given as equation (4.1). It can be rewritten as capacitance per unit diameter thus:

$$\frac{C_L}{D} = \frac{4\epsilon_0\epsilon_x}{\pi} (\ell/D) \left[1 + k_c \frac{(1 + \epsilon_i/\epsilon_x)}{2} \right] \frac{1}{\cos^2 \psi} \quad (9.9)$$

This expression should be compared with the prototype self-capacitance expression (2.6), which can also be written per unit diameter thus:

$$\frac{C_L}{D} = \frac{4\varepsilon}{\pi} (\ell/D) \frac{k_E}{k_H} \frac{1}{\cos^2 \psi}$$

From this we can see that the correction coefficient k_E/k_H is modified to include the effect of the coil former by using the substitution:

$$\frac{k_E}{k_H} = 1 + k_C \frac{(1 + \varepsilon_i/\varepsilon_x)}{2}$$

Where k_E and k_H are the generalised electric and magnetic field non-uniformity corrections, and k_C is the overall correction coefficient that was determined empirically in section 5.

We can use a similar substitution to include the effect of coil-former dielectric in the expression for time-delay capacitance. Also, at this point, we might as well restore the pitch-angle dependence by including the $1/\cos^2 \psi$ factor. Equation (9.8) now becomes:

$$\frac{C_T}{D} = \frac{4\varepsilon_0}{\pi} (\ell/D) \frac{1}{k_L} \frac{1}{\cos^2 \psi} \quad (9.10)$$

where k_L is Nagaoka's coefficient. What has happened here, of course, is that we have taken out the electric field correction, and adopted the current-sheet approximation for inductance so that there is no need to worry about the details of the winding-wire. Thus we have a new overall correction coefficient, which we will call k_{CT} (the time delay part of k_C). Thus:

$$\frac{1}{k_L} = 1 + k_{CT} \frac{(1 + \varepsilon_i/\varepsilon_x)}{2}$$

and, by putting $\varepsilon_i = \varepsilon_x = 1$, we can identify k_{CT} as:

$$k_{CT} = \frac{1}{k_L} - 1$$

Using this, we can write a complete expression for the time-delay capacitance per unit coil diameter thus:

$$\frac{C_T}{D} = \frac{4\varepsilon_0 \varepsilon_x}{\pi} (\ell/D) \left[1 + \left(\frac{1}{k_L} - 1 \right) \frac{(1 + \varepsilon_i/\varepsilon_x)}{2} \right] \frac{1}{\cos^2 \psi} \quad (9.11)$$

Various rearrangements are possible depending on preference, but the following one is interesting:

$$\frac{C_T}{D} = \frac{4\varepsilon_0 \varepsilon_x}{\pi} (\ell/D) \frac{1}{2} \left[\frac{1}{k_L} + 1 + \left(\frac{1}{k_L} - 1 \right) \frac{\varepsilon_i}{\varepsilon_x} \right] \frac{1}{\cos^2 \psi} \quad (9.11a)$$

We can now factor $1/k_L$ from the square bracket thus:

$$\frac{C_T}{D} = \frac{4\varepsilon_0\varepsilon_x}{\pi} (\ell/D) \frac{1}{k_L} \frac{1}{2} \left[1 + k_L + \frac{\varepsilon_i}{\varepsilon_x} (1 - k_L) \right] \frac{1}{\cos^2 \psi}$$

This has restored the form of equation (9.10) except for a relative permittivity factor

$$\varepsilon_r = \frac{\varepsilon_x}{2} \left[1 + k_L + \frac{\varepsilon_i}{\varepsilon_x} (1 - k_L) \right] \quad (9.11b)$$

which uses Nagaoka's coefficient (a function of ℓ/D) to determine the effective average of the internal and external permittivities. Recall also that the limiting behaviour of k_L is: when $\ell/D \rightarrow 0$, $k_L \rightarrow 0$, and when $\ell/D \rightarrow \infty$, $k_L \rightarrow 1$.

Now that we have equation (9.11), of course, we can easily obtain an expression for the induced-field capacitance C_E by subtracting C_T from the total self-capacitance as given by the DAE formula (5.3), i.e.;

$$C_E = C_L - C_T$$

It is more informative however to represent that part of self-capacitance not due to time delay using a modified form of Russell's formula. To do that, we can put (say) equation (9.6) into the form of equation (9.9), starting with $\varepsilon_i = \varepsilon_x = 1$. Thus:

$$\frac{C_L}{D} = \frac{4\varepsilon_0}{\pi} (\ell/D) \left[1 + \frac{1}{k_L} - 1 + \frac{\pi(D/\ell)}{\ln(1 + \pi^2 \ell/D)} \right] \frac{1}{\cos^2 \psi}$$

Comparing this with (9.9), we can immediately see that the function k_C can be written:

$$k_C = \frac{1}{k_L} - 1 + \frac{\pi(D/\ell)}{\ln(1 + \pi^2 \ell/D)}$$

This quantity can be compared with the empirically determined k_C of equation (5.3) and it will be found that the two functions are in good agreement. Now inserting the effects of internal and external dielectrics, we obtain a new formula for self capacitance:

$$\frac{C_L}{D} = \frac{4\varepsilon_0\varepsilon_x}{\pi} (\ell/D) \left[1 + \frac{(1 + \varepsilon_i/\varepsilon_x)}{2} \left(\frac{1}{k_L} - 1 + \frac{\pi(D/\ell)}{\ln(1 + \pi^2 \ell/D)} \right) \right] \frac{1}{\cos^2 \psi} \quad (9.12)$$

Putting $\cos^2 \psi = 1$, $\varepsilon_x = 1$ and $\varepsilon_i = 2.56$ (polystyrene), this formula fits Medhurst's data with an estimated standard deviation of fit of 2.4% and *no variable parameters*⁸⁷. This is not quite as good as the fitted-polynomial DAE formula (5.3), which has an ESD of 2.1%, but there is no reason to presume that the DAE formula will give any more accurate predictions of self-capacitance than (9.12), and the latter has the advantage of being a representation of the preceding arguments relating to the physical origins of self-capacitance.

Now comparing (9.12) with (9.11) we can see that an expression for the axial induced-field capacitance can be obtained by subtraction. Also, although it does not appear to be mathematically rigorous to do so, we must drop the $1/\cos^2 \psi$ factor, because it is not applicable to the induced-field component. The reason for this adjustment is that there is an approximation in the original

⁸⁷ See worksheet **Medhurst.ods**, sheet 4.

derivation (section 2.2) due to the assumption that the self-capacitance of a coil is primarily associated with helical wave propagation. This required the $1/\cos^2\psi$ factor in order to ensure that the conductor length remained correct when ℓ/D was allowed to vary, with any corrections applied being treated as acausal at that point, and therefore a function of conductor-length by default. It turns out, of course, that one part of the correction, the time-delay part, is a function conductor length; but the axial-field part is actually a function of *coil length*.

So, to obtain the axial-field part we subtract (9.11) from (9.12) and delete the $1/\cos^2\psi$ factor, which leaves:

$$\frac{C_E}{D} = \frac{4\epsilon_0\epsilon_x}{\pi} (\ell/D) \frac{(1+\epsilon_i/\epsilon_x)}{2} \left(\frac{\pi(D/\ell)}{\ln(1+\pi^2\ell/D)} \right)$$

i.e., after cancellation and rearrangement:

$$\frac{C_E}{D} = \frac{2\epsilon_0(\epsilon_x + \epsilon_i)}{\ln(1+\pi^2\ell/D)} \quad \cdot \quad \text{Axial induced-field capacitance / unit diameter} \quad (9.13)$$

Thus we obtain a complete expression for axial-field capacitance by a circuitous route and discover that, while the time-delay capacitance (9.11) has a weighting function based on Nagaoka's coefficient to determine the relative contributions of ϵ_i and ϵ_x as the coil shape varies, the axial-field component is only dependent on their average. It derives its long-coil asymptotic behaviour instead from the fact that its contribution dies out completely.

Now we can give the properly corrected new formula for self-capacitance as the sum of (9.11) and (9.13):

$\frac{C_L}{D} = \frac{4\epsilon_0\epsilon_x(\ell/D)}{\pi \cos^2\psi} \left[1 + \left(\frac{1}{k_L} - 1 \right) \frac{(1+\epsilon_i/\epsilon_x)}{2} \right] + \frac{2\epsilon_0(\epsilon_x + \epsilon_i)}{\ln(1+\pi^2\ell/D)}$	<p style="margin: 0;">(9.14) C_L-TDE</p>
--	--

This will be referred to as the TDE (time-delay + induced electric-field) formula. Note that there might be some utility in factoring ϵ_0 and ϵ_x from both major terms during calculation, but the above representation draws attention to the essential separability. Also, it is worth noting that, when modifying the formula to allow for the effect of a hollow coil former, the effective value of ϵ_i will be different for the two parts (see section 8).

Shown in the following box are verified Open Office Basic macro functions for implementing the TDE calculation. Function CTDW(ℓ/D ; ϵ_i ; ϵ_x) performs the time-delay part of the capacitance calculation and returns capacitance per unit diameter, i.e., C_T/D . It ends with 'W' because it uses an approximate formula for Nagaoka's coefficient, W82W(D/ℓ), which is accurate to within ± 20.5 ppm. There is also a version CTDN(ℓ/D ; ϵ_i ; ϵ_x), which uses the full elliptic integral calculation, but given the approximations inherent in self-capacitance calculation, there is no statistically significant gain in using it. Function CIAE(ℓ/D ; ϵ_i ; ϵ_x) returns C_E/D . Self capacitance is calculated using:

$$\frac{C_L}{D} = \frac{\text{CTDW}(\ell/D; \epsilon_i; \epsilon_x)}{\cos^2\psi} + \text{CIAE}(\ell/D; \epsilon_i; \epsilon_x) \quad \cdot$$

The $1/\cos^2\psi$ factor in the first term can be omitted for coils of small pitch angle.

```

Function CTDW(ff as double, ei as double, ex as double) as double
' Calculates solenoid time delay capacitance, CT/D [pF/m]. ff is solenoid length / Diameter
' Quick version using W82W for Nagaoka's coeff. D W Knight. v1.00, 2016-03-16
Dim kct as double, kL as double
kL=W82W(1/ff)
kct = 1/kL - 1
CTDW = 11.27350207*ex*ff*(1+kct*(1+ei/ex)/2)
end function

-----

Function CIAE(ff as double, ei as double, ex as double) as double
' Calculates induced axial E-field component of solenoid self-C, CT/D [pF/m].
' D W Knight. v1.00, 2016-03-16 . ff is solenoid length / Diameter
CIAE = 17.70837564*(ei+ex)/log(1+pi*pi*ff)
end function

-----

Function W82W(byVal x as double) as double
' calculates Nagaoka's coeff. using Wheeler's 1982 eqn (7) as modified by Bob Weaver88.
' Max error is +/- 21ppM. x = Diam/length. D W Knight, v1.00, June 2012.
if x = 0 then
  w82w = 1
else
Dim zk as double, k0 as double, k2 as double, p as double, w as double
zk = 2/(pi*x)
k0 = 1/(log(8/pi)-0.5)
k2 = 24/(3*pi*pi -16)
w = -0.47/(0.755 + x)^1.44
p = k0 +3.437/x +k2/(x*x) +w
W82W = zk*(log(1 + 1/zk) + 1/p)
end if
end function

```

Finally, we can turn to the question of whether or not the axial induced-field capacitance formula (9.13) will also apply to free coils. On the plus side, it does not involve Nagaoka's coefficient, and so is not linked to the uniform-current inductance. We cannot however expect the axial field to remain exactly the same when the current becomes non-uniform. Nevertheless, the determined capacitance will still be approximately valid for short coils, because it is instrumental in maintaining the current, and so its accuracy will die off as its contribution dies off.

⁸⁸ See: **Solenoid Inductance calculation**: D W Knight. http://www.g3ynh.info/zdocs/magnetics/part_1.html. Section 8e. Also: <http://electronbunker.ca/eb/CalcMethods3b.html>

10. Velocity limiting

In sections 1.2, 1.7 and 1.8, we showed solenoid self-resonance data for isolated coils plotted as velocity factor vs. ℓ/D . Medhurst's data can also be plotted in this way; and since the DAE formula is a best-fit curve for Medhurst's measurements when ϵ_i is set to 2.56, it can be used as a smoothed continuous version. The DAE formula moreover has the advantage that ϵ_i can be set to 1, so that it can be compared directly with results for coils in the absence of dielectric material other than air. This, as we will see, is an instructive exercise.

Medhurst's formula for self-capacitance was obtained by fitting measurements to a curve of C_L/D vs. ℓ/D . As he also pointed out however⁸⁹, it is possible to plot the same data as wavelength / conductor length vs. ℓ/D . This gives a curve which, although he did not identify it as such, is proportional to the reciprocal of the apparent velocity factor for helical propagation. He performed his derivation using cgs units, and so we will repeat it using rationalised mks (SI).

Medhurst's formula, and the DAE formula of course, permit the calculation of a capacitance that, if put into the electrical resonance formula with the coil inductance, will give a pseudo-SRF rather than an actual SRF. The discrepancy, as we have already noted, occurs because the data do not fit on the Howe-extrapolation regression-line when the magnitude of the shunt impedance is large (i.e., approaching an open-circuit). It seems therefore that the Howe method produces an in-circuit value of self capacitance, and this points to a virtual self-resonance that is not the same as the actual one. Still, let us assume that this virtual SRF exists and is the resonance that would be seen if a uniform current distribution could be maintained along the conductor at the SRF. So now we have:

$$f_{0s(v)} = \frac{1}{2\pi\sqrt{LC_L}}$$

Where $f_{0s(v)}$ is the virtual self-resonance predicted using the uniform-current inductance L in conjunction with in-circuit measurement techniques for self-capacitance. We have formulae that return C_L/D however, so the resonance becomes a function of diameter thus:

$$f_{0s(v)} = \frac{1}{2\pi\sqrt{L(C_L/D)D}}$$

where (C_L/D) can be the output of a program routine or calculation such as C_LDAE (section 5), or actual data. The free space wavelength associated with this frequency is given by:

$$\lambda_{0s(v)} = \frac{c}{f_{0s(v)}}$$

so that

$$\lambda_{0s(v)} = 2\pi c\sqrt{L(C_L/D)D} \tag{10.1}$$

Now, on the basis that the current-sheet approximation for inductance (better than 2% for coils of small pitch angle) is sufficiently accurate for this investigation, we can substitute for L using the SI formula.

$$L = \mu_0 \frac{\pi D^2}{4 \ell} N^2 k_L \quad \text{Current-sheet inductance}$$

89 Medhurst 1947. Cited earlier. See page 86, Table VI, Fig. 10 and derivation.

where k_L is Nagaoka's coefficient. Using this in (10.1) gives

$$\lambda_{0s(v)} = 2\pi c \sqrt{\mu_0 \frac{\pi D^2}{4\ell} N^2 k_L (C_L/D) D}$$

Now removing D^2 and N^2 from the square-root argument and rearranging we get:

$$\lambda_{0s(v)} = \pi D N c \sqrt{\mu_0 \pi k_L (C_L/D) (D/\ell)} \quad (10.2)$$

but, as was given earlier as equation (2.2), the length of wire used to wind a solenoid coil is:

$$\ell_w = \frac{\pi D N}{\cos \psi}$$

where ψ is the pitch angle. For coils with many turns, $\cos \psi \approx 1$, in which case (10.2) gives:

$$\frac{\lambda_{0s(v)}}{\ell_w} = c \sqrt{\mu_0 \pi k_L (C_L/D) (D/\ell)} \quad \text{Medhurst's "N" (SI version)}$$

The quantity on the right of this equation is referred to by Medhurst as "N" a notation that we will avoid for obvious reasons. It is tabulated in his Table VI, and shown graphically in his Fig. 10, and it is very clear that it has an asymptotic value of 2 in the long-coil limit. This is because the quantity is actually twice the apparent refractive index for helical propagation, on the assumption that the self resonance is a half-wave wire-length resonance, and that waves associated with this resonance propagate at the phase velocity for light in the local medium. This is something that we have demonstrated already in a different way in section 4, it was also something that both Howe and Medhurst knew perfectly well; and it takes us back to a point made in the introduction, which is that self-capacitance can be calculated to a fair approximation on this simple basis (i.e., if we ignore or subtract any end-to-end capacitance). More meaningful than the mongrel quantity given above however, is a nominal phase velocity (i.e., an actual phase velocity were it not for axial-field capacitance), which is generally given (as a velocity factor) by the expression:

$$\frac{v}{c} = \frac{\lambda}{\lambda_0}$$

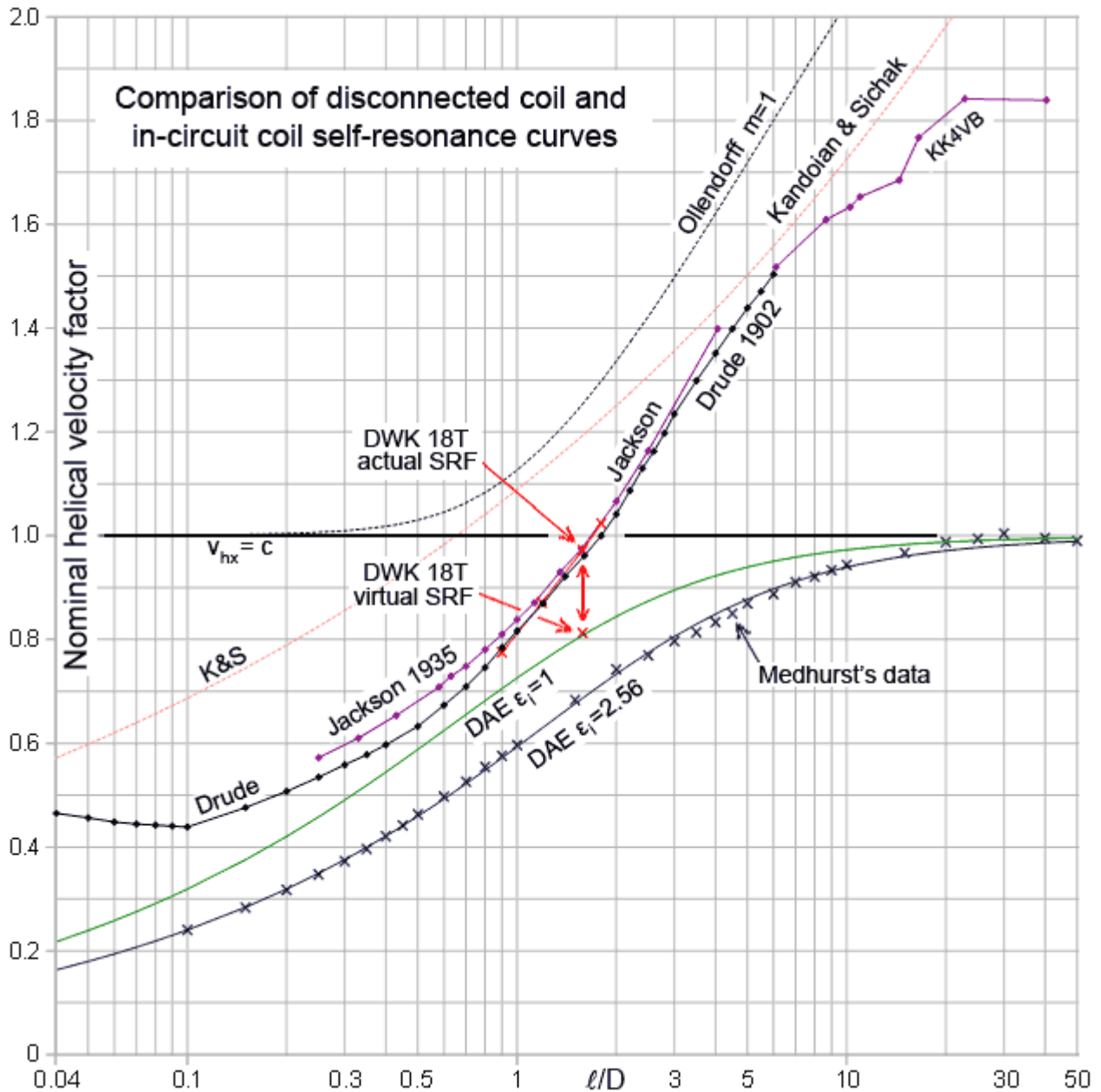
where v is the phase velocity. Thus, since $\lambda = 2\ell_w$ for a half-wave conductor-length resonance, we have the nominal velocity factor for in-circuit self-capacitance measurements as:

$$\frac{\lambda}{\lambda_{0s(v)}} = \frac{2\ell_w}{\lambda_{0s(v)}} = \frac{2}{c \sqrt{\mu_0 \pi k_L (C_L/D) (D/\ell)}} \quad (10.3)$$

In the graph that follows, this expression is used to calculate velocity factors from the DAE formula and from measurement data, so that they can be compared with the disconnected-coil self-resonance data that were introduced in section 1.2. Also plotted are some measurements made by Willis Jackson⁹⁰ in 1935. These were reported as self-capacitances, but they are actually free-coil air-dielectric SRF measurements converted into pseudo-capacitances using the measured inductance and the resonance formula. Consequently, they have long been a source of interpretational difficulty for their failure to agree with in-circuit self-capacitance measurements. They were

90 **The self-capacitance of single-layer coils.** W Jackson. Phil. Mag. Ser. 7, Vol. 19, 128. Apr. 1935. p823-835.

recovered by laying a fine grid on Jackson's Fig. 1 and converted into velocity factors using equation (10.3), whereby it can be seen that they agree fairly well with Drude's work.

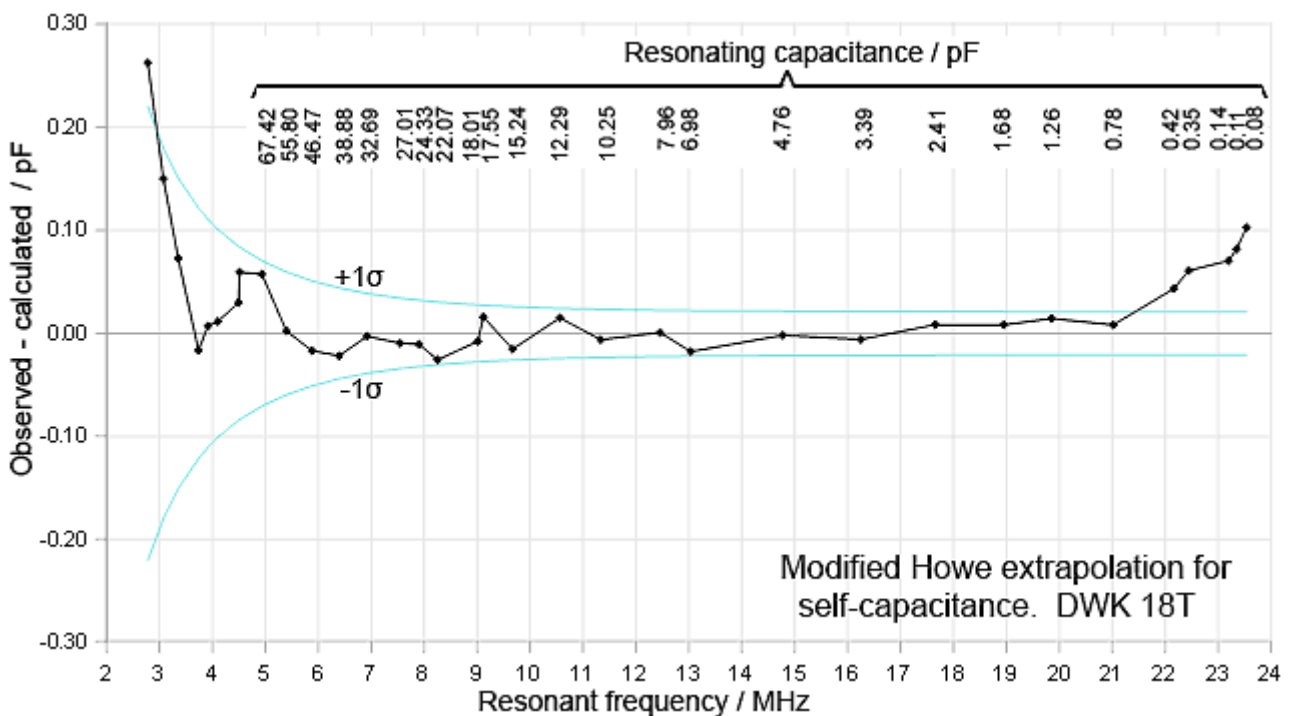


The lower of the curves is produced using the DAE formula for (C_l/D) in equation (10.3) with $\epsilon_i=2.56$, with Medhurst's data (crosses), converted into velocity factors in the same way, falling close-to or on it. This particular curve is included to deflect any possible objections to the effect that, while the DAE formula with $\epsilon_i=1$, might give an asymptote at $v=c$, Medhurst's data might not. As was pointed out in section 4, coils on formers still have the same long-coil asymptote as coreless coils because of cancellation of the radial electric field at the axis.

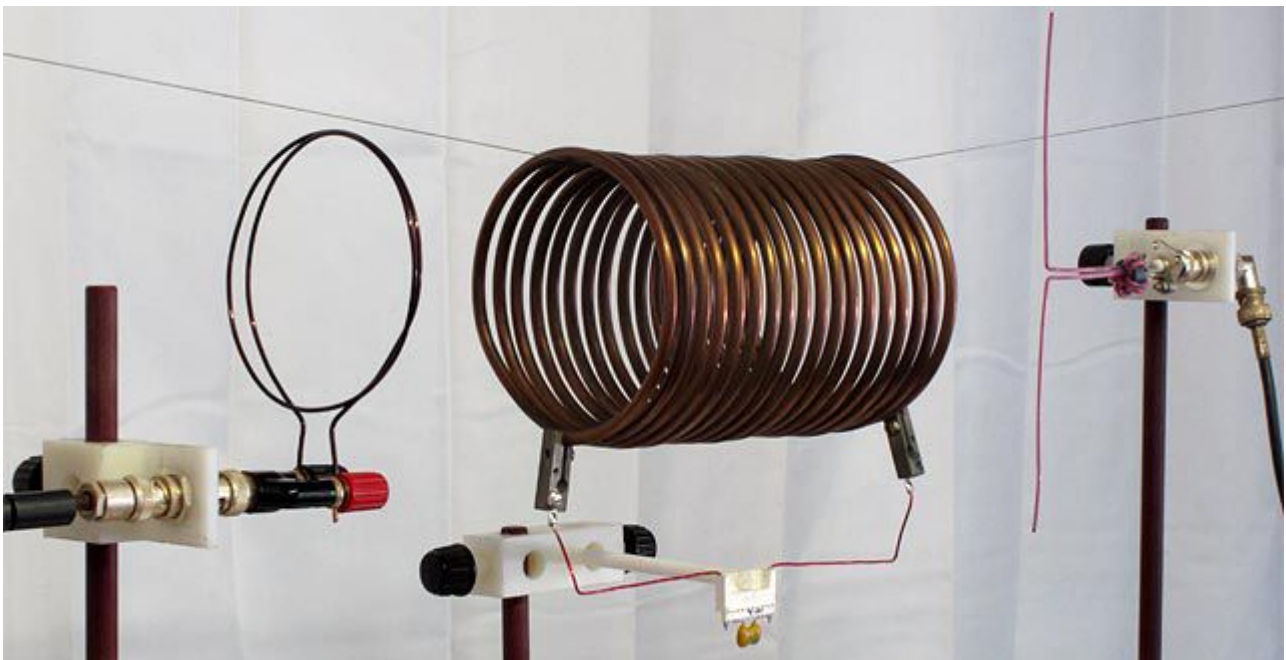
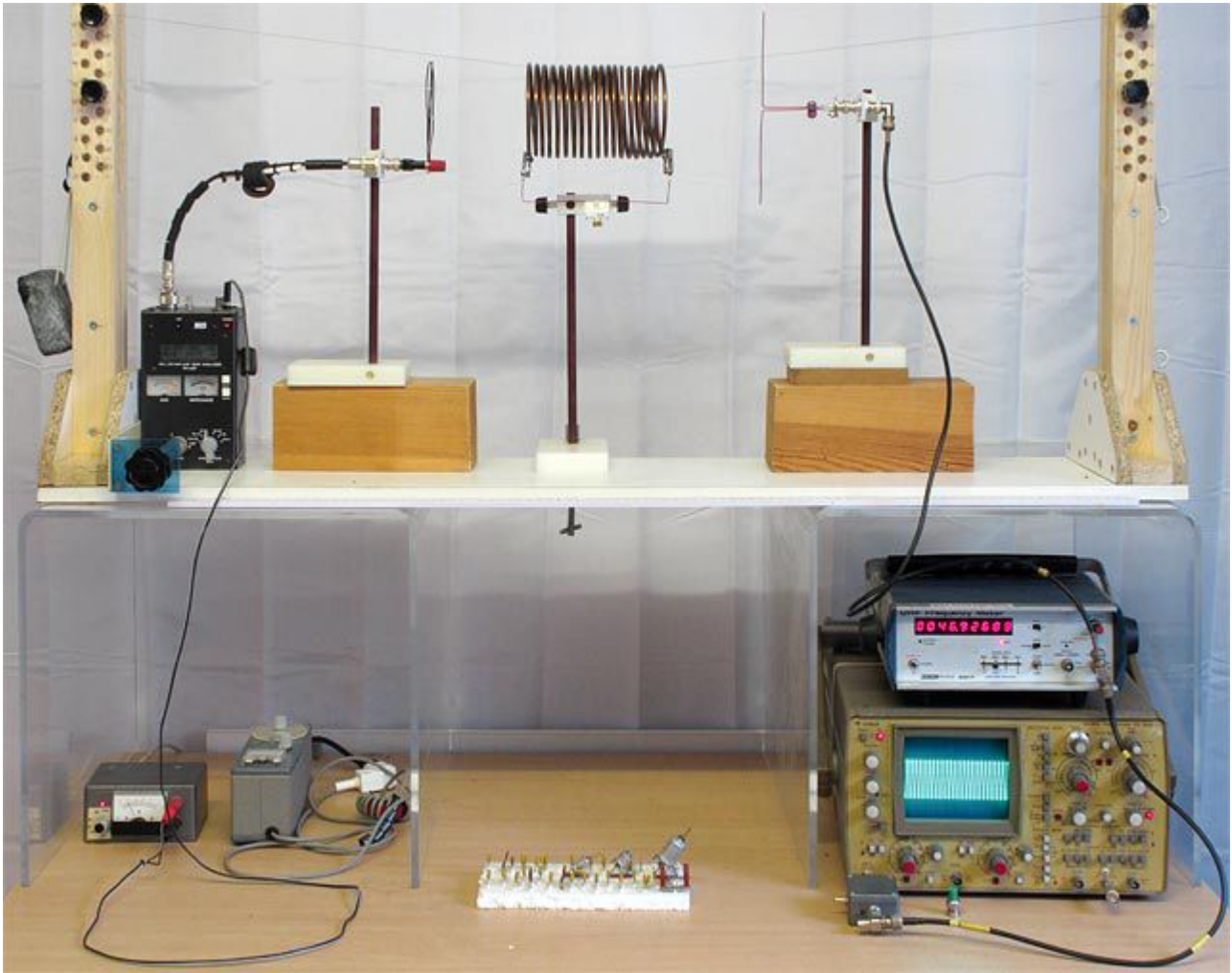
So now we come to the more interesting observation, which is that for air-cored coils with $l/D < 1$, the free-coil and the DAE nominal velocity factors fall fairly close together. The suggestion here is that the axial-field capacitance will provide a substantially uniform current distribution along the length of the wire in the free-coil case, eliminating the difference between the two methods of measurement. It was the author's view while setting-up the calculation that the curves might converge for short coils, but evidently complete coincidence is not achieved, and

Jackson's measurements, probably a little less affected by systematic errors due to residual dielectric than Drude's, are even further away from the DAE curve. It is possible however that the method used to correct the DAE formula is not accurate, although here we have a specific test at $\ell/D=1.6$. where the difference between the $\epsilon_i=2.56$ and $\epsilon_i=1$ curves is at its greatest. For this, note the two crosses marked DWK 18T actual and virtual SRF. These are measurements made on the large 18.1 turn copper tubing coil discussed in section 1.1. The upper measurement, falling on the various free-coil curves, was made using the scattering method with very weak coupling to an induction loop. The lower measurement was made using a modified extrapolation method; whereby the coil is mounted between antennas as for the disconnected measurement, but with stiff-wire leads and a socket attached for the addition of plug-in reference capacitors (see following photographs). The correction of this setup for lead inductance is straightforward, because in the absence of circuit branches, the small positive reactance can simply be added to the negative reactance of the reference capacitor. The capacitance of the holder moreover, although very small (0.08 pF in this case), is easily measured using an RF bridge. Otherwise however, the procedure is the same as the Howe method described in section 1.

The pattern of fitting residuals for the linear regression is shown below (the data have not been smoothed). Note that for measurements made above 22 MHz, as the true SRF (26.6 MHz in the absence of connecting wires) is approached, the points veer away from the horizontal (lumped parameter model) line. We now know what is happening of course. The coil behaviour is crossing over from the DAE curve to the free-coil curve as the shunt impedance increases.



Modified Howe extrapolation for self-capacitance. The curves marked $\pm 1\sigma$ are for an error function determined for the set of reference capacitors prior to the construction of the scattering jig. Evidently these limits are pessimistic, since most of the points fall within the them, but all this means is that the two antenna method for determining resonance gives much reduced experimental scatter in comparison to direct connection methods. The low frequency measurements have the largest uncertainty simply because the large-value reference capacitors were not standardised to two decimal places of pF. The deviation from the model as the true SRF is approached is evident in every self-capacitance measurement made by the author, although it might not be the case for very short coils having large end-to-end capacitance.



Variant of the Howe extrapolation method for self-capacitance. By connecting only the reference capacitor to the coil, the lead correction is greatly simplified. The RF source connected to the induction loop (upper photograph) is an MFJ269 impedance analyser; floated from ground (in addition to the unun in the antenna cable) by placing a ferrite isolator in the power cable, and by attaching the tuning capacitor to a long non-conductive extension spindle and reduction drive.

The nominal velocity factor data for free coils was discussed in relation to Ollendorff's helical waveguide theory in section 1.7. There it was mentioned that the development of a superluminal helical phase velocity in long coils is a genuine effect associated with the production of an axial slow wave (Ollendorff's velocity factor curve for $m=1$ is shown on the graph of collected data given earlier in this section, but recall that the application of an end-correction will shift the curve to the right along the ℓ/D axis).

What we have now established however, is that by attaching the coil to a shunt impedance, it does not take much of a loading before the effective phase velocity in the long coil limit equals that for propagation in the local medium, i.e., for air coils, $v_{hx} = c$. The conclusion towards which we are drawn therefore, is that the conditions giving rise to $v_{hx} > c$ are fragile, easily disrupted, and that external conditions that prevent the establishment of a non-uniform current distribution abolish it. A similar velocity-limiting effect is seen when the helical waveguide is provided with an external coaxial conducting tube, and the tube radius becomes close to the solenoid radius. In that case, of course, slow wave propagation is of less significance, and the helical wire and the outer cylinder behave more like a parallel-conductor transmission-line; in which case $v_{hx} \rightarrow c$ as for any air-spaced line.

Finally, notice that the Kandoian-Sichak curve (discussed in section 1.8) has also been plotted on the comparison graph. This is simply to show that it is far removed from anything that might be used as the basis for a self-capacitance formula. Note however that Medhurst's polystyrene-core ($\epsilon_i=2.56$) data can be made to coincide with it over a limited range if the calculated velocity factors are multiplied by 2. Hence some of Medhurst's measurements are apparently coincident with the K&S formula if they are incorrectly assigned to the $\lambda/4$ resonance and dielectric effects are ignored.

In the introduction, it was mentioned that the author became interested in coil self-capacitance as part of a study of phase-delay in broadband current transformers^{91 92}. The velocity limiting effect actually brings this study full-circle. Although it might not seem like it at first glance, a toroidal coil is simply a long solenoid wound on a magnetic core, with the uniform magnetic field eliminating the need for Nagaoka's coefficient, and a static capacitance across the terminals due to the proximity of the ends. There was a need to understand the phase-shift across the winding in order to devise a correction for the frequency-dependence of the transformer phase error. Reference material on the subject made it seem that this might be difficult, either due to the dispersive nature of the helical transmission line or due to the inconclusive nature of the literature on self-capacitance. It is however best to base any correction on actual data, and so an experiment was devised allowing the relative phase-delay to be measured with an uncertainty that turned out to be better than $\pm 0.008^\circ$ at 1.6 MHz and $\pm 0.0005^\circ$ at 30 MHz. This was achieved by making the current-transformer part of an impedance bridge using an adjustable capacitive voltage-divider with adjustable resistive phase-compensation. The bridge was terminated with a UHF coaxial resistor, and accurate measurements were made of the voltage-divider capacitance and resistance settings needed to achieve balance at a given frequency. The way in which these settings change with frequency can be transformed into relative phase-delay.

What was found was that, after removing the rising frequency response due to shunt inductance, and after accounting for the effect of circuit stray capacitance, the variation of phase error with frequency (degrees / MHz) was a near-perfect straight-line graph with a negative gradient. There was no curvature, as might be expected from the type of dispersion effect predicted by Ollendorff; and although there was some systematic deviation in the pattern of residuals when the results were fitted to a regression line, this was small and explicable as being due to the ordinary polarisation

91 **Evaluation and optimisation of RF current-transformer bridges.** D W Knight, 2007, 2014.

<http://www.g3ynh.info/zdocs/bridges/index.html> . see sections 16 and 16a.

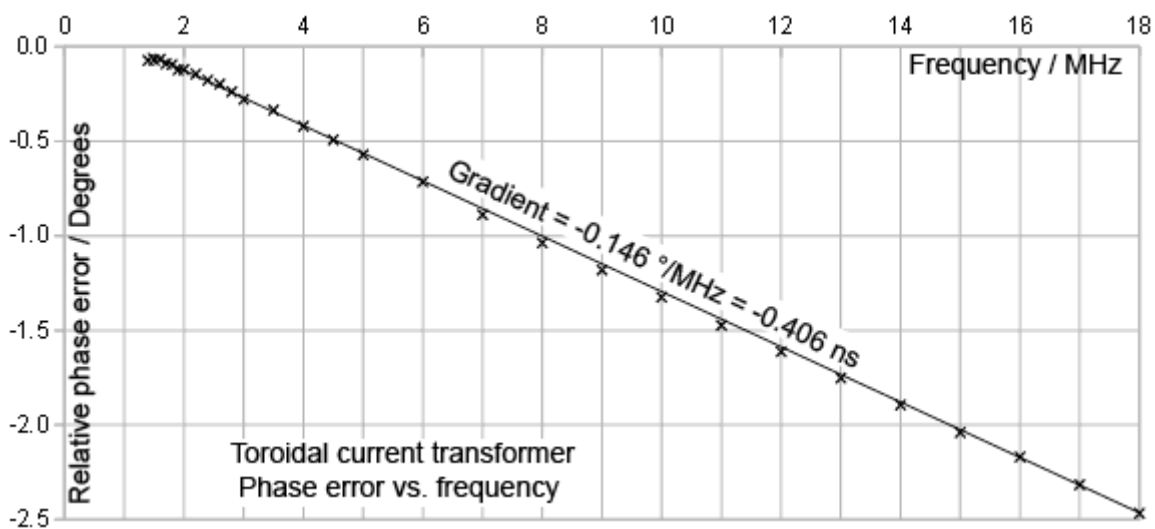
92 **A self-evaluating precision reference bridge.** D W Knight. 2007, 2014.

<http://www.g3ynh.info/zdocs/bridges/index.html>

drop-out dispersion of the ferrite material.

A quantity measured in degrees / MHz is a time, and if it is negative, it is a time delay. Various experiments showed that over a range of at least 5 octaves, the phase delay in the transformer was nothing more than propagation delay. Its value moreover was consistent with the time it would take for a wave to travel half the length of the winding wire with a phase velocity a little less than c . The reason why the propagation distance is half the conductor length is that a magnetic disturbance in the core will affect all points on the wire simultaneously (in the local approximation), sending equal and opposite disturbances upstream and downstream. These disturbances will be seen in superposition at the terminals, with an average propagation distance of half the wire-length. This is true for every point on the wire, which means that all of the disturbances add-together in phase in the absence of non-linearities, dispersion effects and leakage inductance. This is how a transformer cancels most of its own inductance in respect of coupling between primary and secondary windings.

Thus the question of how to compensate for current-transformer phase error was settled experimentally, and the correction methods devised on that basis led to the construction of some extremely accurate broadband transmission bridges. The conclusion was therefore that the coil is not inherently dispersive in the absence of dispersive materials. This, of course, was at odds with the most authoritative material on the subject, but not inconsistent with the basic assumptions used by Medhurst in the process of developing his formula.



Variation of phase error with frequency for a 1:12 toroidal current transformer. The transformer (shown on the right) is wound with 12 turns of 0.9 mm diameter enamelled Cu wire on a Fair-Rite FT50-61 ½" ferrite bead. The phase error vs. frequency graph is a straight line with a gradient of -0.41 ns, i.e., the error is almost entirely due to propagation delay. The secondary winding wire length is 228 mm. The time taken for light to travel half this distance is 0.38 ns, but when other system delays are taken into consideration, the secondary-coil phase velocity comes out at a little less than might be estimated from these numbers.



As was demonstrated in the introduction, self-capacitance measurements made on toroidal coils show the same deviation from the Howe regression-line as solenoids, and although this is explicable as being due to current non-uniformity, it also indicates that they exhibit the Ollendorff dispersion effect when the shunt impedance approaches an open-circuit. The transformer linear phase-delay characteristic is thus another demonstration of the way in which a shunt impedance limits the helical phase-velocity.

11. Free coil SRF calculation

In several places in this document, we have shown graphs of apparent or nominal helical velocity factor vs. ℓ/D for free coils resonating at the first SRF ($\ell_w = \lambda/2$). In that case, the nominal velocity factor for an air-filled coil crosses the $v=c$ line when $\ell/D \approx 1.7$. As was pointed out in section 1.7 however, this is not a true velocity factor, but merely the coil conductor length divided by the free-space half-wavelength; i.e.;

$$\frac{v_{\text{hx(nom)}}}{c} = \frac{2 \ell_w}{\lambda_0} = \frac{2 \ell_w f_0}{c} \quad (11.1)$$

We now know that the energy stored in the axial electric field corresponds to a capacitance that is effectively in parallel with the coil. This induced-field capacitance will resonate with the helical transmission line, reducing f_0 and thereby reducing the apparent phase velocity. In section 9, we obtained a capacitance C_E that models this effect in the case of a coil having a shunt impedance, and this offers us at least a starting-point for modelling short free coils. We must expect however, that in free coils the induced-field capacitance will differ from C_E because the current profile and propagation environment will not be the same.

In the matter of designing helically-loaded vertical antennas and Tesla transformers, it is actually the apparent velocity factor, rather than the true value, that is the main point of interest. This is because it provides a way of calculating the true resonant frequency. The objective therefore is to simulate the apparent velocity factor curve. To do that, we can consider the coil as a short-circuited transmission line operating below its $\lambda/4$ overall length (i.e., $\lambda/2$ conductor-length) resonance frequency, so that it has an inductive input reactance. This line is resonated against a capacitance C_{EF} (free-coil induced electric field capacitance) and its input reactance is therefore such that the sum of the two reactances is zero. The reactance of the short-circuited line expressed using its total conductor length was given earlier as equation (1.2). Here the subscript HG (helical guide) has been added, and a subscript on the wavelength makes it explicit that it is not the free-space value.

$$X_{\text{HG}} = R_0 \tan\left(\frac{\pi \ell_w}{\lambda_{\text{hx}}}\right)$$

Note that when $\lambda_{\text{hx}} \rightarrow 2\ell_w$, the tangent argument $\rightarrow \pi/2$ and $X_{\text{HG}} \rightarrow \infty$. When the line is resonated with a capacitance however, $\lambda_{\text{hx}} > 2\ell_w$, and X_{HG} is finite and positive. Resonance occurs when:

$$R_0 \tan\left(\frac{\pi \ell_w}{\lambda_{\text{hx}}}\right) - \frac{1}{2 \pi f_0 C_{\text{EF}}} = 0$$

i.e.,

$$\frac{1}{2 \pi f_0 C_{\text{EF}}} = R_0 \tan\left(\frac{\pi \ell_w}{\lambda_{\text{hx}}}\right)$$

but $\lambda_{\text{hx}} = v_{\text{hx}}/f_0$. Thus, with some rearrangement:

$$2 \pi f_0 C_{\text{EF}} R_0 \tan\left(\frac{\pi f_0 \ell_w}{v_{\text{hx}}}\right) = 1 \quad (11.2)$$

This is a transcendental equation that can be solved for f_0 , provided that we can evaluate C_{EF} , R_0

and v_{hx} . Generally however, f_0 is a scaleable function of the coil parameters, and so to produce a working formula we want to normalise it. To do that, we can use the substitution given by (11.1), i.e.,

$$f_0 = \frac{V_{hx(nom)}}{2 \ell_w}$$

Hence:

$$\pi \frac{V_{hx(nom)}}{\ell_w} C_{EF} R_0 \tan\left(\frac{\pi}{2} \cdot \frac{V_{hx(nom)}}{v_{hx}}\right) = 1 \quad (11.3)$$

which is a transcendental equation that can be solved for $v_{hx(nom)}$. Note that the unit of CR is time, and so the expression is dimensionless. Also note that when $\ell/D \ll 1$, then C_{EF} is large so that $v_{hx(nom)} \ll v_{hx}$ and the argument of the tangent becomes small. In that case the equation becomes analytically soluble, i.e.;

$$\frac{\pi^2}{2} \cdot \frac{V_{hx(nom)}^2}{\ell_w v_{hx}} C_{EF} R_0 \approx 1$$

which gives

$$\frac{V_{hx(nom)}}{c} \approx \frac{1}{\pi c} \sqrt{\frac{2 \ell_w v_{hx}}{C_{EF} R_0}} \quad \ell/D \ll 1 \quad (11.4)$$

This can be used as a reference function for the limiting short-coil case, but note that it must be a function of ℓ/D in first order. That means that the parameters must either be invariant in first order or functions of ℓ/D themselves. There is a problem in this respect with the quantity C_{EF} , which we expect to be similar to C_E (section 9). C_E is not a function of ℓ/D but C_E/D is. Thus we make the amendment:

$$\frac{V_{hx(nom)}}{c} \approx \frac{1}{\pi c} \sqrt{\frac{2 \ell_w v_{hx}}{(C_{EF}/D) D R_0}}$$

The D so liberated can now be combined with ℓ_w by noting that, for small pitch angles, $\ell_w \approx \pi D N$. Then using $N = \ell/p$ and $\tan \psi = p/\pi D$, we have $\ell_w = \ell / \tan \psi$. Thus:

$$\frac{V_{hx(nom)}}{c} \approx \frac{1}{\pi c} \sqrt{\frac{2 (\ell/D) v_{hx}}{(C_{EF}/D) R_0 \tan \psi}} \quad \ell/D \ll 1 \quad (11.5)$$

The function of course is still not in the required form because $1/\tan \psi$ is strongly dependent on coil parameters and makes a large contribution to the nominal velocity factor. Also recall from section 1.7 that v_{hx} is a function of ℓ/D in first order (it is approximated by Ollendorff's function) and so will not give the required cancellation. Thus it must be the case that the characteristic resistance R_0 has a factor⁹³ at least approximately equal to $1/\tan \psi$.

⁹³ Since winding the conductor into a helix is a way of making a transmission line with a very high characteristic resistance, we would expect there to be a factor that is large for fine pitch and small for coarse pitch.

Helical-line surge resistance

The surge resistance or characteristic resistance of a lossless transmission line is defined as:

$$R_0 = \sqrt{\frac{L_0}{C_0}}$$

where L_0 and C_0 are respectively the inductance and capacitance *per unit length* of the line. The problem of calculating L_0 and C_0 for the infinite helical transmission line (see section 1.8) has been addressed by Chute & Vermeulen⁹⁴, who give the solutions using modified Bessel functions. Assuming that the coil is immersed in air:

$$C_0 = \frac{\pi \epsilon_0}{K_0(x) I_0(x)} \quad [\text{Farads / metre}] \quad (11.6)$$

and

$$L_0 = \frac{\mu_0 \pi (D/2)^2}{p^2} 2 K_1(x) I_1(x) \quad [\text{Henrys / metre}] \quad (11.7)$$

where the Bessel function argument is:

$$x = \gamma \frac{D}{2} \approx \beta_{hx} \frac{D}{2}$$

γ being the radial or circumferential wavenumber, which is approximately equal to the helical propagation constant when the pitch angle is small. Note that at low frequencies, $\gamma D/2 \ll 1$ and $K_1(x)I_1(x) \rightarrow 1/2$. Equation (11.6) then reduces to:

$$L_0 = \frac{\mu_0 \pi D^2}{4 p^2}$$

The pitch distance p however is given by $p = \ell/N$ (coil length / number of turns), and so we have:

$$L_0 = \frac{\mu_0 \pi D^2 N^2}{4 \ell^2} \quad [\text{Henrys / metre}]$$

This is simply the inductance of a long coil divided by its length (i.e., the inductance per unit length); which is to say that if we multiply it by ℓ and Nagaoka's coefficient (k_L) it becomes the standard current-sheet inductance formula.

A further check on the definitions of L_0 and C_0 is given by noting that the propagation constant is given by:

$$\beta_{hx} = \omega \sqrt{2 L_0 C_0}$$

This is slightly different from the propagation constant definition for a 2-wire transmission line,

94 **On the self-capacitance of solenoidal coils.** F S Chute and F E Vermeulen. Canadian Elec. Eng. J., Vol 7(2), 1982, p31-37. See section II, p32. **Transmission line nature of the infinite solenoid.** Note that their β is the helical propagation constant.

requiring L_0 to be multiplied by 2 because we are effectively considering a wave on the whole conductor rather than a superposition of waves on half the conductor. Squaring this expression and using (11.6) and (11.7), we get:

$$\beta_{hx}^2 = \omega^2 \frac{\mu_0 \varepsilon_0 \pi^2 D^2}{p^2} \frac{K_1(x) I_1(x)}{K_0(x) I_0(x)}$$

Now note that $c = 1/\sqrt{\mu_0 \varepsilon_0}$ and that $\omega^2/c^2 = \beta_0^2$. Also, $\tan \psi = p/\pi D$, and the reciprocal of the combination of Bessel functions shown is Ollendorff's function, $W(x)$ (see section 1.7). Thus, with some rearrangement:

$$\beta_0 = W(\beta_{hx} D/2) \beta_{hx} \tan \psi$$

This is the same as equation (1.13), except that the helical propagation constant has been substituted in place of the radial wavenumber.

Now recall that to convert equation (11.5) into a first-order function of ℓ/D , we require R_0 to have a factor approximating $1/\tan \psi$. Notice therefore that (11.7) can be rewritten:

$$L_0 = \frac{\mu_0}{4\pi} \frac{1}{\tan^2 \psi} 2 K_1(x) I_1(x) \quad (11.7a)$$

Thus, combining (11.6) and (11.7a), we have:

$$R_0 = \sqrt{\frac{L_0}{C_0}} = \frac{1}{\tan \psi} \frac{1}{2\pi} \sqrt{\frac{\mu_0}{\varepsilon_0}} \sqrt{2 K_1(x) I_1(x) K_0(x) I_0(x)}$$

but note that $\sqrt{\mu_0/\varepsilon_0} = Z_0$, the impedance of free space (376.73 Ω). Thus:

$$R_0 = \frac{1}{\tan \psi} \frac{Z_0}{2\pi} \sqrt{2 K_1(x) I_1(x) K_0(x) I_0(x)} \quad [\text{Ohms}] \quad (11.8)$$

Uniform current surge resistance

For comparison purposes, we can also calculate a characteristic resistance for a coil operating with uniform current. This becomes possible because the velocity limiting effect (section 10) tells us that the phase velocity will be governed by the local refractive index in that situation. At low frequencies, when the electrical length of the line is small, the transmission line equation reduces to:

$$L = \frac{R_0 \ell_w}{2 v_{hx}}$$

(see equation 1.3). Thus, if (say) the coil is immersed in air, we can substitute $v_{hx}=c$ and rearrange:

$$R_0 = \frac{2cL}{\ell_w} = \frac{2L}{\sqrt{\mu_0 \varepsilon_0} \ell_w}$$

Substituting for L using the current-sheet formula, we then have:

$$R_0 = \frac{2}{\sqrt{\mu_0 \epsilon_0} \ell_w} \frac{\mu_0 \pi D^2 N^2 k_L}{4 \ell}$$

where k_L is Nagaoka's coefficient. Now recall that $\sqrt{\mu_0/\epsilon_0} = Z_0$ and, for small pitch angles $\ell_w \approx \pi D N$. Thus:

$$R_0 = Z_0 \frac{D N k_L}{2 \ell}$$

and recall that $\tan \psi = p/\pi D$ and $\ell = N p$, so we end up with:

$$R_0 = \frac{Z_0}{2\pi} \frac{k_L}{\tan \psi} \quad [\text{Ohms}] \quad (11.8a)$$

Now, bearing in mind that we have established that the coil is not a dispersive propagation environment under uniform current conditions, it will be found that $R_0 \tan \psi$ calculated using this equation differs from the value obtained from equation (11.8). The reason, of course, is that the free coil *is* dispersive. This means that the effect of induced-field shunt capacitance in the free coil will be different from the effect that occurs in circuit. This is a partial explanation for the non-convergence of the free-coil and in-circuit coil nominal phase velocities in the short-coil limit (see section 10).

Nominal VF - short coil limiting case

We can now substitute the quantity $R_0 \tan \psi$ from equation (11.8) into equation (11.5). Before doing that however, we should also note that the helical phase velocity v_{hx} was given by equation (1.8) in section 1.7 as:

$$\frac{v_{hx}}{c} = \frac{W(x)}{\cos \psi} \approx W(x) \quad \text{where} \quad W(x) = \sqrt{\frac{I_0(x) K_0(x)}{I_1(x) K_1(x)}}$$

Hence we can make the combination:

$$\frac{v_{hx}}{R_0 \tan \psi} = \frac{2 \pi c}{Z_0 \sqrt{2}} \frac{1}{I_1(x) K_1(x)}$$

Also note that $c/Z_0 = 1/\mu_0$ and $2/\sqrt{2} = \sqrt{2}$, so that:

$$\frac{v_{hx}}{R_0 \tan \psi} = \frac{\sqrt{2} \pi}{\mu_0 I_1(x) K_1(x)}$$

substituting this into (11.5) gives:

$$\frac{v_{\text{hx(nom)}}}{c} \approx \frac{1}{\pi c} \sqrt{\frac{\sqrt{2}\pi}{\mu_0 I_1(x) K_1(x)} \frac{2(\ell/D)}{(C_{\text{EF}}/D)}}$$

or perhaps more conveniently:

$$\frac{v_{\text{hx(nom)}}}{c} \approx \sqrt{\frac{2\sqrt{2}\epsilon_0}{\pi} \frac{1}{I_1(x) K_1(x)} \frac{(\ell/D)}{(C_{\text{EF}}/D)}} \quad (11.9)$$

With constants evaluated, this becomes:

$$\frac{v_{\text{hx(nom)}}}{c} \approx 2.823396847 \times 10^{-6} \sqrt{\frac{1}{I_1(x) K_1(x)} \frac{(\ell/D)}{(C_{\text{EF}}/D)}} \quad (11.9a)$$

where the factor of 10^{-6} can be dropped if C_{EF}/D is entered in pF/m.

When Chute & Vermeulen derived the characteristic resistance of the helical line, they used the Bessel function argument $x = \beta_{\text{hx}} D/2$. There appears to be no reason however why we cannot truncate the coil in the manner adopted by Ollendorff (section 1.7). In that case, the argument is as given by equation (1.9):

$$x = (m + k_{\text{ff}}) \frac{\pi D}{2 \ell}$$

where $m=1$ for the free coil first SRF case, and k_{ff} is an empirical fringe-field correction that can be set to zero when not required⁹⁵. Thus, with C_{EF} taken to be the same as C_{E} , as calculated using equation (9.13); with $\ell/D=0.04$, equation (11.9a) produces a nominal velocity factor of 0.485. Drude's measurement for that coil-shape corresponds to $v_{\text{hx(nom)}}/c=0.465$. This gives us some confidence that the theory is on track, but note that (11.9) is very much a short-coil limiting case. Thus as the input ℓ/D value increases, the curve veers upwards somewhat wildly; although it does maintain a curvature reminiscent of the data.

Note incidentally, that since (11.9) is a limiting case for large x , we can also insert the large argument limiting forms of the Bessel functions. These are:

$$I_n(x) \approx \frac{e^x}{\sqrt{2\pi x}} \quad x > 10 \quad (\text{Dwight}^{96} \text{ p196, 814.2})$$

$$K_n(x) \approx \sqrt{\frac{\pi}{2}} \frac{e^{-x}}{\sqrt{x}} \quad x > 10 \quad (\text{Dwight p197, 816.2})$$

Thus:

$$I_1(x) K_1(x) \approx \frac{1}{2x} = \frac{1}{\pi} (\ell/D) \quad \ell/D < 0.16$$

Substituting this into (11.9) gives:

⁹⁵ It will turn out that a component of C_{EF} can provide the fringe-field correction in a more general way.

⁹⁶ **Tables of integrals and other mathematical data**, 4th edition, cited in section 1.7.

$$\frac{v_{hx(nom)}}{c} \approx \sqrt{\frac{2\sqrt{2}\epsilon_0}{(C_{EF}/D)}} \quad (11.10)$$

i.e.,

$$\frac{v_{hx(nom)}}{c} \approx 5.004340615 \times 10^{-6} \sqrt{\frac{1}{(C_{EF}/D)}} \quad (11.10a)$$

Once again, the factor 10^{-6} can be dropped if C_{EF} is in pF. The expression above agrees with (11.9) to 4 decimal places at $\ell/D=0.04$.

Nominal VF - Iterative solution

We can now return our attention to the general solution for $V_{hx(nom)}/c$, which is to be obtained from equation (11.3). This was given earlier as:

$$\pi \frac{v_{hx(nom)}}{\ell_w} C_{EF} R_0 \tan\left(\frac{\pi}{2} \frac{v_{hx(nom)}}{v_{hx}}\right) = 1$$

By inspection we can see that, for long coils, as C_{EF} diminishes, $v_{hx(nom)}$ gets closer to v_{hx} and the tangent argument approaches $\pi/2$. Thus the small angle approximations are inappropriate for the general problem and we must develop an iterative method. Before we can do that however, we must satisfy the same requirement as before, which is that all parameters are either invariant in first order or functions of ℓ/D . Thus, once again, we use the substitutions $C_{EF}=D(C_{EF}/D)$ and $\ell_w=\ell/\tan\psi$, and the $\tan\psi$ disappears by virtue of the fact that R_0 , as given by (11.8), has a factor of $1/\tan\psi$. Thus:

$$v_{hx(nom)} (D/\ell) (C_{EF}/D) (R_0 \tan\psi) \tan\left(\frac{\pi}{2} \frac{v_{hx(nom)}}{v_{hx}}\right) = \frac{1}{\pi} \quad (11.11)$$

where

$$R_0 \tan\psi = \frac{Z_0}{2\pi} \sqrt{2 K_1(x) I_1(x) K_0(x) I_0(x)} \quad \text{and} \quad \frac{v_{hx}}{c} = \sqrt{\frac{I_0(x) K_0(x)}{I_1(x) K_1(x)}}$$

Note however, that we want to use the helical *velocity factor* as a parameter, and we want to express the solution as a velocity factor. Thus a preliminary re-grouping on that basis gives a form eligible for trial-and-error solution:

$$\frac{v_{hx(nom)}}{c} = \frac{1}{\tan\left(\frac{\pi}{2} \frac{(v_{hx(nom)}/c)}{(v_{hx}/c)}\right)} \frac{(\ell/D)}{c \pi (C_{EF}/D) (R_0 \tan\psi)} \quad (11.12)$$

The helical velocity factor can be computed using the Basic macro function "Ollendf(x)" (see section 1.7). The OO Basic function $R0\tan(x)$, given in the following box, calculates $R_0 \tan\psi$.

```

Function R0tan(byval x as double) as double
' Calculates R0 Tan(psi) for the sheet helix. D W Knight. Version 1.00, 2016-04-04
Dim I0 as double, I1 as double, K0 as double, K1 as double
Dim ofa as Object
ofa = createUNOService("com.sun.star.sheet.FunctionAccess")
I0 = ofa.callFunction( "Besseli", array(x, 0) )
K0 = ofa.callFunction( "Besselk", array(x, 0) )
I1 = ofa.callFunction( "Besseli", array(x, 1) )
K1 = ofa.callFunction( "Besselk", array(x, 1) )
R0tan = 59.9584916*sqr( 2*I0*K0*I1*K1 )
end function

```

Note that the quantities (ℓ/D) , (C_{EF}/D) , $(R_0 \tan \psi)$ and (v_{hx}/c) are all constant once a value ℓ/D has been selected. We can therefore create some composite parameters in order to put the problem into a more manageable form. These are:

$$a = \frac{\pi}{2 v_{hx}/c} \quad \text{and} \quad b = \frac{(\ell/D)}{c \pi (C_{EF}/D) (R_0 \tan \psi)} \quad (11.13)$$

We will also use y to represent the solution, i.e.;

$$y = v_{hx(nom)}/c$$

Equation (11.12) then becomes:

$$y = \frac{b}{\tan(a y)}$$

To find a solution, one of the instances of y can be replaced with z (say). Thus:

$$y = \frac{b}{\tan(a z)}$$

A guess for z can now be inserted and adjusted until $z=y$. This method was tried manually and, using C_E/D from equation (9.13) in place of C_{EF}/D , served to confirm that the theory as it stands (without empirical corrections) already gives a fairly good simulation of the free-coil data of Drude and Jackson. As a means of solution suitable for programming however, it is ill conditioned. The difficulty lies in the fact that very small changes in z can produce large changes in y , and there is nothing to prevent az from approaching $\pi/2$, in which case the process will crash. That issue can be circumvented by swapping z and y and rearranging thus:

$$y = \frac{1}{a} \arctan\left(\frac{b}{z}\right) \quad (11.14)$$

The arctan function has no argument limits. To solve this equation algorithmically, note that after inserting an initial guess z , any shift in z (δz say) will cause a corresponding shift in y . A solution will be obtained if we can define a shift such that:

$$z + \delta z = y + \delta y$$

Were the system linear, then the shift in y would be equal to the shift in z multiplied by $\partial y/\partial z$. For a non-linear system, this is only approximately true, but if the required shift diminishes after each change in z , then the problem will converge and the computed shift will become progressively more accurate as the solution is approached. Thus we have:

$$z + \delta z \approx y + \delta z \frac{\partial y}{\partial z}$$

which can be rearranged:

$$\delta z \approx \frac{z - y}{\left(\frac{\partial y}{\partial z} - 1\right)}$$

Notice that the problem cannot be solved by this method if $\partial y/\partial z$ can take on a value of 1 during the iteration process. Checking for this type of singularity is easily accomplished using a spreadsheet, and in this case it does not occur. To differentiate (11.14) note that the standard differential for arctan is:

$$\frac{d(\arctan x)}{dx} = \frac{1}{1+x^2}$$

Thus, using the chain rule:

$$\frac{\partial y}{\partial z} = \frac{1}{a} \frac{1}{1 + \left(\frac{b}{z}\right)^2} b(-z^{-2})$$

i.e.,

$$\frac{\partial y}{\partial z} = -\frac{b}{a} \frac{1}{z^2 + b^2}$$

The problem set out in this way turns out to be well conditioned. Using Ollendorff's function (i.e., v_{hx}/c) to provide the initial estimate for $v_{hx(nom)}/c$ (i.e., z), it was found that for small ℓ/D ratios, where $v_{hx}/c \approx 1$ and $y \approx 0.5$, the difference $|z-y|$ was reduced to <1 ppM in 3 rounds of iteration. For $\ell/D > 1$, where the axial induced field capacitance is fairly small, the difference was reduced to <1 ppM after one round. Thus the procedure is highly efficient.

An experimental algorithm for obtaining $v_{hx(nom)}/c$ is shown in the following box. It is experimental because it uses the theoretical 'true' velocity factor and the composite parameter b (see 11.13) as its input arguments. This arrangement is inconvenient for general modelling application, but it permits alteration of the input definitions for the purpose of adjusting the curve shape.

```

Function VFnomx(byval vfh as double, b as double) as double
'Experimental function for calculating nominal helical velocity factor.
'vfh is theoretical 'true' helical VF. D W Knight v 2.01, 2016-04-13.
Dim y as double, z as double, a as double, diff as double, der as double, deltaz as double
Dim n as integer
if vfh <= 0 then vfh = 1
a = pi/(2*vfh)
z = vfh
n = 0
do
y = (1/a)*atn(b/z)
diff = z-y
der = -(b/a)/(z*z+b*b)
deltaz = diff/(der -1)
z = z + deltaz
n = n + 1
loop until abs(diff) < 1E-9 or n > 255
VFnomx = y
end function

```

The output of this function vs. ℓ/D is plotted in the following graph, with data for comparison. Fringe-field correction via the Bessel function argument is not used. The version using the axial field capacitance from the uniform current case (C_E) is marked HTL// C_E (helical transmission line in parallel with C_E).

Note that the model (so far) has no provision for reproducing the flattening-off of velocity factor that occurs for very long coils. Taking that into account, and bearing in mind that C_E diminishes as ℓ/D increases, it is obvious that it takes only the presence of a very small amount of capacitance to shift the transmission-line resonance into the vicinity of the data. In the $\ell/D < 1$ region however, the curve has an inflection that is not evident in the data, and so the uniform-current TDE model capacitance C_E is not correct for the free coil (as was expected).

In order to obtain a curve that is realistic in the $\ell/D < 1$ region, we obviously need to find an expression for C_{EF} . The two empirical formulae shown below are suitable, and give practically identical results. The curve marked HTL// C_{EF} is actually produced by the second formula (11.15), although it makes no visible difference.

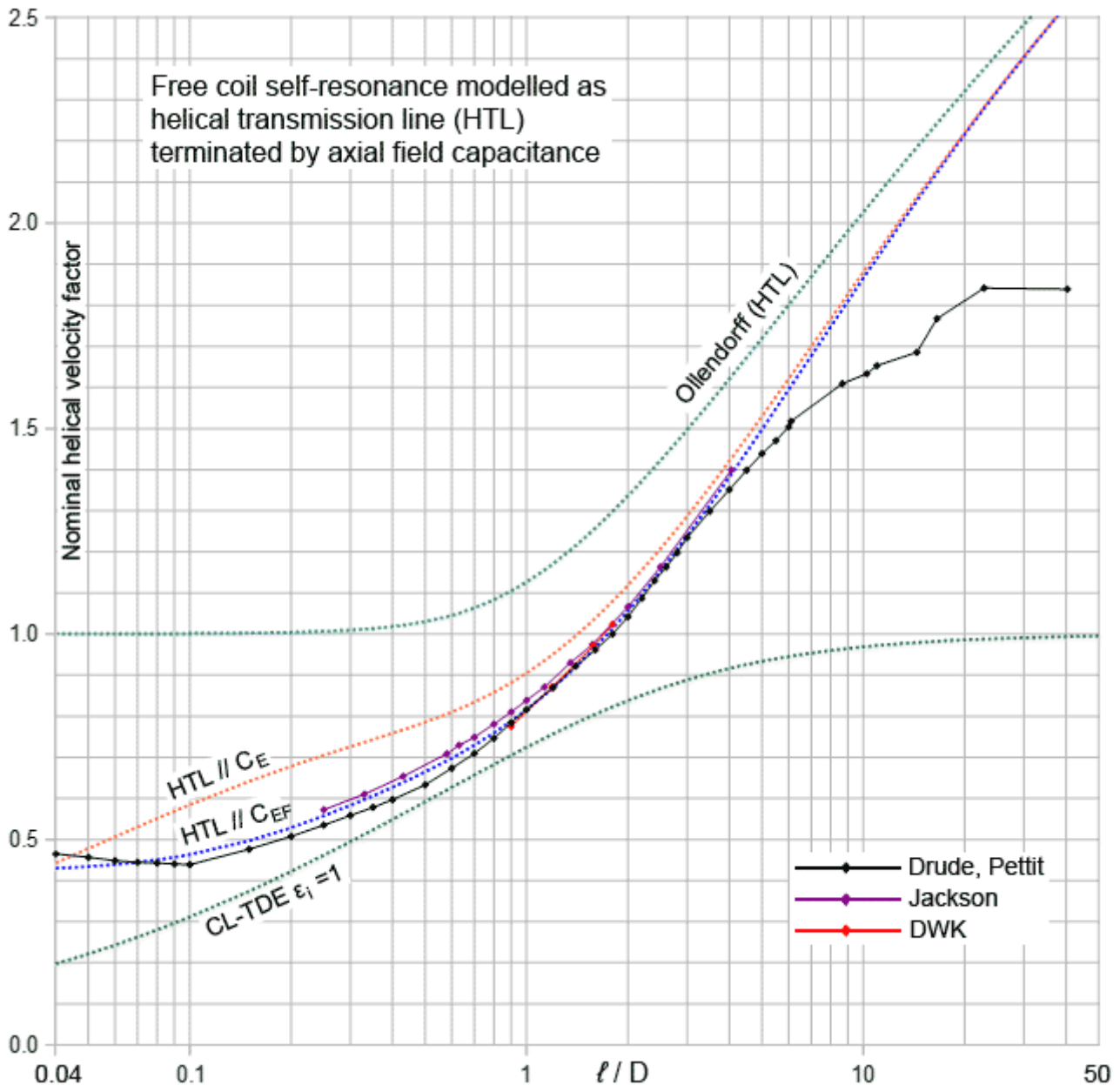
$$\frac{C_{EF}}{D} = \frac{5.5 \epsilon_0}{\operatorname{arccosh}(1.4 + 2.5 \ell/D + 4(\ell/D)^2)}$$

$$\frac{C_{EF}}{D} = 2 \epsilon_0 \left(\frac{1}{1 + \ln(1 + \ell/D)} + \frac{1}{\operatorname{arccosh}(1.015 + (\ell/D)^2)} \right) \quad (11.15)$$

There are various ways in which equation (11.15) can be adjusted, but the only obvious empirical coefficient is the term 1.015 in the argument of the arccosh function. This adjusts the curve in the $\ell/D < 1$ region and allows the spurious inflection to be removed.

What is particularly interesting about (11.15) however is that it corresponds to two separate capacitances, one of which (the first term) provides the fringe-field correction. In the region where

$\ell/D > 1$, this term produces almost exactly the same effect as that of adjusting the Bessel function argument x . It is also fairly obvious that the fringe fields that result from truncating the solenoid will create a capacitance in addition to that which is due to the induced axial field. Correcting for that via x however can only affect the curve in regions where $v_{hx} > 1$, whereas it is actually necessary to correct for it over the whole range. Thus, although adjusting x in order to slide the Ollendorff velocity factor curve along the ℓ/D axis was useful for investigative purposes (see section 1.7) it was never a viable fringe-field correction method overall. The first term in (11.15) therefore represents a capacitance that decays slowly as ℓ/D increases. A constant term would do almost the same job, but is physically unreasonable (an infinitely long coil does not require correction).



Use of (11.15) for the capacitance in parallel with an Ollendorff helical transmission line plants the resulting curve in among the data up to about $\ell/D=4$. Note incidentally, that Drude's measurements for $\ell/D < 0.1$ should probably not be taken too seriously because there is no reason to expect a kink or minimum in that region.

The issue that remains however is that the curve does not follow the data when $\ell/D > 4$. This is a

matter of wave propagation, and has nothing to do with terminating capacitance (which has more or less died out in this region). That the true velocity factor will flatten-off and eventually return to 1 seems physically reasonable, and the data appear to show it. It could also be that helical phase velocity in very long solenoids is no longer primarily dependent on ℓ/D , but the contiguity of Drude's and Alex Pettit's data would seem to mitigate against that view.

It must be noted incidentally that increasing pitch angle will cause a falling-off of observed velocity factor (recall that Ollendorff's function should strictly be divided by $\cos\psi$). As we will see however; the effect is not great enough to account entirely for the failure to fit Alex's data. There is also some evidence of this fall-off in Drude's data, and Drude generally avoided using coils of large pitch (although the details are not always clear). The production of an accurate long-coil velocity-factor model would therefore seem to require either a modification of Ollendorff's function or a modification of the argument passed to that function.

Pitch-angle correction

In the matter of modelling the SRF of a coil as a function of ℓ/D , a second-order effect is by definition a factor that affects the SRF but is not a function of ℓ/D . If such effects become pronounced, the only way in which we can deal with them is by adjusting the data. Such is the case with the effect of pitch.

The helical velocity factor according to Ollendorff's theory is:

$$\frac{v_{hx}}{c} = \frac{W(x)}{\cos\psi}$$

(see equation 1.8). Thus the quantity that we have been assuming to be the true theoretical helical VF is actually:

$$\frac{v_{hx}}{c} \cos\psi = W(x)$$

Thus, in cases where we know the pitch angle, we can in principle apply a correction to the data so that it should better conform to the curve produced by $W(x)$. Of course, there is a complication in doing that in the case of short coils, because they are strongly subject to the effect of the axial-field capacitance, but for long coils the self-shunting effect is greatly diminished, and the gradient of Ollendorff's function becomes similar to that of the data. Thus we can apply a simple second-order correction by dividing the observed values of $v_{hx(nom)}/c$ by $\cos\psi$.

Note incidentally, that this correction implies that an infinitely long coil will have an infinite phase velocity. This is, surprisingly, not paradoxical, the reason being that an infinitely long coil will also have an infinite conductor length. Thus we have, from equation (11.1):

$$f_0 = \frac{v_{hx(nom)}}{2\ell_w} \rightarrow \frac{\infty}{\infty}$$

which simply means that the resonant frequency is undefined. All we are doing therefore is turning large pitch-angle data into small pitch-angle data for the purpose of producing an empirical curve that is correct for small pitch-angles.

Long-coil correction

Once the data have been corrected for the effect of pitch angle, it will be found that there is still a flattening-off of the velocity factor for long coils that is not accounted for by the unmodified Ollendorff transmission-line model.

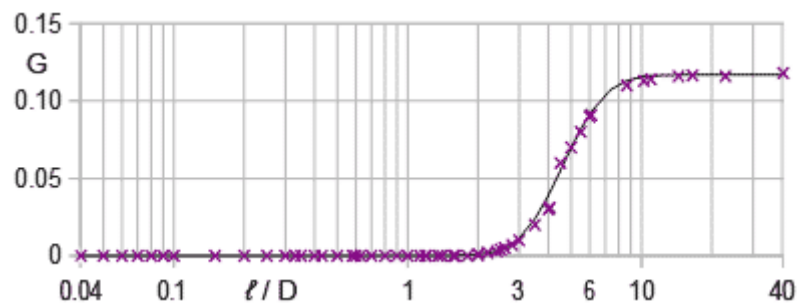
In order to learn more about this effect, various empirical fitting strategies were tried in an attempt to reproduce the actual curve. A complete replacement for Ollendorff's function was found to be impractical because any substitute function would need to be of a very high order in the argument x . This is generally the case with combinations of Bessel functions, and it can be seen from the comparison between Ollendorff's function and the Kandoian-Sichak approximation in section 1.8 that the phase velocity is somewhat wayward. The approach chosen was therefore that of progressively modifying the Bessel function argument. This is a matter of shifting the Ollendorff curve along the ℓ/D axis, as was done for demonstration purposes in section 1.7, but in this case the increment is governed by a function of ℓ/D rather than a constant. Initial attempts to get this to work using simple polynomials and logarithmic functions however failed to produce the desired effect.

Eventually, it was decided that the problem might be solved by finding out what the correcting function should look like. Consequently, with the modified argument defined as $x' = x + \delta x$, a spreadsheet column for δx was created and filled with zeros. Numbers were then entered into this column manually in order to eliminate the fitting residuals (i.e., the difference between the data and the model curve) for $\ell/D > 1$. The resulting noisy correcting curve was then adjusted manually, first for monotonicity and then to make it smooth.

The result was a sigmoid curve, of asymmetric appearance on a linear scale, but symmetric on a logarithmic scale. Such a curve is the Gompertz function⁹⁷:

$$G(t) = k_1 \exp[-k_2 \exp(-k_3 t)]$$

where the parameter k_1 sets the asymptote, k_2 controls the horizontal translation and k_3 controls the rate of growth. The actual Gompertz function used is shown on the right on a logarithmic scale, with the manually determined corrections (crosses) superimposed. It is explicitly:



$$G(\ell/D) = 0.117 \exp[-22 \exp(-0.75 \ell/D)] \quad (11.16)$$

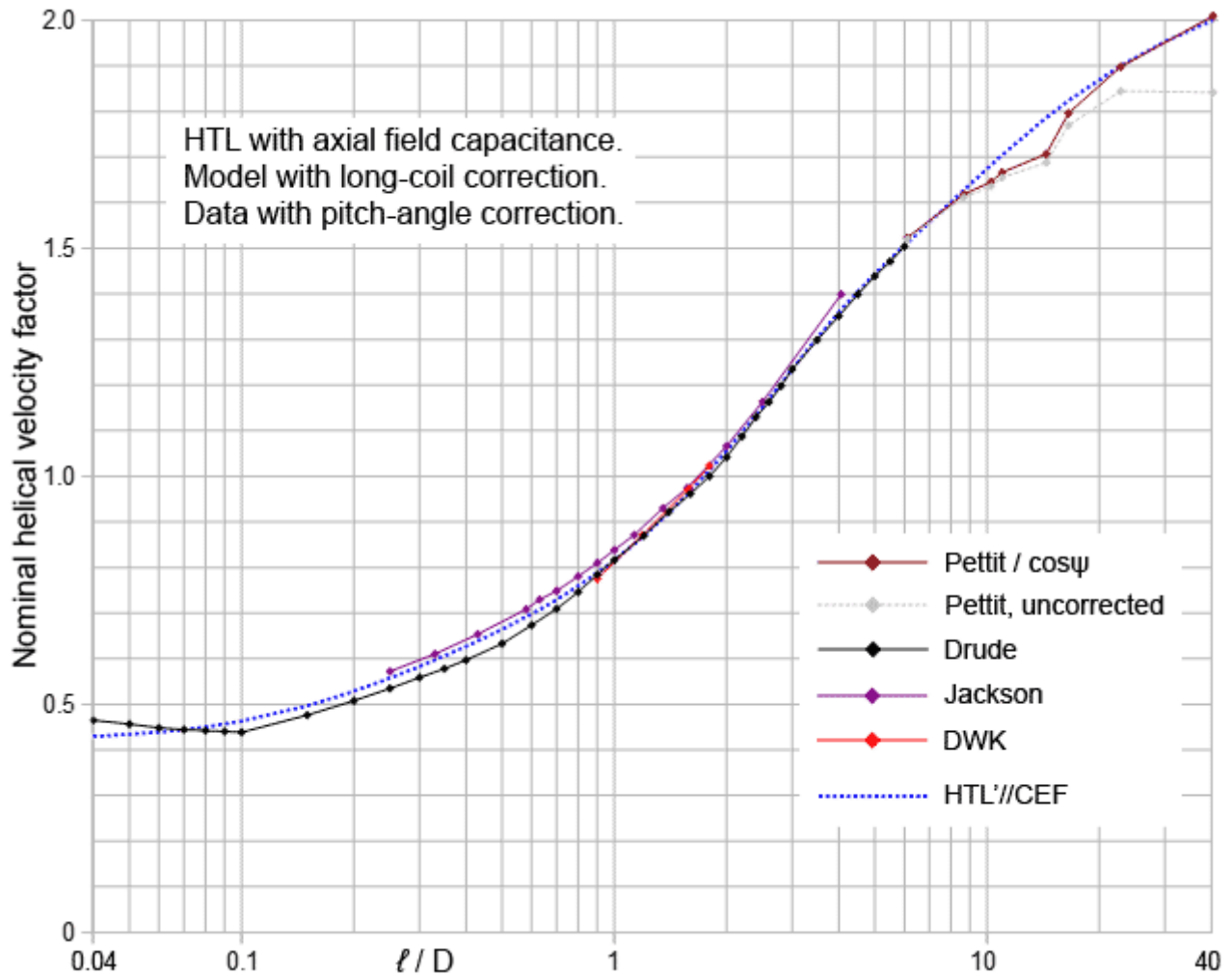
With this correction, the Bessel function argument becomes:

$$x(\ell/D) = \frac{\pi}{2}(D/\ell) + G(\ell/D) \quad (11.17)$$

Note incidentally, that this argument is used both in Ollendorff's function and in the expression for the HTL characteristic resistance (11.8).

⁹⁷ https://en.wikipedia.org/wiki/Gompertz_function

With the correcting function as given the model now fits 62 data points from Drude, Jackson, DWK and Alex Pettit with a standard deviation of 2.1% on 58 degrees of freedom⁹⁸. The four parameters considered adjustable are the three for the Gompertz function and the single adjustable coefficient in equation (11.15). The following graph shows the curve in relation to the data.



Coil former dielectric

A question that might have been asked at various points in this section is: 'why bother with this complicated transmission-line model, when you could simply fit the data to a purely empirical curve?' There are two principal answers to that criticism, the first being that the helical velocity factor veers, in a manner characteristic of behaviour described by Bessel functions. Consequently, there won't be any simple closed-form handbook formulae of any merit⁹⁹. The second point however is more subtle and might be explained as follows.

There is no complete solution for the solenoid self-resonance problem from first principles. Accurate formulae will therefore require some empirical adjustment; but if we keep such adjustments to a minimum, and justify them on physical grounds, then the model can still be adapted in a systematic way.

One very good reason for wanting to adapt the model is that we want to be able to predict the effect of coil former dielectric. This is not completely straightforward, because dielectrics affect different parts of the model in different ways. Correction is therefore not simply a matter of multiplying the nominal VF by a number. If the required correction works moreover, then it suggests that the various pragmatic decisions and empirical adjustments made along the way have not divorced the model too seriously from the underlying physics.

We can start by applying a dielectric correction to the true helical velocity. Instead of writing it as a velocity factor, it can be deconstructed by writing:

$$v_{hx} = c \frac{W(x)}{\cos \psi} = \frac{1}{\sqrt{\mu_0 \epsilon_0}} \frac{W(x)}{\cos \psi}$$

Thus we can see that it can be corrected by multiplying ϵ_0 by a relative permittivity factor. The quantity required in this case is the average relative permittivity for radial propagation, which we will call ϵ_{rad} . This will be a weighted average of the permittivities on either side of the conducting boundary, such that the simple average will apply when the coil is very short, and the external permittivity will dominate when the coil is very long. We have already encountered this type of average in determining self-capacitance, where the effective dielectric constant for the time-delay part was given as equation (9.11b). Here we write the expression with the left-hand side changed to ϵ_{rad} , because that is what it is.

$$\epsilon_{rad} = \frac{\epsilon_x}{2} \left[1 + k_L + \frac{\epsilon_i}{\epsilon_x} (1 - k_L) \right] \quad (11.18)$$

where k_L is Nagaoka's coefficient, and ϵ_i and ϵ_x are the internal and external dielectric constants. Note that using Nagaoka's coefficient to determine the weighting for the free coil is not a rigorous choice. The average obtained however will still be fairly close to the actual, such that we will hopefully not notice any error in a curve that attempts to predict resonance to within a few %.

The velocity factor for helical propagation now becomes:

$$\frac{v_{hx}}{c} = \frac{1}{\sqrt{\epsilon_{rad}}} \frac{W(x)}{\cos \psi} \approx \frac{W(x)}{\sqrt{\epsilon_{rad}}} \quad (11.19)$$

The HTL characteristic resistance was given earlier as equation (11.8). With permittivity and permeability shown explicitly it can be written:

⁹⁹ The Kandoian-Sichak approximation is discussed in section 1.8.

$$R_0 \tan \psi = \frac{Z_0}{2\pi} \sqrt{2 K_1(x) I_1(x) K_0(x) I_0(x)} = \frac{1}{2\pi} \sqrt{\frac{\mu_0}{\epsilon_0}} \sqrt{2 K_1(x) I_1(x) K_0(x) I_0(x)}$$

From this we can see directly that ϵ_0 , once again, needs to be multiplied by the relative permittivity for radial propagation. Thus, the expression for characteristic resistance becomes:

$$R_0 \tan \psi = \frac{1}{\sqrt{\epsilon_{\text{rad}}}} \frac{Z_0}{2\pi} \sqrt{2 K_1(x) I_1(x) K_0(x) I_0(x)} \quad (11.20)$$

The capacitance terminating the transmission line was given by equation (11.15) in a form having two components. Here we will separate those two parts explicitly, because it will be necessary to correct them for coil former dielectric in different ways. Thus we have:

$$C_{\text{EF}} = C_{\text{FF}} + C_{\text{AF}}$$

where C_{FF} is the fringe field capacitance given by:

$$\frac{C_{\text{FF}}}{D} = \frac{2\epsilon_0}{1 + \ln(1 + \ell/D)}$$

and C_{AF} is the axial field capacitance, given by:

$$\frac{C_{\text{AF}}}{D} = \frac{2\epsilon_0}{\text{arccosh}(1.015 + (\ell/D)^2)}$$

Of these two expressions, the second is the easiest to deal with because it represents a fairly straightforward end-to-end capacitance. Consequently, we can expect it to depend on the average dielectric constant in much the same way as was encountered in the self-capacitance case (9.13). Thus, the axial dielectric constant can be taken to be:

$$\epsilon_{\text{ax}} = \frac{\epsilon_1 + \epsilon_x}{2}$$

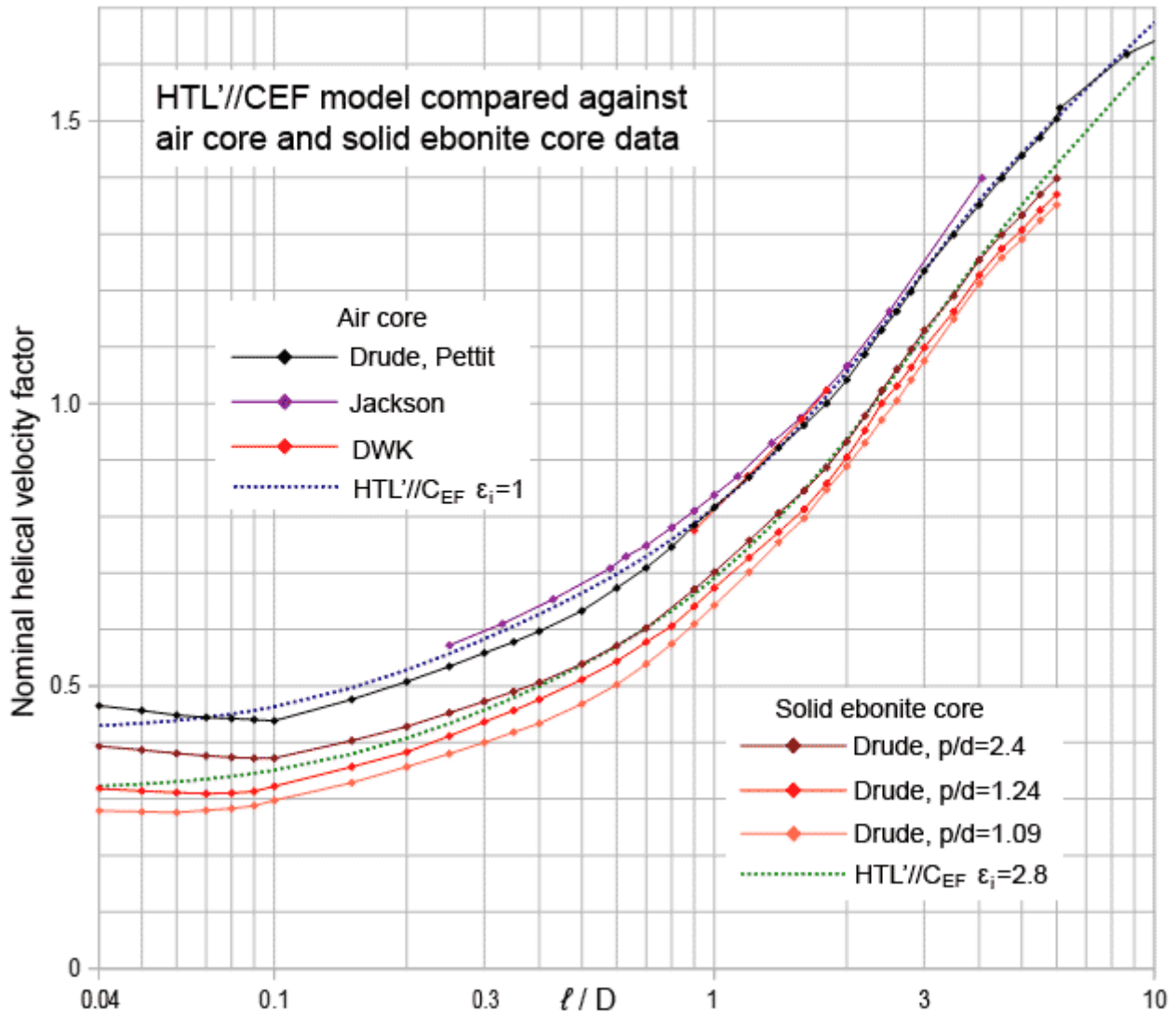
in which case the axial field capacitance per unit diameter becomes:

$$\frac{C_{\text{AF}}}{D} = \frac{\epsilon_0(\epsilon_i + \epsilon_x)}{\text{arccosh}(1.015 + (\ell/D)^2)} \quad (11.21)$$

How to correct the fringe-field capacitance however is a little more difficult to decide, because the associated field lines are neither strictly axial or radial. For that reason both types of correction were tried, and while it can be argued that neither is completely appropriate, the radial type correction was found to give by far the better result. This is because the effect of dielectric needs to die-off faster than the fringe-filed capacitance itself as the length of the coil increases. Thus the fringe -field capacitance per unit diameter becomes:

$$\frac{C_{FF}}{D} = \frac{2\epsilon_0\epsilon_{rad}}{1+\ln(1+\ell/D)} \quad (11.22)$$

With the corrected components (11.19) - (11.22) incorporated, the HTL//C_{EF} model is compared with Drude's data for coils wound on solid ebonite (hard rubber) cores¹⁰⁰ in the graph below¹⁰¹.



Drude actually made four series of measurements of coils on solid ebonite cores, two of which were for p/d=2.4. Those two series are very similar, and so the graph shows the average. The notes given by Drude on coil construction are somewhat ambiguous, but the best interpretation appears to be that the p/d=2.4 measurements refer to coils that had bare copper wire embedded in a shallow helical groove machined into the former. The p/d=1.09 and p/d=1.24 measurements on the other hand, refer to turns of cotton-insulated wire pushed close together on the surface of a bare cylinder. Kaye & Laby¹⁰² gives the dielectric constant of ebonite as falling between 3 and 2.7 for the range from 1 kHz to 1 GHz, so the value ε_i=2.8 was considered reasonable for modelling purposes.

Cotton is cellulose fibre, and cellulose is a highly polar material. Hence cotton fabric can have a

¹⁰⁰On the construction of Tesla transformers. P Drude, English translation cited earlier. Table on p322.

¹⁰¹ Worksheet **Helical_vf.ods**, sheet 10.

¹⁰² http://www.kayelaby.npl.co.uk/general_physics/2_6/2_6_5.html

dielectric constant anywhere between about 2 and 7.5 depending on the state of compression. Also we do not know what oils or waxes were soaked into the cotton to improve its properties. Consequently we should expect the curves for the close-spaced coils to fall below the $p/d=2.4$ curve, and that is what is seen. Thus the wide-spaced case, with only ebonite to consider, is the dataset with which we would like to see the model converge.

The model and the $p/d=2.4$ data agree very closely over the ℓ/D range from 0.4 to 4. There is some divergence at the extremes, but this does not necessarily indicate a problem with the theory. For $\ell/D > 4$, it could simply mean that the coils had a fairly wide pitch and the velocity factor is falling-off slightly as a consequence. For the coils with $\ell/D < 4$, it should be noted that the spacing between Drude's air core and ebonite core curves is uneven, and this looks like an artefact¹⁰³. Thus there is no convincing basis on which to modify the model.

For a final test, the $HTL//C_{EF}$ model was used to predict the self-resonance frequency of a large PTFE cored coil kindly provided by Dr Duncan Cadd¹⁰⁴. The coil, shown in the photograph on the right, has a thick-walled PTFE former and a removable close fitting PTFE rod of 35 mm diameter inserted into it. It thus has an effectively solid PTFE core. The turns are wound into a machined helical groove. The SRF was measured using the scattering jig described in section 1.1 (the coil was suspended using two loops of fishing line). The coil parameters and SRF are listed below.



- Solenoid length: $\ell = 218.1$ mm
- Average diameter : $D = 70.8$ mm
- length / diameter ratio: $\ell/D = 3.08$
- Number of turns: $N = 43.8$
- Wire (tubing) diameter: $d = 4.0$ mm
- Winding pitch: $p = \ell/N = 4.98$ mm
- Pitch to wire diam. ratio: $p/d = 1.24$
- Conductor length: $\ell_w = \sqrt{[(\pi DN)^2 + \ell^2]} = 9.745$ m
- SRF: $f_{0s} = 17.939$ MHz
- $\lambda_0/2$: $= c/(2f_{0s}) = 8.356$ m
- Nominal helical VF: $v_{hx(nom)}/c = 9.745 / 8.356 = 1.166$

The dielectric constant of PTFE is 2.1 over the range from 50 Hz to 3 GHz. Putting this value into the model with $\ell/D=3.08$ yields $v_{hx(nom)}/c = 1.169$. Multiplying this value by c and then using the formula:

$$f_0 = \frac{v_{hx(nom)}}{2 \ell_w}$$

we get a predicted SRF of 17.98 MHz, which is within $\pm 0.23\%$ of the actual value. Such good predictions cannot always be expected of course, but it does indicate that the model is fairly accurate at this particular ℓ/D value.

Incidentally, the SRF of the coil with the 35 mm diameter inner core removed is 18.101 MHz, an increase of 162 kHz.

¹⁰³ Drude hand smoothed all of his data, and short coils are very difficult to construct accurately.

¹⁰⁴ <http://home.freeuk.net/dunckx/>

Model properties, limitations and overall calculation procedure

Since the development of the HTL//C_{FF} model has been a somewhat long process, it is useful to summarise its capabilities and limitations and collect all of the steps required in implementing it.

Firstly, note that the input arguments are the coil length/diameter ratio, ℓ/D , the internal dielectric constant ϵ_i , and the external dielectric constant ϵ_x . Under normal circumstances, ϵ_x will be set to 1, but it can be set to a different value if, for example, the coil is immersed in a bath of liquid. The quantity returned is the nominal helical *velocity factor*, $v_{hx(nom)}/c$, for a free coil (i.e., a coil with no electrical connections) at its SRF. This must be multiplied by c to obtain a nominal velocity. The SRF can then be calculated from the conductor length using:

$$f_0 = \frac{v_{hx(nom)}}{2 \ell_w}$$

If the coil is connected at one end to an infinite ground plane, the SRF will be approximately halved. The SRF obtained is an upper limit, and will be reduced by ball electrodes and other accoutrements.

The model is designed to predict the SRF of coils wound on cylindrical formers of uniform composition. It will be most accurate if the wire is uninsulated, or if the insulation is thin and there is some gap between the turns. If the former is a tube, the SRF will be higher than the value obtained for a solid core. In order to produce accurate predictions for coils wound on tubular formers, the model would need to be extended. If such an extension is attempted, note that the helical propagation process and the axial field capacitance will be affected differently in the event of a discontinuous internal medium.

The following calculations are required.

1) Bessel function argument, (11.16) and (11.17):

$$x = \frac{\pi}{2}(D/\ell) + 0.117 \exp[-22 \exp(-0.75 \ell/D)]$$

2) Nagaoka's coefficient, k_L , for use in the radial permittivity weighting function. Various general purpose inductance calculation utilities can be used, e.g., the Basic macro function W82W(D/ ℓ).

3) Relative permittivity for radial propagation, (11.18):

$$\epsilon_{rad} = \frac{\epsilon_x}{2} \left[1 + k_L + \frac{\epsilon_i}{\epsilon_x} (1 - k_L) \right]$$

4) Actual helical velocity factor(11.19).

$$\frac{v_{hx}}{c} = \frac{W(x)}{\sqrt{\epsilon_{rad}}} \quad \text{Where } W(x) \text{ is Ollendorff's function (1.5).}$$

5) Fringe field capacitance, (11.22):

$$\frac{C_{FF}}{D} = \frac{2 \epsilon_0 \epsilon_{rad}}{1 + \ln(1 + \ell/D)}$$

6) Axial field capacitance, **(11.21)**:

$$\frac{C_{AF}}{D} = \frac{\epsilon_0(\epsilon_i + \epsilon_x)}{\operatorname{arccosh}(1.015 + (\ell/D)^2)}$$

7) Characteristic resistance **(11.20)**:

$$R_0 \tan \psi = \frac{1}{\sqrt{\epsilon_{\text{rad}}}} \frac{Z_0}{2\pi} \sqrt{2 K_1(x) I_1(x) K_0(x) I_0(x)}$$

8) Iterative solution for $v_{\text{hx(nom)}}/c$, **(11.13)** and **(11.14)**:

$$a = \frac{\pi}{2 v_{\text{hx}}/c}$$

$$b = \frac{(\ell/D)}{c \pi [(C_{FF}/D) + (C_{AF}/D)] (R_0 \tan \psi)}$$

$$y = \frac{1}{a} \arctan\left(\frac{b}{z}\right) \quad \text{to be adjusted until } y=z$$

$$\frac{\partial y}{\partial z} = -\frac{b}{a} \frac{1}{z^2 + b^2}$$

$$v_{\text{hx(nom)}}/c = y$$

The complete algorithm is implemented in the Open Office Basic macro function given in the following box. Three external functions are used:

- W82W(D/ℓ) for Nagaoka's coefficient (see section 9),
- Ollendf(x) for Ollendorff's function (section 1.7),
- R0tan(x) for $R_0 \tan \psi$ (given after equation **(11.12)**).

Note that OO Basic has no arccosh function, and so the following identity is used:

$$\operatorname{arccosh}(x) = \ln(x + \sqrt{x^2 - 1})$$

The iterative solution procedure for $v_{\text{hx(nom)}}/c$ is explained in the passage after equation **(11.13)**.

```

Function VFnom(byval lod as double, ei as double, ex as double) as double
' Calculates nominal helical velocity factor for a free coil at its first SRF.
' D W Knight, v1.00, 2016-04-14
' Calls functions W82W(), Ollendf(), R0tan()
Dim x as double, erad as double, kL as double, vf0 as double, vfh as double
Dim Cff as double, arg as double, Caf as double, Rotn as double
Dim n as integer, a as double, b as double, y as double, z as double
Dim diff as double, der as double, deltaz as double
x = pi / (2 * lod)
x = x + 0.117*exp(-22*exp(-0.75*lod))
kL = W82W(1/lod)
erad = (ex/2)*(1 + kL + (ei/ex)*(1-kL))
vf0 = 1/sqr(erad)
vfh = vf0*Ollendf(x)
Cff = erad*2*8.854187818/(1+log(1+lod))
arg = 1.015 + lod*lod
Caf = 8.854187818*(ei+ex)/log(arg+sqr(arg*arg-1))
Rotn = vf0*R0tan(x)
b = 1000000*lod/(299.792458*pi*(Cff+Caf)*Rotn)
a = pi/(2*vfh)
'solve for VFnom
z = vfh
n = 0
do
  y = (1/a)*atn(b/z)
  diff = z-y
  der = -(b/a)/(z*z+b*b)
  deltaz = diff/(der -1)
  z = z + deltaz
  n = n + 1
loop until abs(diff) < 1E-9 or n > 255
VFnom = y
end function

```

12. Pseudo self-capacitance

In the earlier part of the 20th Century, the preferred technique for determining the self-capacitance of a solenoid coil was the extrapolation method of GWO Howe (see introduction, etc.). In 1935 however, as was mentioned in section 10, Willis Jackson published a paper in which he lamented the lack of accurate measurements suitable for comparison with theory. In this he asserted the (by then) common belief that the coil behaves as though it has a uniform current throughout its length right up to the SRF; in which case, poor experimental results could be attributed to failure to account for coil-former dielectric, stray capacitance and connecting leads. He therefore devised an improved method for self-capacitance determination, which he applied to coils constructed with minimal dielectric supporting material.

His solution was to use the resonance extrapolation method to determine the coil inductance; but instead of trusting the self-capacitance that also comes out of that analysis, he trimmed-off the leads, suspended the coil from a thread, and made a separate SRF measurement using an absorption method.

His self-capacitances, calculated from the SRF and the inductance using the parallel resonance formula, came out a lot lower than the results obtained using the Howe method. Anyone who has been paying attention to this article so far will realise why that was; but at the time, only a few months after Palermo's dubious contribution (see section 6), it will have seemed that he had found some serious shortcomings in prior studies.

The result, of course, was more confusion; and in later years some doomed attempts (best left to the reader to discover) to fit free-coil and in-circuit 'self-capacitance' data using the same theory in both cases. As we now know, that doesn't work; and so it is perhaps not surprising that people later fell upon Medhurst's formula with relief and tried not to think too hard about coil former dielectric.

The premise on which this study was based was actually very similar to Jackson's. It was observed that there was some problem with self-capacitance measurements, such that it was not possible to account for them in a consistent way. The difference however, is that this work began with extrapolation measurements made over a wide frequency range; and it became obvious early on that the explanation for the peculiar 'fact' that the lumped element theory holds right up to the SRF is that it is wrong. In retrospect of course, it is obviously nonsense, because, notwithstanding the strange phenomenon of velocity limiting, there cannot be a uniform current in a coil with nothing connected to it. Furthermore, it must be said, that it is not strictly even possible to define inductance for an open circuit, and the problem must therefore be formulated in terms of inductance-per-unit-length. Thus an a-priori indication that it is a transmission-line problem, and by a somewhat lengthy process, we end up with radically different models for the uniform-current and the free-coil cases.

There is however, an issue of measurement technique that remains. This is that the idea that there is no difference between free-coil measurements and in-circuit measurements is so embedded, that people do not distinguish between the two approaches and often do not even report the method used. The models developed here however are now sufficiently mature that they will allow us to distinguish between the two classes of data.

In section 10, we converted self-capacitance curves and measurements into nominal velocity factors for the purpose of comparing them with free-coil data. We can now do the converse, and thereby represent free coil data as pseudo self-capacitances, to be compared with true self-capacitances. It must be understood, of course, that a pseudo self-capacitance is a completely fictitious quantity; because an open-circuit coil does not have an inductance that can be inserted into the resonance formula, but that does not stop people from calculating it.

The inductance used in the reporting of pseudo self-capacitance is usually either calculated from the current-sheet formula or measured by a two-terminal method. For reasonably small pitch

angles, the results are similar in either case; because the current-sheet formula gives the DC inductance without internal inductance, which is close to the RF uniform-current value.

The nominal helical velocity factor as a function of self capacitance was given earlier as equation (10.3). It can be written:

$$\left(\frac{v_{\text{hx(nom)}}}{c}\right)^2 = \frac{4\epsilon_0 \ell/D}{\pi k_L (C_L/D)}$$

where k_L is Nagaoka's coefficient. For a nominal helical VF of arbitrary origin therefore, we can rearrange this to obtain an alleged 'self-capacitance' per unit diameter:

$$\frac{C_L}{D} = \frac{4\epsilon_0}{\pi} \frac{\ell/D}{k_L (v_{\text{hx(nom)}}/c)^2} \quad (12.1)$$

For the purpose of generating free-coil pseudo self-capacitances, we can either feed this formula using actual SRF measurements, i.e. using:

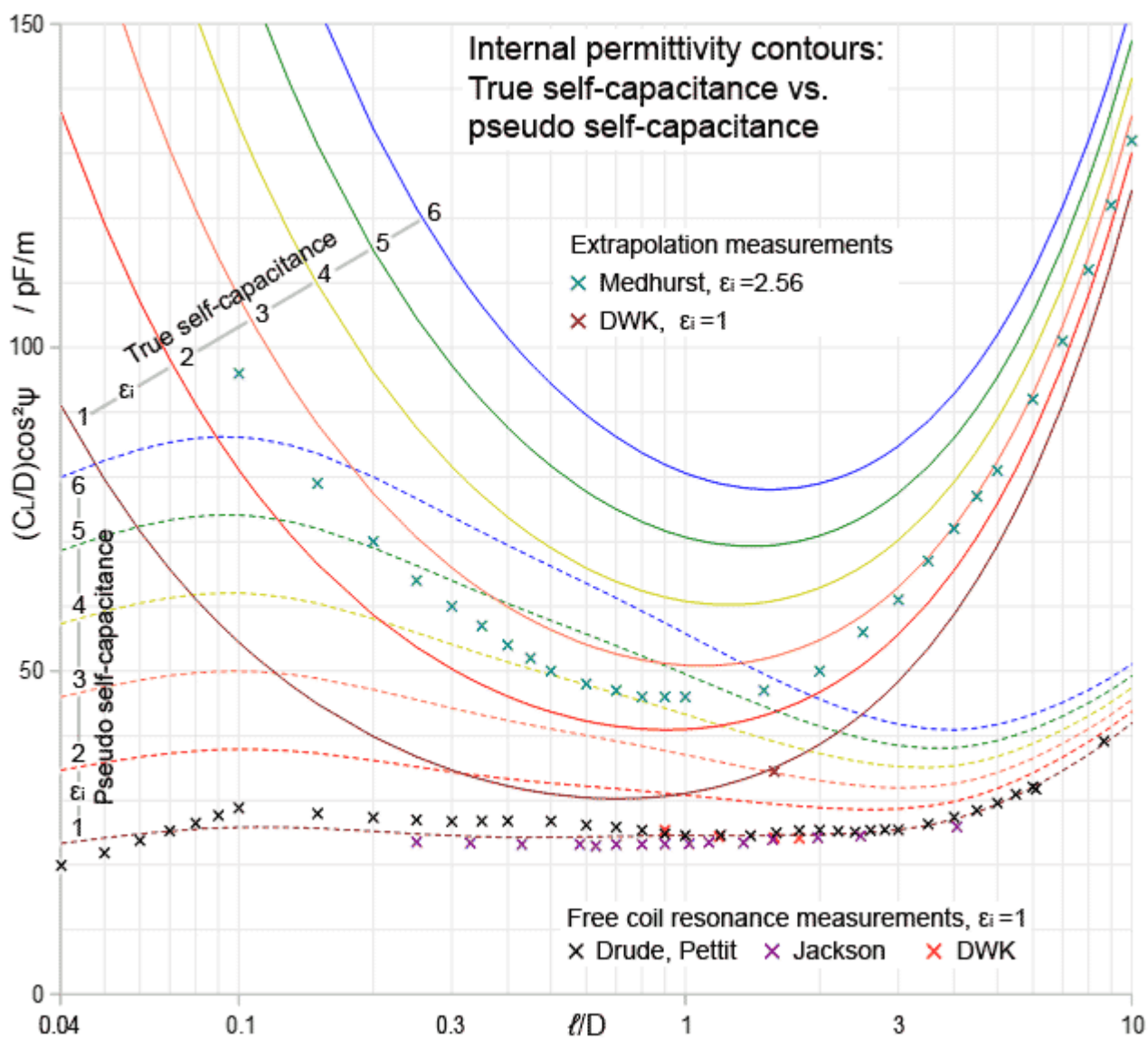
$$\frac{v_{\text{hx(nom)}}}{c} = \frac{2f_0 \ell_w}{c}$$

or we can use the output of the HTL//CEF model developed in the previous section.

A Basic macro that converts velocity factors into self-capacitance per unit diameter is given below.

```
Function V2Cw(vfnom as double, loD as double) as double
' Converts nominal VF into CL/D in pF/m. D W Knight. v1.00, 2016-04-17
' loD is coil length / Diam. Calls function W82W for Nagaoka's coeff.
Dim kL as double
if vfnom <= 0 then vfnom = 1
kL = W82W(1/loD)
V2Cw = 11.27350207*loD/(kL*vfnom*vfnom)
end function
```

Recall that in section 7, a graph was given showing various self-capacitance measurements against a set of coil-former relative permittivity contours generated using the C_L -DAE formula. The following graph has true self-capacitance permittivity contours as before (solid lines), but it also has pseudo-self-capacitance contours (dashed lines) produced using equation (12.1) and the HTL//CEF program¹⁰⁵. Jackson's 'self capacitance' per unit diameter measurements taken from his paper are plotted for comparison, along with pseudo C_L/D values created using air-core free-coil data from Drude, Alex Pettit and DWK. It is obvious that the two types of data are very different, and they can be distinguished fairly easily if the solenoid internal permittivity is known.



13. Discussion and summary

The matter of radio-frequency solenoid reactance and resonance prediction has had a remarkably troubled history. In this article however, we have uncovered the various difficulties giving rise to that situation, particularly the velocity limiting effect that renders the Ollendorff helical waveguide theory inapplicable to coils carrying uniform current. Cleared of that obstacle, it has been possible to develop practical calculation methods for both free-coil self-resonance and uniform current self-capacitance and show that they agree with a substantial body of experimental data. Theoretical issues however remain, particularly in the matter of why wave propagation along a helix is affected by external influences on current distribution, and in the matter of how to derive the induced axial field and fringe field capacitances from first principles.

For those who wish to develop this subject further, or who simply want to understand the solenoid resonator for the purpose of using it, the following general points have been established.

1) A free coil, i.e., a coil without connections, has its fundamental resonance when the wire length is $\lambda/2$ (where λ is the electrical wavelength). When one end of the coil is connected to an infinite ground plane, the fundamental SRF occurs when the conductor length is $\lambda/4$. The removal of the impedance discontinuity at one end effectively doubles the length of the single-conductor transmission line.

When an impedance is connected in parallel with a coil, the impedance terminates the transmission line. The coil behaves as a short-circuited two-wire line of half its conductor length, which is the same as a one-wire transmission line of length equal to its conductor length. A two-wire line presents a high impedance at its terminals when its electrical length is $\lambda/4$, i.e., when the length of the wire in it is $\lambda/2$. Thus when the line is resonated against a variable reference capacitor, the data extrapolated to zero capacitance point to the $\lambda/2$ wire length resonance (provided that the test frequency is not too close to the SRF). ***This is true regardless of whether or not one terminal of the coil is grounded***, because the ground is not involved in resonating the coil.

That grounding one end of the coil has very little effect on the parallel resonance of an LC network is easily verified by removing and replacing the ground connection (the small changes that do occur are due to stray capacitance).

2) A long free coil exhibits a superluminal helical phase velocity that declines with increasing frequency. When a shunt impedance is connected across the coil terminals, and provided that its magnitude is low enough to render the current distribution reasonably uniform, the superluminal effect is abolished and waves travel along the helix at the velocity of light for the local medium. Hence ***free-coil waveguide theories do not apply to coils connected in circuit***.

For those unfamiliar with electromagnetic theory, please note that a superluminal phase velocity does not imply transmission of information at a velocity faster than that of light. A phase velocity is the apparent velocity of a superposition of incident and scattered waves, all of which have a true velocity of c .

A generator of relatively low output impedance connected across the coil will have the same effect as a shunt impedance. Hence network analyser (virtual) SRF measurements are not equivalent to free-coil measurements.

3) The variability of the superluminal phase velocity is what is being referred-to when it is said that a helical transmission line is dispersive. When external circuitry provides a shunt impedance sufficient to abolish the superluminal effect, the line is not dispersive in the absence of an environment composed of dispersive material. Thus coils in circuit are in general not dispersive, and propagation delay can be estimated on the simple basis that a wave travels along the coil-winding at a velocity governed by the local refractive index (the refractive index is the reciprocal velocity factor for the surrounding medium).

4) The elevated helical phase velocity effect is not abolished by immersing the system in a medium of high refractive index. All apparent velocities are simply scaled in proportion. Thus, although a guided wave might not have a phase velocity $> c$, it is still effectively superluminal if its phase velocity is greater than that of an unguided wave.

5) The time-varying current associated with an electromagnetic wave propagating along a helical conductor produces a time-varying magnetic field in the direction of the coil axis. By Faraday's law, an electric field is induced around any loop that encloses this changing magnetic flux. There will be a component of this induced circumferential field, $E\cos\psi$, at the surface of the helix acting in the helical direction. Assuming a perfect conductor, this field must be exactly cancelled at the conducting wall (a perfect conductor cannot sustain an electric field within its body). For that requirement (i.e., EM boundary condition) to be satisfied, an electric polarisation must occur in the helical direction. This causes a voltage to appear across the ends of the coil, and hence an axial electric field in addition to the axial magnetic field. The energy stored in this axial electric field is equivalent to a capacitance. Thus there is an apparent static capacitance between the two ends of the coil.

6) When a coil is short, the induced axial field capacitance renders the current distribution more uniform than would otherwise be expected, and this tends to abolish the superluminal effect even when the coil is unconnected.

7) The axial field capacitance is also present in coils connected in circuit. It renders the current substantially uniform in short coils, allowing them to be modelled as a lumped inductance in parallel with a fixed capacitance. In longer coils, the self-shunting effect is less pronounced, and superluminal helical phase velocity is restored as the parallel impedance increases in magnitude (i.e., becomes more like an open-circuit) and the SRF is approached.

8) It is tempting to attribute the axial field capacitance to a series combination of capacitances assumed to exist between adjacent turns. The problem here is that if the number of turns is increased, the voltage per turn required to cancel the surface helical component of the induced field goes down. Hence the axial field capacitance is unaffected by the number of turns (at least, to a good first-order approximation). For that reason, inter-turn capacitance theories have no predictive power in the case of single-layer solenoid coils (i.e., they are wrong).

Also, the axial field is not concentrated in the gaps between the turns. It is actually fairly uniform on the inside of the solenoid, allowing the the internal average dielectric constant to be calculated from the area average.

There is, of course, static inter-layer capacitance in multi-layer coils. Also, a spiral coil can be considered to be a single-turn multi-layer coil, and this topology gives a relatively large self-capacitance.

Glossary

// = parallel impedance operator, defined such that: $\mathbf{a} // \mathbf{b} = \mathbf{ab} / (\mathbf{a} + \mathbf{b})$

$\beta = 2\pi/\lambda = \omega/v$ = propagation constant (wavenumber).

$\beta_0 = 2\pi/\lambda_0 = \omega/c$

$\gamma = \sqrt{(\beta^2 - \beta_0^2)}$ = radial wavenumber

$\epsilon = \epsilon_0 \epsilon_r$ = electric permittivity

$\epsilon_0 = 1/(\mu_0 c^2) = 8.854187818 \text{ pF/m}$ = permittivity of free space

ϵ_r = relative permittivity (dielectric constant in the lossless approximation).

ϵ_{rad} = relative permittivity for radial wave propagation

ϵ_f = dielectric constant (relative permittivity) of coil-former material.

ϵ_h = relative permittivity of a space occupied by a helical scattering element

ϵ_i = relative permittivity inside the solenoid

ϵ_x = relative permittivity outside the solenoid

η = volume fraction

$\lambda = v / f$ = wavelength in the surrounding medium

$\lambda_0 = c / f$ = wavelength in free space

λ_{ax} = axial wavelength

λ_{hx} = helical wavelength

$\mu = \mu_0 \mu_r$ = magnetic permeability

$\mu_0 = 400\pi \text{ nH/m}$ = permeability of free space

μ_r = relative permeability (neglecting losses)

χ^2/v = reduced chi-squared = variance of an observation of unit weight.

$\psi = \arctan(p/\pi D)$ = pitch angle

$\omega = 2\pi f$ = angular frequency [radians / sec.]

$c = 1/\sqrt{(\mu_0 \epsilon_0)} = 299\,792\,458 \text{ m/s}$ = Velocity of light

C_0 = Capacitance per unit length of transmission line

C_{ee} = End-effect capacitance

C_E = Capacitance due to axial induced electric field

C_{EF} = Axial induced field capacitance of free coil

$C_L = C_T + C_E$ = Self-capacitance of an inductor

C_T = time delay expressed as a capacitance

D = Average or effective diameter of solenoid

DAE = "Doubly asymptotic, empirical"

d = wire diameter

DFM = Digital Frequency Meter

ESD = estimated standard deviation

f = frequency

f_0 = resonant frequency

f_{0s} = self-resonant frequency (SRF)

$f_{0s(v)}$ = virtual SRF, calculated from uniform current inductance and self-capacitance.

g = Geometric mean distance (GMD)

$G(x)$ = Gompertz function

GDO = Grid-dip oscillator

h = height

HTL = Helical transmission line

$H_n^{(1)}(x)$ = Hankel function of the first kind of order n and argument x .

$I_n(x)$ = Modified Bessel function of the first kind

$J_n(x)$ = Bessel function of the first kind.
 $K_n(x)$ = Modified Bessel function of the second kind.
 k_C = capacitance correction coefficient
 k_E = electric correction factor
 k_H = Generalised magnetic field inhomogeneity coefficient
 k_L = Nagaoka's coefficient (current-sheet field inhomogeneity coeff.)
 L = Low-frequency inductance
 $L' = X_L' / (2\pi f)$ = Apparent inductance
 L_0 = Inductance per unit length of transmission line
 $\ell = Np$ = Length (or height) of solenoid.
 ℓ/D = coil length to diameter ratio.
 $\ell_w = 2\pi rN/\cos\psi$ = Wire (or conductor) length (often approximated by setting $\cos\psi=1$)
 ℓ_{TL} = physical length of a transmission line
 $m = 1, 2, 3, \dots$ = Counting index for overtones.
 n_{ax} or n_z = Apparent refractive index for axial wave propagation.
 n_{hx} = Apparent refractive index for helical wave propagation (Drude's f).
 N = Number of turns
 $N/\ell = 1/p$ = Number of turns per unit length
 $p = \ell/N$ = pitch distance (i.e., distance between turns, wire centre to wire centre).
 $r = D/2$ = Effective radius of solenoid ($r < r_a$)
 R_0 = Characteristic resistance of a transmission line
 r_a = Average radius of solenoid (measured to middle of wire)
 r_i = inside radius of tubular coil-former
 r_o = outside radius of coil-former
SRF = Self-resonance frequency
 T_0 = Lowest helical waveguide propagation mode (radially symmetric).
TDE = "time delay + induced electric field"
TL = Transmission line
UHMWPE = ultra-high molecular weight polyethylene
unun = unbalanced-to-unbalanced transmission-line transformer
 v = phase velocity, i.e., apparent propagation velocity (in medium. $v = c$ in vacuo)
VF = velocity factor
 v_p = phase velocity
 $v/c = 1/n$ = velocity factor
 $v_{ax}/c = 1/n_{ax}$ = axial velocity factor
 $v_{hx}/c = 1/n_{hx}$ = helical velocity factor
 $v_{rad} = v_{hx} \cos\psi$ = radial phase velocity
VNA, VNWA = Vector Network Analyser
 w = relative wall thickness
 w_i = statistical weight of the i^{th} observation
 x = Generalised function argument. Polynomial root. Horizontal graph axis.
 $W(x) = v_{rad}/c$ = Ollendorff's function (free-coil radial velocity factor).
 X = reactance
 $X_{CL} = -1/(2\pi f C_L)$ = reactance attributable to self-capacitance
 $X_L = 2\pi f L$ = Inductive reactance
 $Z_0 = \sqrt{(\mu_0/\epsilon_0)} = 376.7303134 \Omega$ = Impedance of free space
 $Z_0/2\pi = 59.9584916 \Omega$

Revision history

- 2008-09: Refitted version of Medhurst's formula with correction for coil-former dielectric + comparison with inter-turn capacitance theories first published online as HTML
- 2010-05-09: v 0.01: 1st draft PDF, ported from HTML and reformatted and put online .
- 2013-02-01: v 0.03. Loaded vertical antenna discussion.
- 2013-04-23. v 0.06: Helical resonators.
- 2013-05-02: v 0.07: Notation updated to comply with SI conventions.
- 2016-03-03: v 0.09: Presentation of evidence for the velocity limiting effect.
- 2016-03-16: v 0.12: Introduced the CL-TDE formula.
- 2016-03-27: v 0.14: Changed 'sheath-helix' to 'sheet-helix'. Macro code for Ollendorff's function. Iterative solution for wavenumber problem. Comparison with the K&S approximation. Added K&S to the collected VF curve (section 10).
- 2016-03-31: v 0.15: Correction in discussion of K&S curve & Medhurst's data. Misassignment to the $\lambda/4$ resonance doubles the apparent velocity factor.
- 2016-04-07: v 0.16: Correction to formula in section 1.2.
- 2016-04-19: v 0.17: Completed section 11. Added section 12.
- 2016-04-21: v 0.18: Made more accurate (VNA two-antenna) measurements on the large PTFE coil, both with and without the inner PTFE core. HTL//CEF prediction is actually within 0.23%.
- 2016-05-02: v 0.19: Shorter abstract. Minor changes to text and formatting.
- 2016-05-03: v 0.21. Section 1.0 edited and renamed. Pocklington ref. added.
- 2016-05-04: v 1.00. Extended title. Additional comments in discussion.

